Modulation of functional properties of bifunctional S-Adenosylmethionine decarboxylase/Ornithine decarboxylase of *Plasmodium falciparum* by structural motifs in parasite-specific inserts

by

Suretha Roux

Submitted in partial fulfillment of the requirements for the degree *Magister Scientiae* in the Faculty of Natural and Agricultural Science

Department of Biochemistry
University of Pretoria
Pretoria

March 2006

Acknowledgements

- Prof. A.I. Louw my supervisor and mentor. For his invaluable lessons in academics and in life, which shaped me to be a better scientist and a stronger person.

- Dr. Lyn-Marie Birkholtz, my co-supervisor, for her friendship, advice and ever willingness to help.

- For Gordon Wells, who helped me with the Molecular Dynamics and Secondary Structure predictions.

- The NRF for the Grant Holders Bursary that made it possible to be a full time student.

- To my parents, who gave me the opportunity to follow my dreams, supported me throughout and for their unconditional love. My brother, who believes that I can do anything and for his support, love and encouragement. For Christiaan, my love, for his patience, love, support and his ever optimistic view that scientists will prosper.

- God, for leading me down the road of Biochemistry. For the opportunity to discover something new every day of this wonderful world He created. For granting scientists the opportunity to glimpse pieces of the complex puzzle of biology and for the knowledge that one day He will let us in on it all.

Contents

List of Figures

List of Tables

List of Abbreviations

ACC	Acetyl-CoA carboxylase
AHT	Anhydrotetracycline
AdoMetDC	S-Adenosylmethionine decarboxylase
Brij-35	Polyoxyethyleneglycol dodecyl ether
BSA	Bovine serum albumin
CS	Circumsporozoite protein
CSA	Chondroitin sulphate A
cSAT	N^1-acetyltransferase
dcAdoMet	Decarboxylated *S*-Adenosylmethionine
DFMO	α-Diflouromethyl ornithine
DHFR-TS	Dihydrofolate reductase-thymidylate synthase
DHODH	Dihydroorotate dehydrogenase
DHPS-PPPK	Dihydropteroate synthase-pyrophosphokinase
DTT	Dithiothreitol
EDTA	Ethylene diamine tetra-acetic acid
eNOS	Endothelial cell nitric oxide synthase
FAS I	Type I fatty acid synthase
FAS II	Fatty acid synthase type II
GPI	Glycosylphosphatidylinositol
HABA	4-hydroxy azobenzene-2-carboxylic acid
HS	Heparan sulphate
ICAM-1	Intercellular adhesion molecule-1
IFN-γ	Interferon gamma
IgM	Immunoglobulin M
IL-1	Interleukin-1
iNOS	Inducible nictric oxide synthase
LB	Luria-Bertani
MAT	S-Adenosylmethionine synthetase
ME	Multi-epitope
MR	Methionine recycling
MSP-1	Merozoite surface protein 1

MTA	Methylthioadenosine
MVA	Mevalonate
MVA	Modified vaccinia Ankara virus
NMVA	Non-mevalonate pathway
NO	Nitric oxide
OD	Optical density
ODC	Ornithine decarboxylase
PAGE	Polyacrylamide gel electrophoresis
PAO	Polyamine oxidase
PECAM-1	Platelet-endothelial cell adhesion molecule-1
PfEMP1	*P. falciparum* erythrocyte membrane protein-1
Pfu	*Pyrococcus furiosis*
PLP	Pyridoxal 5'-phosphate
PMSF	Phenylmethylsulfonyl fluoride
SDS	Sodium dodecylsulphate
SpdSyn	Spermidine synthase
SpmSyn	Spermine synthase
STET	Sucrose, Triton X-100, EDTA, Tris
TEMED	N,N,N',N'-tetramethylenediamine
TNF-α	Tumor necrosis factor alpha
TRAP	Thrombospondin-related adhesion protein
Tris-HCl	Trishydroxy (methyl-amino) methane / Hydrochloric acid
TSP	Thrombospondin
WT	Wild type

Chapter 1
Introduction

The occurrence of malaria dates back to more than 4 000 years ago when periodic fevers, the so-called 'king of diseases', have been mentioned for the first time. Egyptian mummies of about 3 000 years old have been found to contain enlarged spleens, which are most probably due to malaria. After 200 B.C., malaria was evident in Italy, especially in the marshes of the Roman Campagne. In Roman literature, the symptoms of malaria were accurately described and it was thought that the marshes were the source of this disease, which became known as *mal'aria* meaning bad air (Sherman, 1998). Charles Laveran (1845 – 1922) observed that malaria incidences increased remarkably close to the equator and stated that 'swamp fever' is caused by a germ and not by the swamp itself. In 1880, Laveran concluded that malaria is caused by a parasite and not a bacterium as was believed previously; he also recognized all the stages of *Plasmodium falciparum* in that year. In 1907, Laveran received the Nobel Prize for his discovery of the parasite *P. falciparum*, the causative agent of malaria. In 1897, Ronald Ross (1857 – 1932) demonstrated the transmission of malaria by mosquitoes and received the Nobel Prize for his finding in 1902 (Sherman, 1998).

1.1 The burden of malaria

Malaria is returning to areas from which it had been exterminated and it enters new areas such as Eastern Europe and Central Asia. In addition, more people are dying each year from malaria than 30 years ago. Malaria deaths range between 0.7 – 2.7 million each year, with more than 70% of the victims being African children and pregnant woman (Hartl, 2004; Phillips, 2001). The malaria burden falls most heavily on sub-Saharan Africa, where more than 90% of the deaths occur and 5% of children die from malaria before the age of 5 (Phillips, 2001). Globally, malaria presents a threat to 2.4 billion people per year throughout the world and is responsible for 300 – 500 million clinical cases. The resurgence of malaria is due to the following factors: emergence and spread of drug resistant parasites, the evolution of pesticide-resistant mosquitoes, increased population density, global warming (this allowed the mosquitoes to migrate to places previously out of their range) and continuing poverty (especially in Africa) (Hartl, 2004). The Malaria Foundation International calculated that 76% more productive life years are lost because of malaria than

cancer throughout the world whereas funding for cancer research still exceeds malaria funding 10- to 50 fold. One major reason for the lack in malaria research funding is the fact that pharmaceutical companies do not see economic sense in developing new antimalarials (Phillips, 2001). It is therefore up to malaria endemic countries to find solutions to the spread and resistance of malaria.

1.2 Pathogenesis of malaria

Malaria is caused by one of four species of *Plasmodium*; *P. falciparum, P. vivax, P. ovale* and *P. malaria* of which *P. falciparum* is the causative agent of almost all the malaria-related deaths (Webster and Hill, 2003).

P. falciparum is the most malignant form of malaria and the only one which causes severe complications including cerebral malaria, severe anemia, severe respiratory distress, hypoglycemia, pulmonary oedema, renal failure and placental malaria. Cerebral malaria and severe anemia are, however, the most common causes of hospitalization and death, especially in patients that had no prior exposure to the parasite (Rasti, *et al.*, 2004).

P. falciparum spread through the bite of the infected female *Anopheles* mosquito, which transfers from 15 to 100 sporozoites into the blood stream of the human host (Phillips, 2001; Webster and Hill., 2003). The sporozoites migrate to hepatic cells and infection occurs within 30 to 45 minutes. Once inside the liver cells, the sporozoites mature into liver-stage trophozoites and then into schizonts, a process that takes an estimated 6 to 7 days. Upon schizont rupture, 20 000 – 40 000 merozoites are released into the blood stream and in a matter of 15 to 20 seconds, attach to and invade erythrocytes (Phillips, 2001; Webster and Hill, 2003). During the asexual erythrocytic cycle, the merozoites multiply inside erythrocytes causing rupture and invade new erythrocytes every 48 hours until the infection is controlled or the host dies. Some of the ring-forms in the erythrocytic cycle differentiate into male and female gametocytes that are taken up by a feeding mosquito. After fertilization in the mosquito mid-gut, a zygote is formed that matures into the motile ookinete within 24 hours. The ookinete moves through the midgut wall and stagnate on the basal lamina where it develops into an oocyst. Mitotic division inside the oocyst gives rise to a number of sporozoites and upon rupture of the oocyst, the sporozoites move to the

salivary glands where it is available for infection of the human host (Phillips, 2001; Webster and Hill, 2003). A schematic of the parasitic lifecycle is depicted in Figure 1.1.

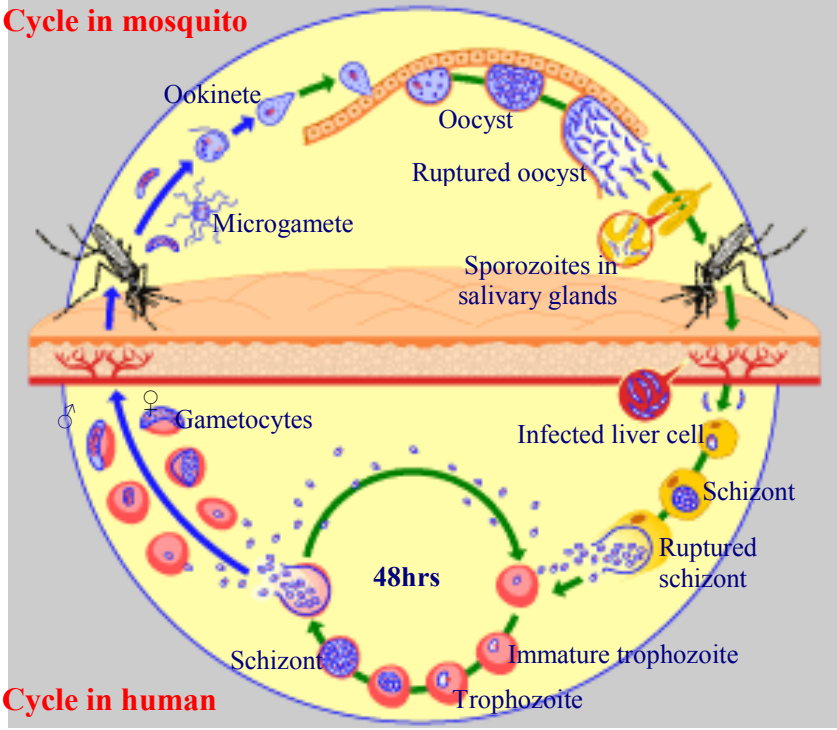

Figure 1.1: The malaria parasite life cycle. (adapted from www.who.int/tdr/diseases/malaria /lifecycle.htm)

P. falciparum has the ability to invade erythrocytes of all ages, which causes extremely high parasitaemias and enhanced growth; furthermore it also has the capacity to adhere to vascular endothelium through the process of sequestration. These two features are unique to *P. falciparum* and are responsible for its disease severity and pathogenesis (Heddini, 2002). Infected erythrocytes are known for their adhesive qualities: they adhere to endothelial cells (cytoadherence) and uninfected erythrocytes (rosetting) and also causes the aggregation of infected cells (autoagglutination) or the aggregation of cells mediated by platelets (clumping) (Heddini, 2002). The adherence traits of infected erythrocytes are responsible for the accumulation of parasites in vascular beds causing organ damage and preventing clearance of *P. falciparum* by the immune system.

The adhesive properties of infected erythrocytes are a result of parasite-derived proteins expressed on the erythrocyte surface. *P. falciparum* evades the immune system in a number of ways, including the expression of variant surface antigens such as *P. falciparum* erythrocyte membrane protein-1 (PfEMP1) (Cooke, *et al.*, 2000; Rasti, *et al.*, 2004). The

parasite uses PfEMP1 to adhere to several host receptors including chondroitin sulphate A (CSA), CD36, heparan sulphate (HS), intercellular adhesion molecule-1 (ICAM-1), immunoglobulin M (IgM), platelet-endothelial cell adhesion molecule-1 (PECAM-1)/CD31 and thrombospondin (TSP) thereby avoiding spleen clearance (Cooke, *et al.*, 2000; Heddini, 2002). The interacting molecules are illustrated in Figure 1.2.

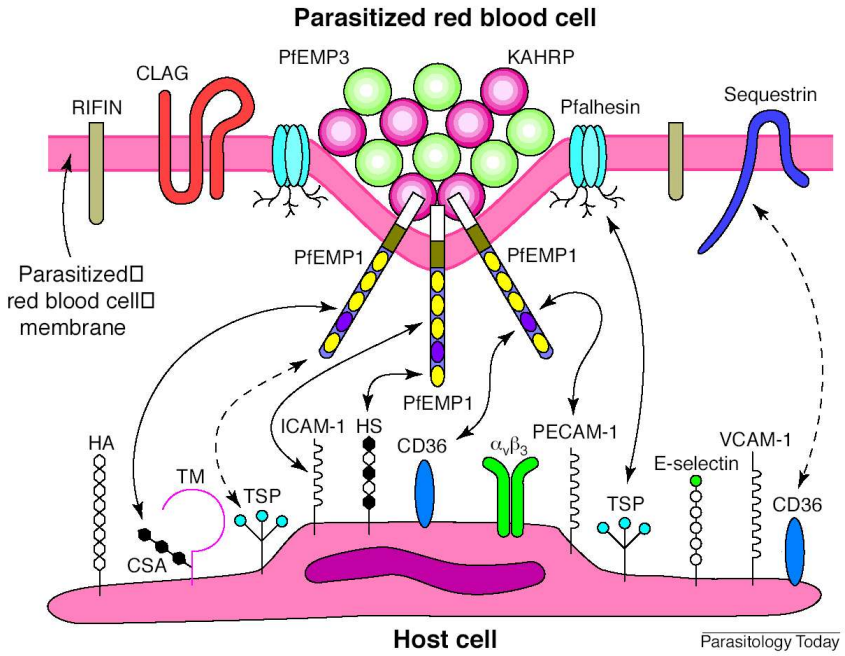

Figure 1.2: The interacting molecules between the *P. falciparum* infected red blood cell and the host cell endothelium. Abbreviations: chondroitin sulphate A (CSA), cytoadherence-linked asexual gene (CLAG), heparan sulphate (HS), hyaluronic acid (HA), intercellular adhesion molecule-1 (ICAM-1), immunoglobulin M (IgM), knob-associated His-rich protein (KAHRP), *P. falciparum* erythrocyte membrane protein-1 (PfEMP1), platelet-endothelial cell adhesion molecule-1 (PECAM-1), parasite-modified form of the native RBC anion transport protein Band 3 (Pfalhesin), thrombospondin (TSP), thrombomodulin (TM), vascular cell adhesion molecule 1 (VCAM-1) (Cooke, *et al*., 2000).

Upon schizont rupture, the malaria debris including glycosylphosphatidylinositol (GPI), induces the release of pro-inflammatory cytokines. These cytokines include tumor necrosis factor alpha (TNF-α), interferon gamma (IFN-γ), interleukin-1 (IL-1), and IL-6 and play a major role in the onset of severe malaria, particularly fever and malaise (White, 1998). The cytokines, especially TNF-α and IFN-γ, induce an upregulation and redistribution of endothelial receptors (Heddini, 2002; Rasti, *et al.*, 2004). The upregulation of host receptors facilitate the adhesion of the *P. falciparum* infected erythrocytes. At sites of sequestration, TNF-α stimulates inducible nictric oxide synthase (iNOS) from circulating leukocytes as

well as endothelial-cell NOS (eNOS) to produce nitric oxide (NO) (Heddini, 2002; White, 1998). NO causes many of the pathological features of severe malaria, including hypotension, lactic acidosis and hypoglycemia. NO also crosses the blood-brain barrier and acts as an inhibitor of the central nervous system, resulting in the onset of coma (Heddini, 2002).

1.3 Malaria control strategies

Three main strategies to control malaria are presently under investigation: vaccination, vector control and anti-parasitic drugs. Rapidly spreading resistance to available drugs urges the development of mechanistically novel drugs and vaccines that are efficient, nontoxic and cost effective. Vaccines and anti-parasitic drugs are discussed in the following sections.

1.3.1 Vaccine development

P. falciparum has a complicated life cycle consisting of several stages (refer to Figure 1.1) with each stage expressing different antigens. This makes vaccine development extremely complex. Another setback is the polymorphism and antigenic variation of various malaria proteins, which potentially limits the efficacy of any vaccine not incorporating distinct variants of antigen (Richie and Saul, 2002). Immunity against malaria is normally species-specific, needs repeated exposure to the specific parasite and is short-lived (Phillips, 2001).

Despite all these complications, several studies showed that malaria vaccines are possibly viable. First, immunization of rodents, monkeys and humans with irradiated sporozoites showed a degree of protection against sporozoite infection (Richie and Saul, 2002; Webster and Hill, 2003). This suggests that a multivalent, pre-erythrocytic stage vaccine might induce immunity. Second, repeated infection of individuals with malaria leads to gradual achievement of naturally acquired immunity, which protects against clinical disease (Webster and Hill, 2003). Third, currently existing vaccine candidates showed protection against malaria infections in both humans and animals during clinical studies (Richie and Saul, 2002; Webster and Hill, 2003). Lastly, transmission-blocking vaccines proved to be successful in protecting mosquitoes against *P. falciparum* and *P. vivax* infections (Richie and Saul, 2002). The most effective vaccine will be one targeted at the asexual blood-stages of the parasite since this is the stage that causes pathogenesis and clinical symptoms.

Candidate vaccines of each of the major stages of the parasite life-cycle are being evaluated in clinical trials. It is still difficult to elicit a sufficiently strong and long lasting immune response in humans even though the same vaccine preparations are often strongly immunogenic in animal models (Richie and Saul, 2002). Currently, three vaccine candidates are studied in target populations in field trials; two pre-erythrocytic vaccines RTS,S/ASO2A and MVA-ME TRAP; and the blood-stage vaccine MSP-1/ASO2A (Ballou, *et al.*, 2004).

RTS,S/ASO2A is a hybrid protein containing the circumsporozoite protein (CS) fused to the hepatitis B surface antigen. ASO2A is a potent oil-in-water adjuvant including the immunostimulant monophosphoryl lipid A and the saponin derivative QS-21 (Ballou, *et al.*, 2004; Richie and Saul, 2002; Webster and Hill, 2003). RTS,S/ASO2A has been shown to be safe and highly immunogenic. The immunity obtained however is short-lived (Ballou, *et al.*, 2004). A RTS,S/ASO2A trial performed in Mozambique in children aged 1 to 4 showed a 30% efficacy against malaria infection of which the prevalence of *P. falciparum* infection was approximately 37% (Alonso, *et al.*, 2004).

The MVA-ME TRAP vaccine is constructed from a modified vaccinia Ankara virus (MVA) vector, containing a multi-epitope (ME) string of T- and B-cell epitopes, fused to the entire thrombospondin-related adhesion protein (TRAP) coding region (Ballou, *et al.*, 2004; Webster and Hill, 2003). Clinical trials to date proved this vaccine safe and highly immunogenic and effective against a heterologous strain, sporozoite challenge (Webster and Hill, 2003).

MSP-1/ASO2A contains a 19-kDa carboxy-terminal fragment from the merozoite surface protein 1 (MSP-1). Antibodies to the C-terminal region of MSP-1 protected West African children against clinical malaria (Webster and Hill, 2003) and immunization studies with mice and *Aotus* monkeys with recombinant and native MSP-1 proteins, showed an induction of protective antibody (Phillips, 2001). Clinical studies showed that this vaccine is also effective in humans although some suffer hypersensitivity reactions after the third dose (Webster and Hill, 2003). Adjustment of the vaccine formulation should prove to be effective against these side effects and the vaccine may protect against high parasitaemias in the host and therefore prevent the onset of clinical disease.

The best approach to develop an effective vaccine is the use of multistage (combining antigens of all the parasitic life-stages) and multivalent vaccines (a combination of epitopes from the same stage). This approach should solve the problem of antigenic variation and diversity (Phillips, 2001). The limited successes of vaccine candidates in clinical trials, suggests that an effective vaccine will not be available in the short-term.

1.3.2 Anti-parasitic drugs

Drugs are still the preferred method to combat malaria even though resistance against anti-malarial drugs has increased over the last 20 years. Under-investigation and shortage of research funds have contributed to the current situation where few replacements for compromised drugs are available. Over the past 25 years, pharmaceutical companies marketed less than 1% of new drugs for tropical diseases, which account for more that 90% of the worldwide disease burden (Trouiller, *et al.*, 2002). The problems and limitations of current drugs are listed in Table 1.1.

Table 1.1: Problems and limitations of existing antimalarials. Adapted from Milhous and Kyle, 1998 and Ridley, 2002

Drugs	Main problems and limitations
Chloroquine	Resistance worldwide (except Central America)
	Compliance, safety, resistance
Quinine	Safety, resistance
Amodiaquine	Psychoses (Safety), resistance, cost
Mefloquine	Cardiotoxicity (Safety), poor absorption, cost
Halofantrine	Resistance, cost
Artemisinins (artemether, arteether, artesunate)	Recrudescence, neurotoxicity (safety), compliance, cost
Sulphadoxine-pyrimethamine	Resistance
Atovaquone-proguanil	Rapid resistance when Atovaquone is used alone,
	Proguanil causes mouth ulcers, world-wide resistance,
	cost
Lumefantrine-artemether	Compliance, resistance potential, cost

In order to obtain selective toxicity of new drugs, the antimalarial targets must be essential for parasitic growth or survival and, if present in the human host, must be significantly different from that of the host. Perceived drug targets have been identified in the lysosomal food vacuole, apicoplast, mitochondrion, cytosol and plasma membrane of the parasite (Figure 1.3). Survival and proliferation of parasites in host erythrocytes require adaptations

of their metabolic processes. These alterations present potential novel drug targets and are discussed in the following sections.

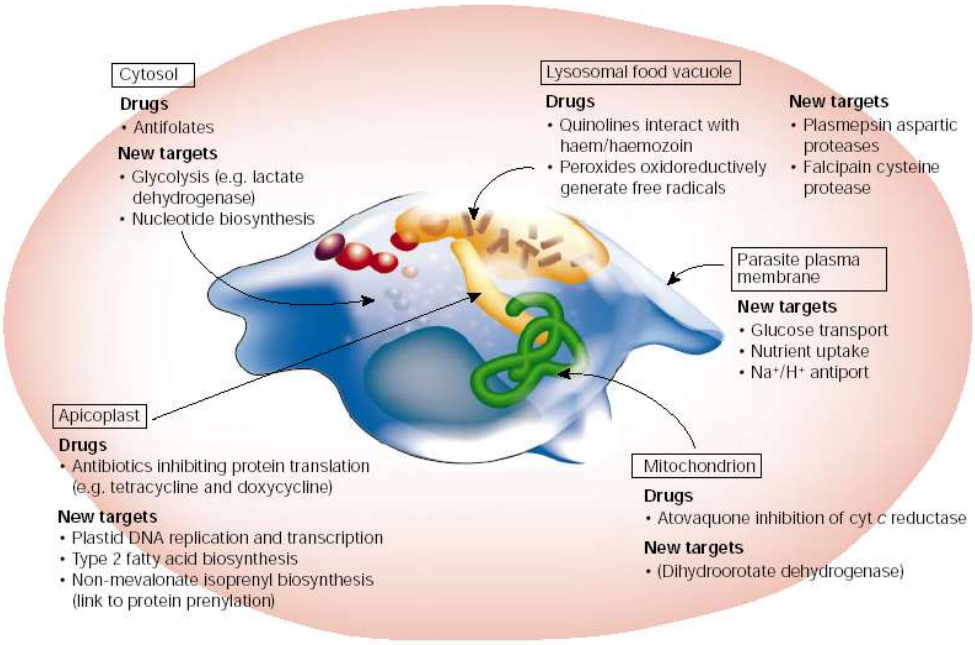

Figure 1.3: Drug interaction sites in the trophozoite stage of the malaria parasite (Ridley, 2002).

1.3.2.1 Hemoglobin processing in the lysosomal food vacuole

The food vacuole appears at the trophozoite stage of the parasitic life cycle. It has lysosomal properties because of its acidic nature and presence of hydrolytic enzymes but is specialized for the degradation of hemoglobin. The enzymes present in the *P. falciparum* food vacuole are the cysteine protease falcipain, the aspartic proteases plasmepsin I and plasmepsin II (Rosenthal and Meshnick, 1998), as well as many peptidases including a metallopeptidase (Ridley, 2002). The malaria parasite degrades up to 80% of the host hemoglobin during the 48 hours of growth and releases the resulting products in the infected erythrocyte (Ridley, 2002). The digestion of hemoglobin results in the production of amino acids used for protein synthesis, and ferrous-protoporphyrin IX (Fe(II) haem). The Fe(II) haem monomers are rapidly oxidized to ferric-protoporphyrin IX (Fe(III) haem) that is toxic to the parasitic cell because of the ability to generate oxygen radicals (Olliaro, 2001). Instead of being degraded, the haem monomers polymerize by linkage of the ferric ion of one haem to the side chain of another haem to form an insoluble, biologically inactive pigment, hemozoin (Berman and Adams, 1997; Olliaro, 2001; Pandey, *et al.*, 2003).

Quinolines (Chloroquine, Quinine, Amodiaquine and Mefloquine) block the formation of hemozoin. The mechanism involves quinoline binding non-covalently to haem through π-π stacking of their planar aromatic structures and competing with the hemozoin polymers for this molecule (Berman and Adams, 1997; Ridley, 2002). Quinolines can also bind to hemozoin and thus prevent further polymer elongation or induce depolymerization. The buildup of toxic levels of free haem or haem-quinoline complexes in the food vacuole results in toxicity to the parasite (Olliaro, 2001; Rosenthal and Meshnick, 1998).

Artemisinin contains an endoperoxide bond, which is necessary for its antimalarial activity. Interaction between artemisinin and haem results in the cleavage of the peroxide bond that generates free-radicals, which directly alkylate haem and other proteins in its immediate vicinity (Berman and Adams, 1997). Fe(II) haem and Fe(III) haem are required for the activation of artemisinin into an activated alkylating agent, which damages proteins (Meshnick, 2002). Covalent binding of artemisinin to haem might also inhibit hemozoin formation or induce hemozoin degradation (Meshnick, 2002).

Proteases that hydrolyze hemoglobin are potential drug targets for the control of *P. falciparum*. *In vitro* studies show that inhibition of the trophozoite cysteine proteases (falcipain) results in the accumulation of undegraded hemoglobin in the lysosomal food vacuole (Lee, *et al.*, 2003).

1.3.2.2 Apicoplast metabolism

The apicoplast is a novel, non-photosynthetic plastid organelle in Apicomplexa (including *Plasmodium spp., Toxoplasma gondii, Eimeria spp., Theileria spp.* and *Cryptosporidium;* (Kim and Weiss, 2004) originating from endosymbiotic cyanobacteria (Ralph, *et al.*, 2001). Plastids host a couple of anabolic processes of which the products get exported to the rest of the cell and are therefore indispensable to the parasite (Ralph, *et al.*, 2001). Parasites without their apicoplasts have been shown to lose their ability to invade erythrocytes or to establish a parasitic vacuole inside the host cell (Gornicki, 2003). DNA replication, transcription, translation and post-translational modification are some of the well-known processes occurring in the apicoplast (Ralph, *et al.*, 2001). Several nuclear-encoded proteins targeted to the apicoplast have been identified and it seems that they play a role in fatty acid synthesis and isoprenoid synthesis (Gornicki, 2003). The metabolic processes in the

apicoplast differ from that of the eukaryotic host because of its prokaryotic origin, making the apicoplast an ideal target for drug intervention.

DNA replication in the apicoplast requires the involvement of DNA gyrase, a prokaryotic type II topoisomerase, in order to replicate the circular plastid genome of *P. falciparum*. Ciprofloxacin is a fluoroquinolone and inhibits DNA gyrase; it is known to inhibit apicoplast DNA replication in *P. falciparum* (Ralph, *et al.*, 2001). Ciprofloxacin resistance already occurred in bacterial cells and there is a danger that the use of this compound as an effective anti-malarial will be short lived. Despite the possible resistance against ciprofloxacin, inhibition of DNA replication is still a viable strategy to control malaria.

Transcription and translation in plastids are being investigated as potential targets for drug intervention. Transcription of the plastid is inhibited by the treatment of parasites with rifampicin, which acts against the DNA-dependent RNA polymerase. Translation is interrupted by a number of drugs of which the precise mechanisms are unclear. Some of these drugs including doxycycline, clindamycin and spiramycin, are used clinically for the treatment of malaria and toxoplasmosis (Ralph, *et al.*, 2001).

The fatty acid synthase type II (FAS II) protein is present in bacterial as well as plant plastids and is also found in the apicoplast of *P. falciparum*. Type I fatty acid synthase (FAS I) is only present in the cytosol of mammalian cells and the gene encoding FAS I has not been found in the apicomplexan genome (Gornicki, 2003). Acetyl-CoA carboxylase (ACC) provides malonyl-CoA for fatty acid synthesis and is the metabolic regulator of this pathway. ACC in plants is inhibited by two classes of herbicides; aryloxyphenoxypropionates (fops) and cyclohexanediones (dims). *In vitro* studies show that the apicomplexan parasite, *T. gondii*, is inhibited by two fops and one dim (Gornicki, 2003). These results are indicative of the potential use of herbicides as antimalarials. The antibiotics thiolactomycin, triclosan and cerulenin are well known inhibitors of bacterial fatty acid synthesis and have been indicated in the inhibition of *in vitro P. falciparum* cultures. The targets for these antibiotics are β-ketoacyl-ACP synthase and β-enoyl-ACP reductase (Mitamura and Palacpac, 2003).

Isopentenyl diphosphate, the common precursor for isoprenoids, is synthesized by the mevalonate (MVA) as well as the non-mevalonate (NMVA) pathways. The MVA is present

in the majority of organisms whereas the NMVA is only present in bacterial and plant cells and the apicoplast. Fosmidomycin is an inhibitor of 1-deoxy-D-xylulose-5-phosphate synthase (an enzyme in the NMVA pathway) and strongly hinders parasite growth (Ridley, 2002).

1.3.2.3 Mitochondrial electron transport

The preference of *P. falciparum* parasites for an oxygen-deficient environment is due to its remarkable mitochondrial physiology and morphology. The malaria parasite lacks NADH-ubiquinone oxidoreductase and rather depends on certain redox reactions for the generation of a proton-motive force (Ridley, 2002; Vaidya, 1998). Dihydroorotate dehydrogenase (DHODH) together with two other proteins feed the electron transport chain in the absence of NADH-ubiquinone oxidoreductase. The malaria parasite solely depends on the *de novo* synthesis of pyrimidines making DHODH, which oxidizes dihydroorotate to orotate, the key enzyme in the pyrimidine biosynthetic pathway (Vaidya, 1998). Atovaquone inhibits electron transport by interfering with cytochrome c reductase coupling to DHODH (Ridley, 2002).

1.3.2.4 Cytoplasmic drug targets

The folate pathway is probably the best studied in terms of drug action and resistance. The arsenal of antifolates includes the diaminopyrimidines (such as pyrimethamine and trimethoprim), the biguanides (proguanil and chlorproguanil) and the sulfadrugs (including sulfonamides and the sulfones) (Phillips, 2001). The parasite relies on *de novo* synthesis of folate and the two main targets for antiparasitic intervention are dihydrofolate reductase-thymidylate synthase (DHFR-TS). DHFR is inhibited by pyrimethamine and proguanil. The dihydropteroate synthase (DHPS) domain of the bifunctional pyrophosphokinase-dihydropteroate synthase (PPPK-DHPS) is inhibited by the sulfur drugs (Olliaro, 2001). Pyrimethamine resistance is due to point mutations in *dhfr*; similarly sulphadoxine resistance is due to point mutations in *dhps* (Ridley, 2002). The extensive knowledge on how resistance in the folate pathway is achieved and the structural information of the enzymes makes it possible to develop new improved antifolates against *P. falciparum* (Yuvaniyama, *et al.*, 2003).

Another cytoplasmic biosynthetic pathway in the parasite is the polyamine pathway that shows promise for the development of new antiparasitic drugs. The polyamine pathway is

the focus of the current research study and will be discussed in detail in the following section.

1.4 Mammalian polyamine metabolism

Polyamines are ubiquitous in nature except for two orders of Archaea: Methanobacteriales and Halobacteriales (Wallace, *et al.*, 2003). Most eukaryotic cells contain three polyamines, the diamine, putrescine (1,4-diaminobutane), and its derivatives, spermidine and spermine (Cohen, 1998; Müller, *et al.*, 2001; Wallace, *et al.*, 2003). The structures are shown in Figure 1.4.

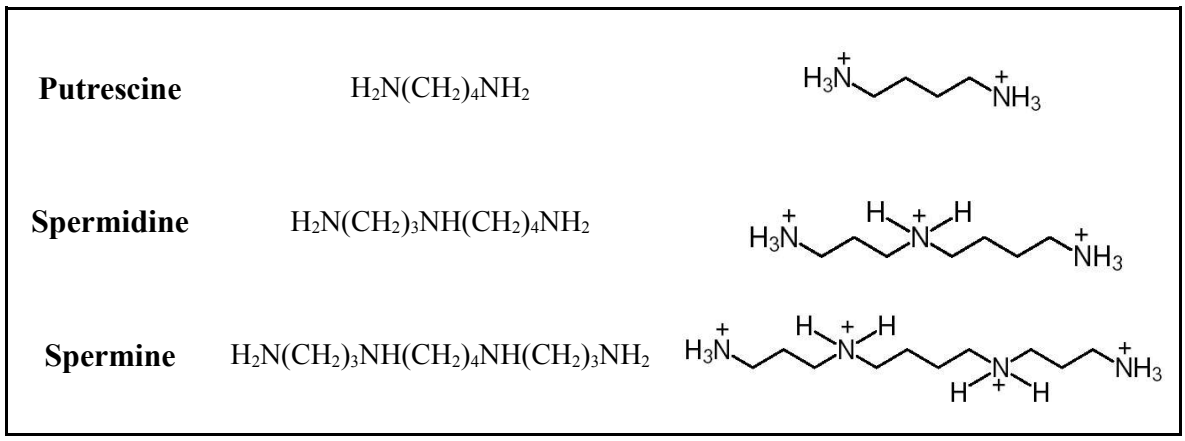

Figure 1.4: Structures of the polyamines. Taken from Seiler, 2005.

The polyamines are organic cations with a multitude of functions in cell proliferation, differentiation and cell death of eukaryotic cells (Thomas and Thomas, 2003). The functions of polyamines are directly related to their chemical structures. At physiological pH, the polyamines are charged at every nitrogen atom and the charge is distributed along the length of the carbon chain (Wallace, *et al.*, 2003). This property separates the polyamines from other cations like calcium or magnesium and the positive nature makes the polyamines ideal interacting molecules (Yerlikaya, 2004). Polyamines interact electrostatically with macromolecules in a specific or non-specific manner because of its cationic nature, water-solubility and length. Interacting macromolecules include DNA, RNA, membrane and soluble proteins, phospholipids, enzymes, and nucleotide triphosphates (Criss, 2003; Thomas and Thomas, 2003).

Polyamines regulate transcription by inducing conformational changes in DNA structure. Spermidine and spermine preferentially bind to pyrimidine residues in the secondary structures of DNA and is known to act as a bridge between major and minor grooves of DNA thereby holding together the molecule or mediating the interaction between different molecules. Polyamine depletion in the nuclei of the cell results in the partial unwinding of DNA strands thereby exposing binding sites for transcription (Wallace, *et al.*, 2003). Micromolar concentrations of polyamines induce a DNA conformational change from right-handed B-DNA to left-handed Z-DNA thereby inhibiting transcription (Thomas and Thomas, 2003). In addition to ligand-DNA interactions for the control of transcription, the polyamines also enhance the binding of several gene-regulatory proteins to regulatory sequences (response elements) on DNA (Thomas and Thomas, 2003). Polyamines also play important roles in protein-protein interactions, signal transduction, enzyme regulation and apoptosis (Criss, 2003).

The role of polyamines is evident when normal tissue is compared with tumor tissue which has a higher requirement for polyamines. If hepatic tissue dedifferentiate to a hepatoma, the following changes in the polyamine metabolism occur (Suya Subbayya, *et al.*, 1997):

i) The activity of ornithine transcarbamylase, which normally channels ornithine into the urea cycle, nearly disappears;
ii) The activity of the transaminase, which catalyses the first step in the formation of glutamate and proline from ornithine, decreases;
iii) ODC regulation gets altered resulting in an over-expression of ODC and an increase of cellular polyamines;

Recently, increased expression of cytosolic N^1-acetyltransferase (cSAT) and decreased expression of polyamine oxidase (PAO) was demonstrated in breast carcinoma cells (Wallace, *et al.*, 2003).

The polyamines are generally present at relatively high levels in most mammalian tissues. The intricate intracellular control mechanisms of the polyamine biosynthetic pathway and the limited knowledge thereof, encourages further investigation and development of chemotherapeutic strategies aimed at the polyamine pathway.

The biosynthesis of polyamines depends on the decarboxylation of ornithine to putrescine and the subsequent attachment of aminopropyl groups to its terminal amino substituents to form spermidine and spermine, respectively. Ornithine decarboxylase (ODC, EC 4.1.1.17) and S-Adenosylmethionine decarboxylase (AdoMetDC, EC 4.1.1.50) are the rate limiting enzymes in the polyamine pathway. ODC catalyzes the conversion of ornithine to putrescine using pyridoxal 5'-phosphate (PLP) as a cofactor whereas AdoMetDC provide the aminopropyl groups for spermidine and spermine synthesis (Figure 1.5). Addition of aminopropyl groups to putrescine and spermidine is catalyzed by spermidine synthase (EC 2.5.1.16) and spermine synthase (EC 2.5.1.22), respectively (Müller, *et al.*, 2001).

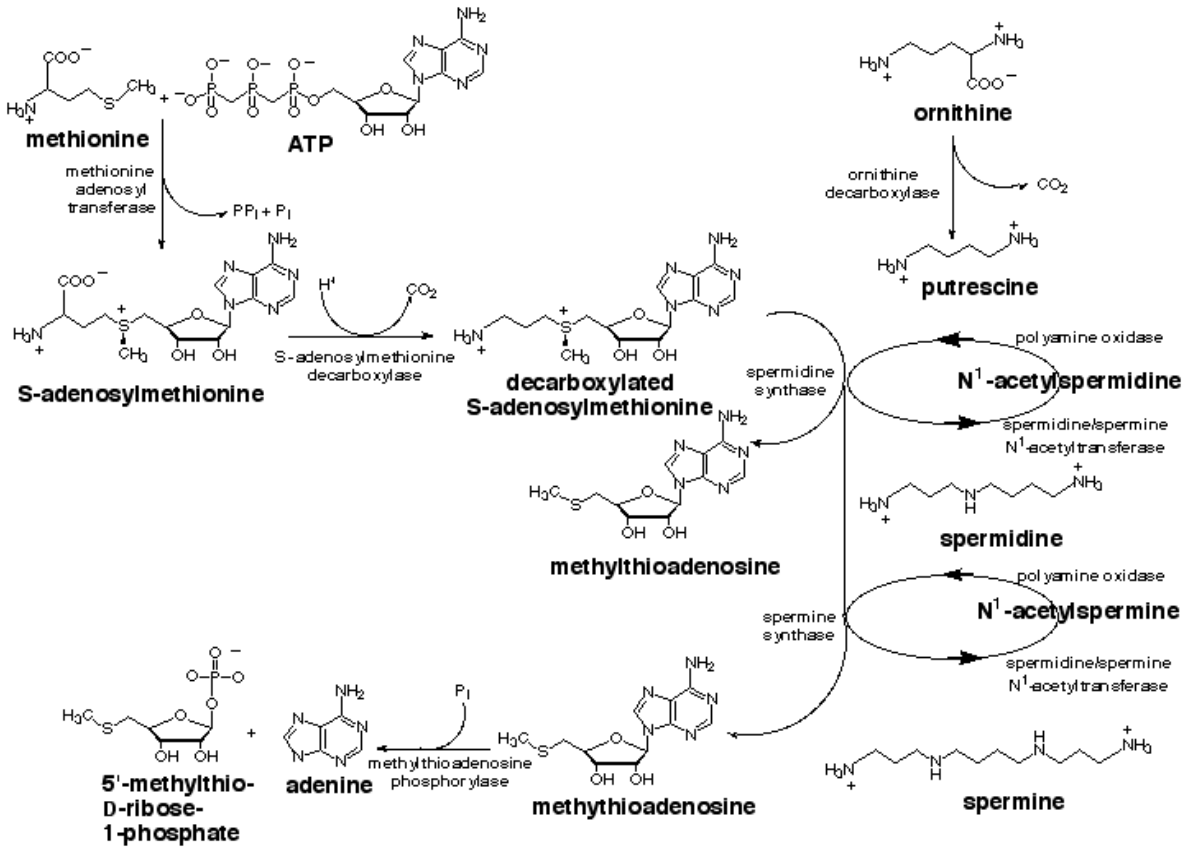

Figure 1.5: Polyamine metabolism in mammalian cells. *(arginine.chem.cornell.edu)*

In mammalian cells, spermine and spermidine are back-converted to putrescine. The first step is an acetylation step catalyzed by cytosolic spermidine/spermine N^1-acetyltransferase (EC 2.3.1.57) to form respectively, acetylspermidine and acetylspermine. The acetylated polyamines are either exported from the cell or it is oxidized by an FAD-dependent polyamine oxidase (EC 1.5.3.11) to form putrescine and spermidine, H_2O_2 and

acetoamidopropanol (Wallace, *et al.*, 2003). The biosynthetic polyamine pathway is compartmentalized in both the cytoplasm and the nuclei of mammalian cells and the resulting polyamine products may play different roles in the cytoplasm and nuclei (Criss, 2003).

1.5 Ornithine Decarboxylase (ODC)

ODC (E.C.4.1.1.17) catalyzes the decarboxylation of ornithine to putrescine, using PLP as co-factor. The active form of ODC is a homodimer with the two active sites situated at the dimer interface (Myers, *et al.*, 2001; Wallace, *et al.*, 2003). Mammalian ODC has a very short half-life of about 20 min and is regulated inside the cell at the gene amplification, transcription, translation and post-translational modification steps, which include oligomer assembly and protein degradation (Ceriani, *et al.*, 1992).

Mammalian ODC is inhibited by the natural products putrescine and cadaverine, and by 1,3-diaminopropane and some aromatic diamines, such as *p*-phenylenediamine (Cohen, 1998). Intracellular mammalian ODC levels is feedback-regulated by the polyamines, where high concentrations decrease ODC expression and the reverse is true for increased expression (Wallace, *et al.*, 2003). The level of ODC activity in less active cells is very low but synthesis of the enzyme is greatly and rapidly induced by a wide variety of growth-promoting stimuli including hormones, growth factors and tumor promoters (Kilpelainen and Hietala, 1998).

1.6 S-Adenosylmethionine decarboxylase (AdoMetDC)

AdoMetDC (E.C.4.1.1.50) is responsible for the conversion of adenosylmethionine to decarboxylated adenosylmethionine in order to provide aminopropyl groups for further polyamine synthesis. Mammalian AdoMetDC is synthesized as a 38 kDa proenzyme (333 residues) which has no catalytic activity unless it is autocatalytically cleaved into a 31 kDa α-subunit (266 residues) and an 8 kDa β-subunit (67 residues) by serinolysis (Yerlikaya, 2004). Putrescine stimulates both processing and catalytic activity (Seiler, 2003). The mammalian enzyme consists of a dimer of these non-identical subunits $(\alpha\text{-}\beta)_2$, and contains two active sites that functions independently of each other (Hillary and Pegg, 2003). The small subunit contributes residues to the active site of AdoMetDC and therefore both subunits are necessary for catalytic activity (Yerlikaya, 2004). The amino acid sequence of

the protein is highly conserved (more than 90% identical) among mammalian species (Persson, *et al.*, 1998). AdoMetDC translation is regulated by intracellular changes in spermidine and spermine levels where accumulated levels negatively influence protein synthesis (Shantz and Pegg, 1999).

1.7 Inhibition of polyamine biosynthesis

α-Diflouromethyl ornithine (DFMO), the ODC specific inhibitor, was the first successful drug targeted at the polyamine pathway and was initially used as an antitumor drug. Despite initial excitement of its possibilities, *in vivo* studies showed that DFMO is a cytostatic rather than a cytotoxic inhibitor (Müller, *et al.*, 2001; Seiler, 2003; Wallace and Fraser, 2004). The inefficiency of DFMO to arrest cell proliferation is most likely as a result of increased polyamine uptake by the cell in response to the low intracellular polyamine levels. The studies with DFMO did however demonstrate that polyamine depletion does prevent the growth of tumor cells (Wallace, *et al.*, 2003). DFMO has since been found to be effective against West African sleeping sickness caused by the parasite, *Trypanosoma brucei gambiense.* It is unfortunately not effective against the East African human form of the disease caused by *T. brucei rhodesiense* (Müller, *et al.*, 2001).

It is also known that DFMO inhibits the *in vitro* maturation of *P. falciparum* parasites beyond trophozoites during the blood stage of the parasitic lifecycle (Heby, *et al.*, 2003). Irreversible inhibition of AdoMetDC of *P. falciparum* results in inhibition of trophozoite development (Heby, *et al.*, 2003). The separate treatments of *P. falciparum* with DFMO and AdoMetDC inhibitors are both cytostatic. Combination therapy that inhibit both regulatory proteins of the polyamine pathway and polyamine transport appears to be the most effective strategy in targeting malaria through this pathway (Müller, *et al.*, 2001). It was shown that DFMO in combination with bis(benzyl)polyamine analogs are cytotoxic in the treatment of *P. berghei* infected mice (Bitonti, *et al.*, 1989).

1.8 *Plasmodium* polyamine metabolism

Usually, the rate limiting enzymes AdoMetDC and ODC are individually regulated on the transcriptional, translational and post-translational level. In *P. falciparum,* both these enzymes are encoded by a single open reading frame (Müller, *et al.*, 2000). The ODC domain is located at the C-terminal and is connected to the N-terminal AdoMetDC region

by a hinge region (Müller, *et al.*, 2000) (Figure 1.6). Unlike other bifunctional Plasmodial proteins (DHFR-TS, PPPK-DHPS) that allows substrate channeling to catalyse subsequent reactions, the *Pf*AdoMetDC/ODC catalyses reactions in two separate legs of the polyamine biosynthetic pathway. Other advantages of the bifunctional organization include intramolecular communication and interaction between the different domains for regulatory purposes as well as coordinated transcription and translation of the rate limiting enzymes.

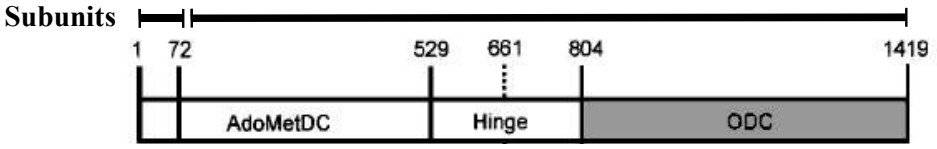

Figure 1.6: Schematic organization of the *P.falciparum* AdoMetDC/ODC heterodimeric polypeptide. Numbers correspond to amino acid residues. The AdoMetDC domain comprises amino acid residues 1-529. Residues 530-804 form the hinge region. The ODC domain consists of amino acids 805-1419 (Müller, *et al.*, 2000).

The polyamine pathway of *Plasmodium* (Figure 1.7) is relatively simple compared to that of the mammalian pathway (Figure 1.5). The ODC activity of the bifunctional *Pf*AdoMetDC/ODC is more strongly feedback regulated by its product putrescine compared to the mammalian enzyme, and *Plasmodium* AdoMetDC activity is not stimulated by putrescine whereas the mammalian enzyme is. The mammalian ODC and AdoMetDC have extremely short half-lives (ca. 15 min and 35 min, respectively) compared to *P. falciparum* AdoMetDC/ODC that has a half-life of more than 2 h (Müller, *et al.*, 2001). The slow turnover of *Pf*AdoMetDC/ODC is advantageous for inhibition by antimalarials because of the slow replacement of inhibited proteins.

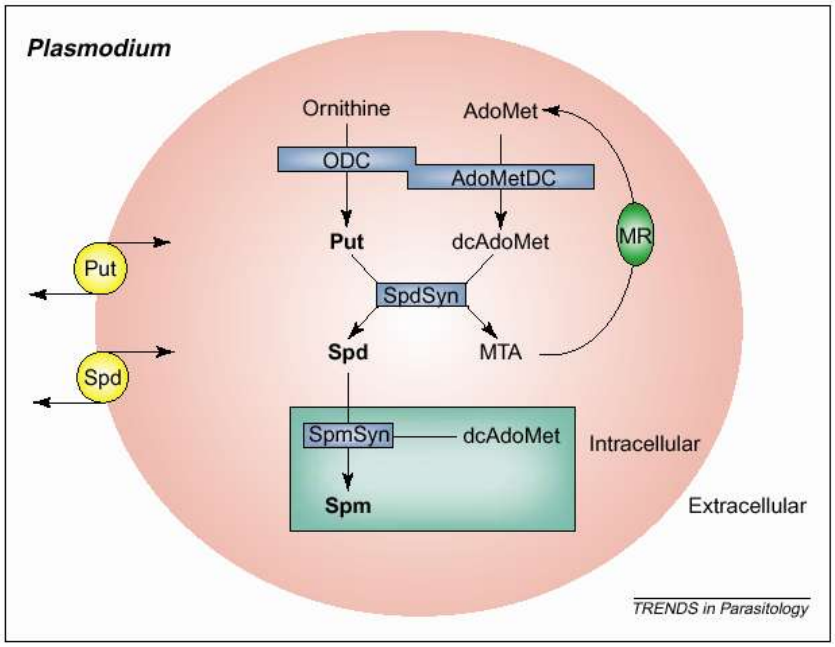

Figure 1.7: Polyamine metabolism in *Plasmodium*. Abbreviations: AdoMet: S-adenosylmethionine; AdoMetDC: S-adenosylmethionine decarboxylase; dcAdoMet: decarboxylated S-adenosylmethionine; MR: methionine recycling pathway; MTA: methylthioadenosine; ODC: ornithine decarbocylase; Put: putrescine; Spd: spermidine; SpdSyn: spermidine synthase; Spm: spermine; SpmSyn: spermine synthase (Müller, *et al*., 2001).

The bifunctional *Pf*AdoMetDC/ODC complex has a predicted molecular mass of ~330 kDa and is a heterotetrameric structure consisting of the two heterodimeric polypeptides (Figure 1.6). Monofunctional AdoMetDC exists as a heterotetramer and monofunctional ODC as a homodimer (Birkholtz, *et al.*, 2003; Müller, *et al.*, 2000). In previous studies it was shown that single mutations in the active site or inhibition of the activity of one domain decreased activity of that specific domain but the neighbouring domain activity was not affected (Wrenger, *et al.*, 2001). These results indicated that the two decarboxylase activities of the bifunctional *Pf*AdoMetDC/ODC function independently. However, deletions of parasite-specific regions outside the active site in one domain greatly influence both domain activities suggesting that the two domains interact and that these interactions are necessary for the stabilization of the active bifunctional *Pf*AdoMetDC/ODC protein (Birkholtz, *et al.*, 2004).

1.9 Parasite-specific inserts in *Pf*AdoMetDC/ODC

A further unique property of AdoMetDC/ODC in *Plasmodia* is the presence of parasite-specific inserts in both domains compared to other homologous proteins. These inserted regions are responsible for the much larger parasite proteins (Müller, *et al.*, 2000).

Various proteins in *Plasmodium* are characterized by parasite-specific inserts, which are species-specific, hydrophilic, rapidly diverging, and most probably form non-globular flexible domains protruding from the core of the proteins and not affecting the core fold (Pizzi and Frontali, 2001). In a small number of *P. falciparum* proteins analyzed, parasite-specific inserts were additionally also predicted to contain low-complexity areas (Figure 1.8) (Pizzi and Frontali, 2001). Another unmistakable feature of the low-complexity regions in *P. falciparum* is the abundance of Asn and Lys residues, which is not elevated in more complex regions (Pizzi and Frontali, 2001).

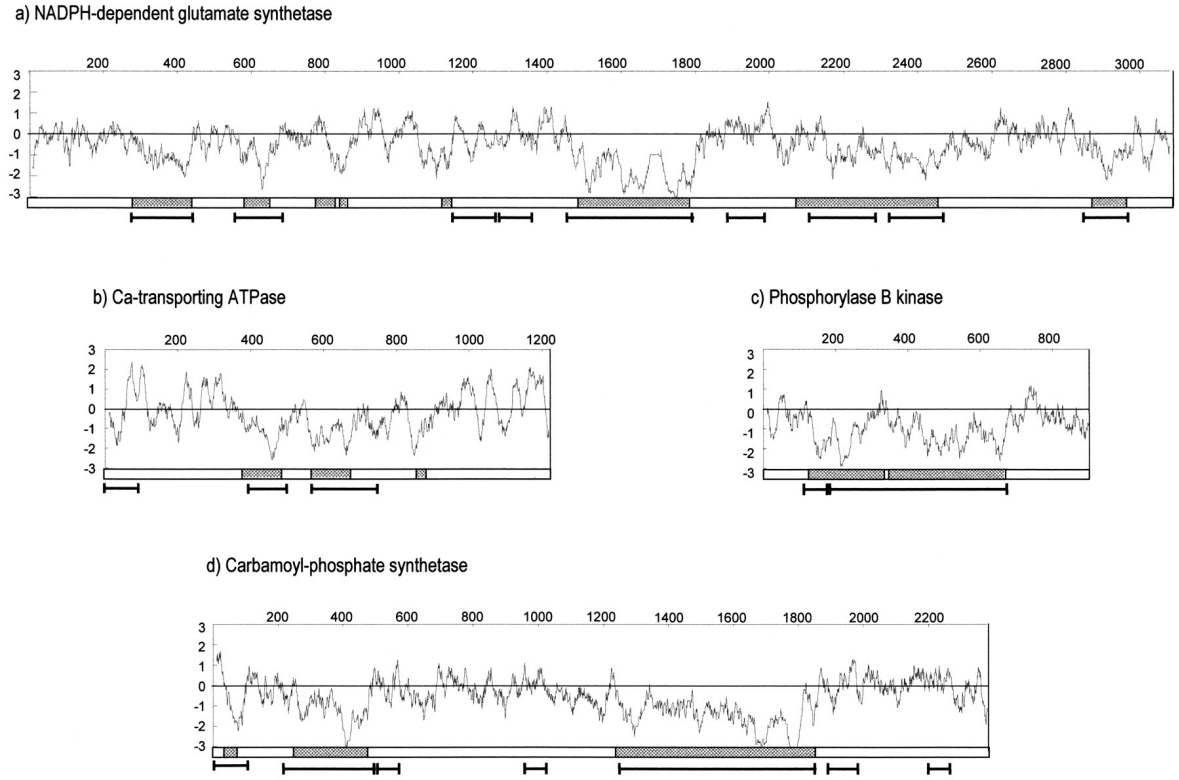

Figure 1.8: Hydrophobicity profiles, parasite-specific inserts and predicted low-complexity regions of various *P. falciparum* proteins. The parasite-specific inserts are indicated with the gray blocks, the predicted low-complexity regions are indicated with the underlying black bars (Pizzi and Frontali, 2001).

In the *P. falciparum* bifunctional AdoMetDC/ODC protein, six parasite-specific inserts are found. In the AdoMetDC domain the inserts consists of amino acids 57-63 (A_1), amino acids 110-137 (A_2) as well as residues 259-408 (A_3) (Wells, 2004). In the ODC domain the inserts include residues 1047-1085 (O_1) and 1156-1301 (O_2) (Birkholtz, *et al.*, 2003). The hinge region connecting these domains consists of residues 573-752 (H) (Müller, *et al.*, 2000) (Figure 1.9).

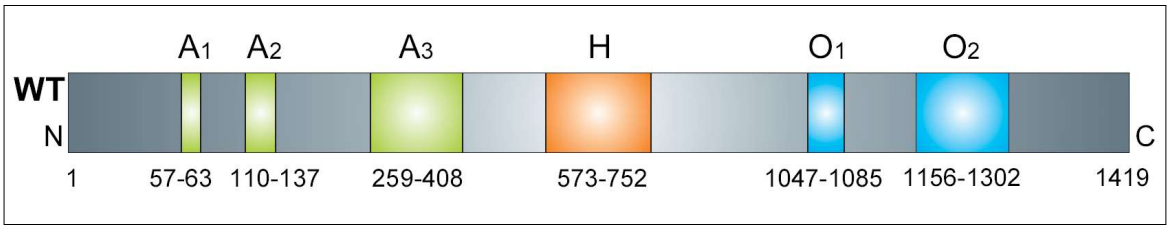

Figure 1.9: Parasite-specific inserts in the bifunctional protein. The figure shows the wild type *Pf*AdoMetDC/ODC with the indicated positions and residue numbers of the parasite-specific inserts (A_1, A_2, A_3, H, O_1, O_2) (Birkholtz, *et al*., 2004; Müller, *et al*., 2000; Wells, 2004). The N- and C-terminals are also indicated.

It seems that the large inserts of the different domains of the bifunctional enzyme are conserved between murine *Plasmodia* sequences (*P. berghei* and *P. yoelii*) but differ in sequence composition and length from *P. falciparum*. The parasite-specific inserts in *Pf*AdoMetDC/ODC are predominantly hydrophilic because of the abundance of the charged residues Asn, Asp, Lys, Ser, Glu as well as the hydrophobic residues Leu and Ile (Birkholtz *et al.*, 2004). Analysis of the *P. falciparum* genome indicated that ~1300 proteins contain areas exceptionally rich in Asn, these areas are known as prion-like domains, which are involved in amyloid structure formation (Singh, *et al.*, 2004). The *P. falciparum* proteome consists of ~36% homorepeat containing proteins compared to *H. sapiens* (~9%) and *P. yoelii* (~13%). The content of the *P. falciparum* homorepeats consists mainly of Asn (~60%) and Lys (~23%) residues (Singh, *et al.*, 2004).

The *Pf*AdoMetDC A_3 insert is ~100 residues longer than the murine protein A_3 inserts and has a bias towards Asn and Lys residues (Wells, 2004). The large *Pf*ODC insert (O_2) contain ~26 extra residues and contains $(Asn\text{-}Asn\text{-}Asp)_x$ sequence repeats in comparison to the O_2 inserts of the murine species. The hinge and O_2 regions are rich in Asn residues, with the hinge containing 15% and the O_2 insert 29% Asn residues. The A_3, hinge and the O_2 inserts contain areas of low-complexity, show considerable variation between the

Plasmodium species, are not very antigenic and it is predicted that the inserts are non-globular with a tendency to form unstructured loops (Birkholtz, *et al.*, 2003).

However, insert O_1 in the ODC domain is the exception because it does not contain low-complexity regions and is better conserved between the *Plasmodium* species both in terms of sequence composition and length. The 38 amino acid insert O_1, has a high abundance of Lys residues at 21% of its composition as well as areas with well defined secondary structures (Birkholtz, *et al.*, 2004). The above-mentioned features suggest that the O_1 region has a more defined function compared to other larger inserts.

Deletion of the inserts in their respective domains rendered the specific decarboxylase inactive and also reduced the activity of the neighbouring decarboxylase. This clearly indicates that the parasite-specific inserts mediate physical interactions between the two domains (Birkholtz, *et al.*, 2004). Deletion mutagenesis of the parasite-specific inserts in the separately expressed AdoMetDC and ODC monomers, yielded enzymes that did not have significant decarboxylase activity. This implies that these inserts have parasite-specific properties that are important for enzyme activity. The O_1 and hinge regions has also been shown to be important for the hybrid bifunctional complex formation (Birkholtz, *et al.*, 2004). However, finer delineation of the exact areas in these parasite-specific inserts that are important for activity and protein-protein interactions are needed.

The unique features of the *P. falciparum* AdoMetDC/ODC protein, including the bifunctional organization and parasite-specific inserts offers new possibilities for intervening with polyamine biosynthesis in these parasites. This could include strategies where one inhibitor can be used to inhibit both decarboxylase activities. In order for this to be achieved, a better understanding of the *Pf*AdoMetDC/ODC protein properties and interactions needs to be attained.

1.10 Research Aims

This study was aimed at further elucidating the functions of the parasite-specific inserts in both the ODC domain and the connecting hinge region of the bifunctional *Pf*AdoMetDC/ODC protein. Two distinct topics were studied in this regard.

- **Chapter 2: Mobility of the O_1 insert and its role in the function of the AdoMetDC and ODC domains.** In addition to the fact that the O_1 insert is conserved, structured and important in protein-proteins interactions, it is also flanked by Gly residues that contribute to its flexibility. The flexibility of the insert may be an important factor in the function of this insert.
- **Chapter 3: Secondary structures in the parasite-specific inserts of the *Pf*AdoMetDC/ODC protein.** The O_1 insert contains three predicted secondary structures, in addition it was found that the larger parasite-specific inserts (A_3, H and O_2) also contain areas of predicted secondary structures despite their low-complexity nature. This study focuses on the disruption of secondary structures in the ODC and Hinge parasite-specific inserts (O_1, O_2 and H) and their influence on the enzyme function of both domains.
- **Chapter 4: Concluding Discussion.** Provides a concluding discussion and future perspectives on the studies performed in this dissertation.

Chapter 2
Mobility of the O_1 insert and its role in the function of the AdoMetDC and ODC domains

2.1 Introduction

The dynamics of protein structures have become recognized as a key aspect of function. Protein segments called loops or lids are common in enzyme activity where it prevents reactive reaction intermediates from escaping the active site into the surrounding environment (Taylor and Markham, 2003). S-Adenosylmethionine synthetase (MAT) of *E. coli* is a tetramer with the active sites situated at the subunit interfaces, the protein also contains a polypeptide loop consisting of 18 amino acids that is positioned in such a way that it acts as a lid that gates access of substrate to the active site pocket. The loop has a disordered region of 5 amino acids and a conformational change is initiated upon ligand binding (Taylor and Markham, 2003). The same is observed in human salivary amylase, which possesses two loops that surround the active site. One of the loops is 7 amino acids in length, extremely flexible, rich in Gly residues and acts as a gateway for substrate binding and release of product (Ramasubbu, *et al.*, 2003). A number of other proteins contain flexible loops: *E. coli* undecaprenyl-pyrophosphate synthases contain a 12 amino acid loop that is important for catalysis and substrate binding (Ko, *et al.*, 2001); Metallo-β-lactamase from *Stenotrophomonas maltophilia* has a flexible loop of 13 amino acids, which extends over the active site of the enzyme and is important for clamping down the substrate and stabilizes the reaction intermediate (Garrity, *et al.*, 2004). The leupeptin binding site of calpain is flanked by two flexible loops of 13 and 10 amino acids, respectively. The loops fold onto and encapsulate leupeptin in the active site. The loops define the width of the active site and provides the amino acids necessary for specificity and selectivity of leupeptide binding (Moldoveanu, *et al.*, 2004). It is apparent that numerous proteins contain flexible loops, each with a specific function.

The O_1 loop is situated in the ODC domain of the bifunctional protein *Pf*AdoMetDC/ODC and it consists of 38 amino acids. The insert is conserved between *Plasmodia* species with a 50% sequence identity and similar length suggesting a highly specific functional role for the

O_1 insert (Birkholtz, *et al.*, 2004). O_1 differs from the other *Pf*AdoMetDC/ODC inserts in that it does not contain low complexity areas but instead one very short, conserved β-plate and one α-helix (more detail in Chapter 3, Figure 3.4). The loop is composed of 20.5% Lys residues (Birkholtz, *et al.*, 2004). As yet there is no firm conclusion as to the exact orientation of the loop in space but is proposed to have a surface localization and to protrude on the same side of the ODC monomer as the active site entry (Birkholtz, *et al.*, 2003).

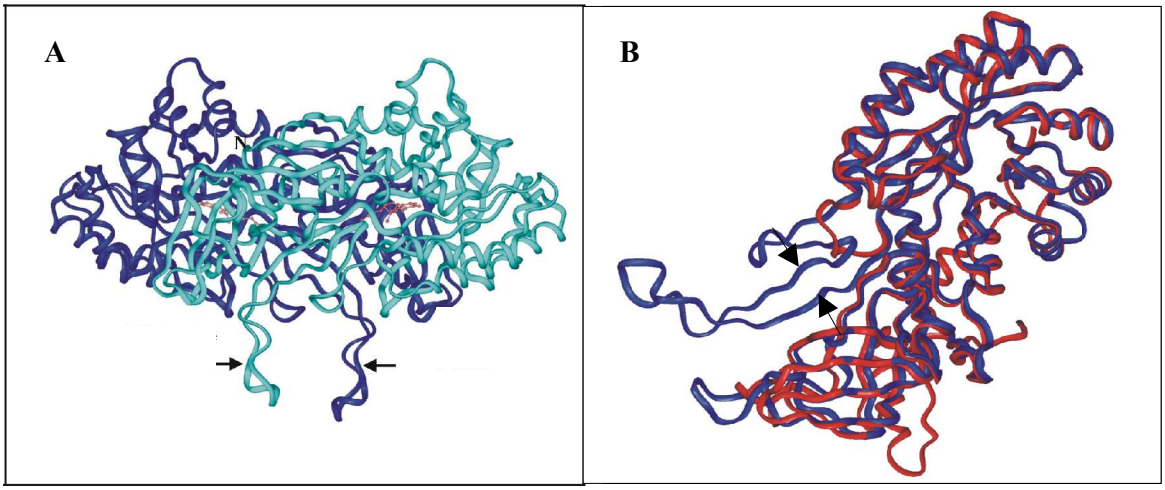

Figure 2.1: The ODC homology model indicating the location of insert O_1. A: The two ODC dimers are indicated with different colours. The O_1 loops of both subunits are indicated with the arrows. PLP (co-factor) and DFMO (competitive inhibitor) are indicated by the red ball-and-stick models and are located in the two active sites formed between the two monomers. B: The *Pf*ODC monomer (blue) and the human ODC monomer (red) superimposed. Arrows indicate the start and end of the O_1 insert (Birkholtz, *et al.*, 2003).

Deletion of O_1 in the bifunctional *Pf*AdoMetDC/ODC decreased the ODC activity with 94% and that of AdoMetDC with 77% (Birkholtz, *et al.*, 2004). Hybrid complex formation of the bifunctional enzyme is possible between the wild type *Pf*ODC and *Pf*AdoMetDC monofunctional domains. However, no physical interaction is observed between the AdoMetDC wild type monofunctional domain and the ODC domain containing the O_1 deletion (Birkholtz, *et al.*, 2004). The deletion of O_1 furthermore disrupts ODC subunit interaction/homodimerization possibly by altering the conformation of ODC at the dimer interface. Therefore ODC homodimer (~180 kDa) formation seems to be needed for the association with heterotetrameric AdoMetDC (~150 kDa) and these interactions are mediated by O_1 (Birkholtz, *et al.*, 2004).

The O_1 insert is flanked by Gly residues ($Gly_{1036-1038}$ and Gly_{1083}) that may function as hinges to allow flexibility and mobility of the loop. Gly has only a hydrogen atom as side chain and can adopt a wide range of phi (Φ) and psi (Ψ) angles that are normally sterically impossible to other amino acids (Bourne and Weissig, 2003; Brandon and Tooze, 1999). Gly therefore introduces flexibility into a protein because of the wide range of conformations it assumes.

This chapter focuses on the mobility of the O_1 loop and its involvement in either the dimerization of the ODC monomers and/or in the activity of *Pf*AdoMetDC/ODC. The participation of the flanking Gly residues in mediating this proposed flexibility/mobility of O_1 is investigated here.

2.2 Methods

2.2.1 Amplification and cloning of *Pf*AdoMetDC/ODC

Amplification and cloning of *Pf*AdoMetDC/ODC into an expression vector was essentially conducted by Müller, *et al* (2000). Briefly, the entire coding region of the AdoMetDC/ODC from *P. falciparum* 3D7 cells (PlasmoDB accession number: Pf10_0322) was amplified with the sense oligonucleotide, 5'-GCGCGCGGTCTCCAATGAACGGAATTTTTG-AAGG-3' and the antisense oligonucleotide, 5'-GCGCGCGGTCTCCGCGCTCCAA-TGTTTGTTTGGTTGCCCC-3' using *Pfu* DNA polymerase (Stratagene) and genomic DNA of *P. falciparum* as a template. The PCR product was digested with *Bsa*I (BioLabs) and cloned into a *Bsa*I cut pASK-IBA3 expression vector (Institut für Bioanalytik).

2.2.2 Plasmid isolation

Transformed cells were grown in 5 ml Luria-Bertani liquid medium (1% (w/v) tryptone, 0,5% (w/v) yeast extract, 1% (w/v) NaCl, pH 7), containing 50 µg/ml ampicillin (Roche, Switzerland), overnight at 30°C in a shaking incubator at 300 rpm. The cells were collected by centrifugation for 10 min at 3000 x g in a Microlitre Centrifuge Z252M (Hermle Labortechnik). The High Pure Plasmid Isolation kit from Roche was used for plasmid purification and the manufacturers protocol was followed throughout. The principle of the isolation technique is DNA binding to glass fibres in the presence of chaotropic salts after the conventional alkaline lysis of the cells. The pellet was suspended in 250 µl suspension buffer (50 mM Tris-HCl, 10 mM EDTA, pH 8) to which 250 µl lysis buffer (0.2 M NaOH, 1% (w/v) SDS) was added. The suspension was incubated at room temperature for 5 min whereafter 350 µl binding buffer (4 M guanidine hydrochloride, 0.5 M K-acetate, pH 4.2) was added. After 5 min incubation on ice and centrifugation at 13 000 x g for 10 min, the clear supernatant was transferred to a filter-tube and centrifuged for 1 min at 13 000 x g. The filter was washed consecutively with 500 µl and 200 µl wash buffer II (20 mM NaCl, 2 mM Tris-HCl, pH 7.5). The purified DNA was free of salts, proteins and other cellular impurities and was eluted in 50 µl of a low salt buffer (1 mM Tris-HCl, pH 8.5). The concentration was determined spectrophotometrically as described in section 2.2.4.

2.2.3 Agarose gel electrophoresis

Isolated plasmid and digested products were run on 1% (w/v) agarose (Promega) in TAE (40 mM Tris-acetate, 1 mM EDTA, pH 8.0) gel at 7.8 V/cm in a Minnie Submarine HE33 Agarose Gel unit (Hoeffer Scientific systems). A final concentration of 1.25 ng/ml ethidium bromide (EtBr) was incorporated in the agarose gel and the DNA was visualized at a wavelength of 312 nm on a Spectroline TC-312A UV transilluminator (Spectronics Corporation). Gel images were captured digitally with a 4.0 mega pixel Canon Powershot G2 camera using the G2Remote version 1.2 software (Breeze Systems, Ltd.).

2.2.4 Nucleic acid quantification

The concentrations of the plasmids were determined on a GeneQuant*pro* spectrophotometer (Amersham Biosciences). The yield for double stranded DNA (plasmid) (where one absorbance unit = 50 µg/ml) was estimated from the absorbance at 260 nm. The purity of the DNA was determined by the $A_{260/280}$ ratio between the absorbance at 260 nm and 280 nm. Pure double stranded DNA should have a ratio of 1.7 – 1.9 (Sambrook, *et al.*, 1989).

2.2.5 Primer design

The mutagenesis primers were designed following the suggestions in the QuikChange Site-Directed Mutagenesis Kit (Stratagene): The primers were between 49 and 58 nucleotides in length (Inqaba Biotechnical Industries); the sites of mutation were situated near the middle of the primer; the primers anneal to the same sequence on opposite strands of the plasmid and the primers were terminated with either a G or C nucleotide at the 3' end. The designed oligonucleotides were analyzed with the Oligo 4 Primer Analysis Software program (Molecular Biology Insights, MBI) for internal stability, secondary structure formation and possible self-annealing. Primers used are indicated in Table 2.1. Two sets of primers were designed; the ODC-G1 set of primers was used to incorporate three Ala at the $Gly_{1036\text{-}1038}$ positions and the ODC-G2 set was used to incorporate an Ala at the Gly_{1083} position. The Tm was calculated with the following formula:

$$\mathbf{Tm = 81.5 + 0.41(\%T + \%C) + 16.6 \times \log[Na^{+}] - 500/length}$$

2.2.6 PCR mutagenesis

The QuikChange Site-Directed Mutagenesis Kit (Stratagene) was used for the conversion of the O_1 flanking Gly residues to Ala. This rapid procedure generates mutants with greater than 80% efficiency. The basic procedure utilizes a supercoiled double-stranded DNA vector containing a coding region of interest and a forward and reverse oligonucleotide, both containing the desired mutation. The oligonucleotides, each complementary to opposite strands of the vector, are extended during temperature cycling by *Pfu* polymerase, without oligonucleotide displacement thereby generating a mutated plasmid. The wild type plasmid containing the *Pf*AdoMetDC/ODC sequence was used as a template for the ODC-G1 primers, the resulting mutated plasmid was then used as a template for the ODC-G2 primers to produce the double mutant. The PCR reactions contained 50 ng of wild type plasmid, 125 ng of both the forward and the reverse primer, 2 mM each of dNTP's and 6 U *Pfu* DNA polymerase (Fermentas). *Pfu* DNA polymerase from *Pyrococcus furiosis* has a 3'-5' proofreading exonuclease activity and replicates both plasmid strands with high fidelity and without displacing the mutant oligonucleotide primers. The enzyme was added to a 50 µl reaction at 80°C using a Hot Start protocol after the initial denaturing step of 94°C for 30 sec. After another denaturation step at 94°C, 18 cycles were conducted of denaturation at 94°C for 30 sec, primer annealing at 60°C for 1 min and primer extension at 68°C for 12 min.

2.2.7 Isolation of the mutated plasmid

After PCR mutagenesis, the PCR products were treated with *DpnI* (New England Biolabs). The *DpnI* endonuclease (target sequence 5'-Gm^{6}ATC-3') is specific for methylated and hemimethylated DNA and is used to digest the parental DNA template and to select for mutation-containing synthesized DNA. DNA isolated from almost all *E. coli* strains is *dam* methylated and therefore susceptible to *DpnI* digestion.

To the 50 µl PCR product, 1 µl (20 U) *DpnI* was added and the reaction was performed at 37°C for 3 hours. After *Dpn*I digestion, the volume was adjusted to 100 µl with double distilled, deionised H_2O (dddH_2O). The digested parental DNA templates were removed using the standard protocols described in the High Pure PCR Product Purification Kit (Roche). (The kit relies on the same principle as the High Pure Plasmid Isolation Kit

mentioned in section 2.2.2). 500 µl binding buffer (3 M guaninidine-thiocyanante, 10 mM Tris-HCl, 5% ethanol (v/v), pH 6.6) was added to the 100 µl digestion product. The liquid was transferred to a filter-tube and centrifuged for 1 min at 13 000 x g and 22°C. The eluate was discarded and 500 µl wash buffer (80% ethanol, 20 mM NaCl, 2 mM Tris-HCl, pH 7.5) was added followed by centrifugation as above. The wash step was repeated with 200 µl wash buffer. The pure plasmid DNA was eluted from the filter with 50 µl elution buffer (10 mM Tris-HCl, pH 8.5) and the pure mutated DNA was stored at –20 °C until further use.

2.2.8 Transformation

Electroporation was the chosen method used for transformation.

2.2.8.1 Preparation of electrocompetent cells for transformation

Electrocompetent cells were prepared by the method described in Sambrook (1989). A single colony of *E. coli* DH5α cells (Gibco BRL, Life Technologies) was inoculated in 15 ml LB liquid medium and was grown overnight at 37°C with shaking at 300 rpm. From the overnight culture, 10 ml was inoculated into 2 x 500 ml LB broth and grown at 37°C with shaking until an OD_{600} of ~0.5 – 0.6. The culture was incubated on ice in pre-chilled 250 ml centrifuge bottles for a further 20 min. All subsequent steps were carried out on ice. The cells were pelleted at 5 000 x g in a Beckman Avanti J-25 centrifuge with a fixed angle rotor for 10 min at 4°C whereafter the supernatant was discarded. The pellets were kept on ice and were resuspended in ice-cold $dddH_2O$. The pellets were washed and then gently resuspended in 240 ml ice-cold $dddH_2O$. The suspension was centrifuged at 5 000 x g for 10 min at 4°C. The supernatant was poured off immediately and the pellets were resuspended by swirling in the remaining liquid. This wash step was repeated twice. The supernatant was then discarded and the pellets were resuspended in 10 ml cold 10% glycerol in water followed by incubation on ice for 30 min. The cells were pelleted at 5 000 x g for 10 min at 4°C. The supernatant was poured off and each pellet was resuspended in 800 µl 10% glycerol. The cells were aliquoted in sterile micro-centrifuge tubes and were frozen at -70°C.

2.2.8.2 Transformation of electrocompetent cells

The pure, mutated DNA (obtained with HP PCR purification) stored at -20°C was used for transformation into electrocompetent expression cells. The DNA was concentrated by means of precipitation. To the 50 µl DNA eluate 10% (v/v) tRNA (10µg/ml), 10% (v/v) Na-acetate (3M, pH 5) and 3 volumes cold 100% ethanol was added. The suspension was incubated at -70°C for 1 hour and centrifuged at 13 000 x g for 20 min. The pellet was washed with 100 µl 70% ethanol and centrifuged for 10 min at 13 000 x g followed by drying *in vacuo*. The pellets were dissolved in 5 µl dddH_2O.

The competent cells were thawed on ice and 90 µl cells and 5 µl DNA were gently mixed in a chilled microcentrifuge tube. The DNA-cell mixture was transferred to a chilled electroporation cuvette. The cells were pulsed with 2000 V at a field strength of 20 kV/cm for 5 msec in a Multiporator system (Eppendorf). After pulsing of the cells, the suspension was transferred to 900 µl of pre-warmed (30°C) sterile LB liquid medium with 20 mM added glucose. The cell suspension was incubated at 30°C for 1 hour with moderate shaking to allow cell recovery after exposure to the high voltage. 50 µl of the transformation culture was plated out onto solid LB-Agar plates (1% (w/v) agar, 1% (w/v) tryptone, 0,5% (w/v) yeast extract, 1% (w/v) NaCl, pH 7) containing 0.1 mg/ml ampicillin and the plates were incubated overnight at 37°C. 50 ng/µl pBluescript (Stratagene) was transformed as a positive control.

2.2.9 Plasmid isolation and confirmation of mutations

2.2.9.1 STET-prep screening

The method used is a variation of the STET (Sucrose, TritonX-100, EDTA, Tris) -prep method described in Sambrook (1989). Single colonies from the plates were incubated in 5 ml liquid LB medium containing 50 µg/ml ampicillin and grown overnight at 30°C with agitation. From the liquid overnight culture, 1.5 ml was centrifuged for 10 min at 13 000 x g in a Microlitre Centrifuge Z252M (Hermle Labortechnik) at 22°C. The supernatant was partially discarded and the pellet was resuspended in the remaining supernatant. To the cell suspension, 300 µl STET buffer (8% (w/v) sucrose, 5% (v/v) Triton X100, 50 mM EDTA, 50 mM Tris pH 8) was added together with 25 µl of a 4 mg/ml lysozyme stock solution. The

mixture was then incubated in boiling water for 1 min and was centrifuged for 15 min at 13 000 x g. The pellet was discarded and the plasmid DNA was precipitated with 300 µl isopropanol (NT Laboratory Supplies) followed by centrifugation for 15 min at 13 000 x g and 22°C. The supernatant was removed and the pellets were dried on the bench by evaporation of the remaining liquid. The DNA pellets were resuspended in 25 µl TE (10 mM Tris, 1 mM EDTA pH 7.5) with a final concentration of 0.5 mg/ml RNAse (Roche).

2.2.9.2 Restriction enzyme mapping

The correctness and size of the insert in the STET-prep-isolated recombinant plasmids was verified by means of restriction enzyme digestion. *Hind*III (Promega) was used for confirmation of the plasmid size. The G1 mutation removed an *EcoR*V (Promega) restriction site and its presence could therefore be verified by restriction digestion. The restriction reaction was set up in a total volume of 10 µl that contained 100 to 300 ng of plasmid together with 10 U of the required restriction enzyme and 1x of the enzyme specific buffer. The reaction was incubated at 37°C for 3 hours or overnight. The digestion products were analysed by electrophoresis as discussed in section 2.2.3.

The clones with the correct restriction digestion profile were purified from cell culture using the High Pure Plasmid Purification Kit from Roche as described in section 2.2.2. The purified plasmids were sequenced in order to verify the new mutations.

2.2.10 Automated nucleotide sequencing

The primer used for sequencing, ODCseq1, is sequence-specific and was designed to be 172 nucleotides upstream from the G1 mutation site. The nucleotide sequence for the primer is as follows:

ODC seq1: 5' TATGGAGCTAATGAATATGAATG 3'

The sequence reaction contained 200 – 500 ng plasmid DNA, 5 pmol of the sequence specific primer, 3 µl 5 x sequencing buffer and 2 µl Terminator Big-Dye Ready reaction mix version 3 (Perkin Elmer) in a final volume of 20 µl. The reaction was made up to a final volume of 20 µl with dddH_2O. The sequencing cycles were performed in a GeneAmp 9700 thermocycler (Perkin Elmer) with an initial step at 96°C for 1 min followed by 25 cycles of

denaturation at 96°C for 10 sec, annealing at 50°C for 5 sec and extension at 60°C for 4 min. The labeled extension product was purified by either size exclusion filtration or ethanol precipitation. For size-exclusion, a column was prepared in a micro-filtration tube by the addition of 600 µl G50 superfine Sephadex (Pharmacia) swollen overnight in dddH_2O (66.7 mg/ml), followed by a 2 min centrifugation step at 750 x g. The PCR product was loaded onto the column and was eluated with centrifugation for 2 min at 750 x g into a sterile microcentrifuge tube. The eluated product was dried *in vacuo* and stored at –20°C in the dark until sequencing. For precipitation cleanup, 2 µl NaOAc (pH 5.2) and 60 µl ice-cold absolute ethanol was added to the 20 µl PCR product. The reaction was incubated on ice for 10 min and centrifuged at 13 000 x g and 4°C for 30 min. The pellet was washed twice with 50 µl 70% ethanol and centrifugation for 10 min at 13 000 x g at 4 °C. The pellet was dried *in vacuo* and stored at -20°C in the dark.

Sequencing was performed on an ABI PRISM 3100 capillary sequencer (Perkin Elmer). The sequences obtained were analyzed with the BioEdit version 5.0.6 software program (Hall 2001, North Carolina State University, Department of Microbiology, USA).

The correct mutated plasmid was subsequently used for protein expression in an expression cell-line.

2.2.11 Recombinant protein expression

The pASK-IBA3 vectors containing the *Pf*AdoMetDC/ODC wild type sequence and the various mutated sequences were transformed into AdoMetDC and ODC defficient EWH331 *E.coli* expression cells (kindly provided by Dr.H.Tabor (Hafner, *et al.*, 1979)) with the electroporation method described in section 2.2.8. The transformed cells were plated onto LB-Agar plates and incubated at 37°C overnight. For each of the transformants a single colony was incubated in 10 ml LB liquid medium containing 50 µg/ml ampicillin overnight at 30°C with moderate shaking. The culture was diluted to a 1:100 ratio in 500 ml liquid LB (with 50 µg/ml ampicillin) and was incubated at 37°C in a shaking incubator until the OD_{600} reached 0.5. Expression of the pASK-IBA vectors is under tight control of *tet*-promoter/operator. Protein expression was therefore induced with the addition of 200 ng/ml anhydrotetracycline (AHT) and cells were incubated at 22°C for an additional 16 hours. The

recombinant proteins were expressed as *Strep*-tag (NH_2-Trp-Ser-His-Pro-Gln-Phe-Glu-Lys-COOH) fusion proteins, with the tag situated at the C-terminal of the protein. The short *Strep*-tag does not interfere with the folding or activity of the recombinant proteins according to the manufacturers (Institut für Bioanalytik).

2.2.12 Isolation of the *Strep*-tag fusion proteins

The cells were harvested by centrifugation for 30 min at 4°C and 15 500 x g in a Beckman Avanti J-25 centrifuge with a fixed angle rotor (Beckman). The supernatant was removed and the cell pellet was resuspended in 10 ml cold Buffer W (150 mM NaCl, 1mM EDTA, 100 mM Tris, pH 8). All subsequent steps were performed on ice. A final concentration of 0.1 mg/ml lysozyme was added to the cell suspension together with 100 µg/ml phenylmethylsulfonyl fluoride (PMSF, Roche), 1 µg/ml aprotinin (Roche) and 2.5 µg/ml leupeptin (Roche) to inhibit protease activity together with 0.02% Brij-35 (Fluka), a non-ionic detergent. The suspension was incubated on ice for 30 min. The cells were sonified by pulsing for 10 cycles at an output control of 2/90 for a 30 sec cycle with a Sonifier Cell Disruptor B-30 (Instrulab) with a microtip. The tubes were balanced to the second decimal and centrifuged for 2 hours at 28 000 x g and 4°C. The supernatant was filtered through a 0.45 µm syringe filter before affinity chromatography.

Affinity chromatrography was performed at 4°C. The total protein extract obtained in the centrifugation step was subjected to a *Strep*-Tactin affinity column (Institut für Bioanalytik); *Strep*-Tactin is streptavidin that is engineered to have higher affinity for the *Strep*-tag. The protein containing supernatant was run through the affinity column (with a $1cm^3$ bed volume) three times. The column was washed two times with Buffer W (150 mM NaCl, 1mM EDTA, 100 mM Tris, pH 8) and the protein was eluated with 5 ml Buffer E (150 mM NaCl, 1mM EDTA, 2.5 mM desthiobiotin, 100 mM Tris, pH 8). The eluate was run through the column three times. Desthiobiotin is a reversibly binding specific competitor of the *Strep*-tag. The column was regenerated with Buffer R (150 mM NaCl, 1mM EDTA, 1mM 4-hydroxy azobenzene-2-carboxylic acid (HABA, Sigma), 100 mM Tris, pH 8). HABA displaces the desthiobiotin on the streptavidin column.

To each of the 5 ml eluted protein solutions, a final concentration of 100 µg/ml PMSF, 0.02% Brij 35, 1 µg/ml aprotinin and 2.5 µg/ml leupeptin was added. The protein eluate was dialyzed overnight in Snakeskin Pleated Dialysis Tubing (with a 10 000 Da molecular weight cut-off, Pierce) against cold buffer A (1 mM EDTA, 1 mM dithiothreitol (DTT), 0.1 mM PMSF, 0.02% Brij, 50 mM Tris, pH 7.5) at 4°C with continual stirring.

2.2.13 Protein Quantitation

The protein concentration was determined by the Bradford method (Bradford, 1976) where a shift in absorbancy of the dye occurs from A_{465} to A_{595} due to electrostatic binding of the basic and aromatic amino acid residues to the dye. Bovine serum albumin (BSA) was used to set up the standard range. A 10 mg/ml BSA stock solution was used to make dilutions of 5, 10, 12.5, 25, 35 and 50 µg/ml. 100 µl of the protein solutions were added to a 96 well microtitre plate in a 1:1 ratio with the Coomassie Protein Assay Kit (Pierce). The absorbancy was measured at 595nm with a Multiskan Ascent scanner (Thermo Labsystems).

2.2.14 SDS-PAGE analysis

Denaturing SDS Polyacrylamide gel electrophoresis (PAGE) was performed on an acrylamide gel consisting of a 5% stacking gel (5% acrylamide, 0.14% N,N'-methylenebisacrylamide, 0.125 mM Tris-HCl (pH 6.8), 0.1% w/v SDS, 0.1% v/v TEMED, 0.1% w/v ammonium persulfate) and a 12% acryl-bisacrylamide separating gel containing 0.5 mM Tris-HCl (pH 8.8), 0.1% w/v SDS, 0.2% v/v TEMED and 0.1% w/v ammonium persulfate. The samples were diluted 1:1 in a 2x SDS sample buffer (0.125 M Tris-HCl (pH 6,8), 2% w/v SDS, 30% v/v glycerol, 5% v/v β-mercaptoethanol and 1% w/v bromophenol blue) and boiled for 5 min. Electrophoresis was performed with a 25 mM Tris, 0.2 M glycine buffer (pH 8.3) in a Hoefer SE 600 Ruby gel electrophoresis unit (Amersham Pharmacia Biotech) with an EPS 601 electrophoresis power supply unit (Amersham Pharmacia Biotech).

Silver staining was used to visualize the low protein concentrations on the gels. The gels were fixed overnight in a 30% ethanol, 10% acetic acid solution followed by a 30 min sensitization step with 30% ethanol, 0.5 M sodium acetate, 0.5% v/v glutaraldehyde and

0.2% $Na_2S_2O_3$. The gels were washed three times with $dddH_2O$ for 10 min before silver impregnation for 30 minutes with 0.1% $AgNO_3$ and 0.25% formaldehyde. The gels were washed two times briefly with ddH_2O and were subsequently developed with 3.5% Na_2CO_3 and 0.01% formaldehyde. The reaction was stopped with the addition of 0.05 M EDTA (Merril, *et al.*, 1981). The Protein Molecular Weight Marker from Fermentas (Catalogue number: SM0431) was used for size comparison of the bands.

2.2.15 Activity assays of AdoMetDC and ODC

AdoMetDC and ODC activity were measured by trapping the release of $^{14}CO_2$ from S-adenosyl-[methyl-^{14}C]methionine (60.7 mCi/mmol, Amersham) and L-[1-^{14}C]ornithine (55 mCi/mmol, Amersham) as described (Krause, *et al.*, 2000; Müller, *et al.*, 2001; Birkholtz, *et al.*, 2004). Briefly, the AdoMetDC reaction contained 12.5 mM KH_2PO_4, pH 7.5, 250 µM DTT, 250 µM EDTA, 24 nM AdoMet and 325 nCi [^{14}C]AdoMet. The ODC reaction mixture was set-up with 10 mM Tris-HCl, pH 7.5, 250 µM DTT, 250 µM EDTA, 10 nM PLP, 24.5 nM ornithine and 55 nCi [^{14}C]ornithine. Both reactions were made-up to 100 µl with $dddH_2O$. The reactions were started in a 50 ml glass tube with the addition of between 1.5 µg and 4.5 µg protein. The tubes were sealed with rubber stoppers and the reactions were incubated at 37°C for 30 min in a shaking incubator. The released $^{14}CO_2$ was captured on filter paper treated with hydroxide of hyamine (Packard), which was incubated with the reaction in the glass tube and separated from the reaction by means of an open-ended inner tube. The reaction was stopped with 500 µl of 20% trichloro-acetic acid and 50 mM $NaHCO_3$ was added to the reaction to neutralize $^{14}CO_2$ that was not absorbed by the filter paper. The filter paper was transferred to a Pony-Vial H/I (Packard) and 4 ml Ultima Gold XR scintillation fluid (Packard) was added. The radioactivity was counted with a Minaxiβ Tri-Carb 4000 series liquid scintillation counter (Packard, United Technologies) for 15 min. The results obtained are the mean of 3 independent experiments performed in duplicate and are expressed as specific activity (nmol/min/mg). The specific activity is calculated with the following formula:

$$\frac{\text{CPM x nmol substrate}}{\text{[Mg protein] x minutes x total CPM}}$$

2.2.16 Statistical analysis

The significance of the results were calculated with a two-tailed t-Test assuming unequal variances. Results with p values smaller than 0.05 were accepted to be significant.

2.2.17 Molecular dynamics

The *Pf*ODC homology model was build based on the crystal structure of the *T. brucei* enzyme (Grishin, *et al.*, 1999; Birkholtz, *et al.*, 2003). The ODC homology model was used in molecular dynamic studies performed in consultation with G.A. Wells of the Bioinformatics and Computational Biology Unit of the Biochemistry Department at the University of Pretoria. The Gly$_{1036\text{-}1038}$Ala mutant *Pf*ODC model and the double Gly$_{1036\text{-}1038}$Ala and Gly$_{1083}$Ala mutant *Pf*ODC model were made in PyMOL (DeLano Scientific). In Charmm vs. 29b2 (Brooks, *et al*., 1989), the following steps were done: hydrogens were added to all available atoms of the various protein models at physiological pH, the proteins were then minimized for 50 steps with steepest descents with a distant dependent dielectric and a nonbond cutoff of 12 Å. The proteins were then minimized with conjugate gradients, a distant dependent dielectric and a nonbond cutoff of 12 Å. Moleculard dynamics were performed for 1000 000 steps with 1 fsec per step. The initial temperature was 48K and was heated to 298K with 10K increments every 500 steps. The data obtained was visualized in RasMol version 2.5.1 (Sayle 1996, University of Edinburgh, Biocomputing Research Unit, UK).

2.3 Results

Figure 2.2 summarizes the mutation sites of the O_1 insert with the positions of the Gly residues mutated to Ala. The three Gly residues on the N-terminal side of the insert are conserved between *Plasmodia* species (Birkholtz, *et al.*, 2004).

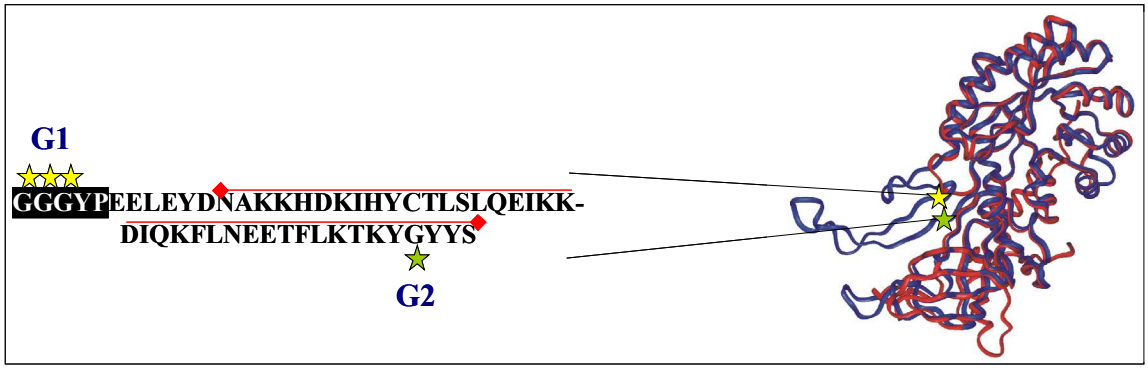

Figure 2.2: The sites of the mutated Gly residues in perspective to the O_1 insert and its sequence. The yellow stars on the ODC monomer homology model indicate the three conserved Gly residues that were mutated, termed the G1-mutant. The green star indicates the single Gly residue at the other end of the O_1 insert mutated to produce the double mutant (G1G2). The red bar on top of the sequence indicates the residues of the O_1 insert. The two superimposed homology models are the human (red, without O_1 insert) and the *P. falciparum* (blue, with the O_1 insert) ODC monomers (homology model figure from Birkholtz, *et al*, 2003).

2.3.1 Primers used for site-directed mutagenesis

According to the site-directed mutagenesis protocol of Stratagene, the oligonucleotides used must have a GC content of 40%. This was impossible to reach because of the high AT-richness of the *Plasmodia* genome. The primers were a bit longer than proposed in the protocol in order to terminate in a G or C to allow the 3' end to bind with a high binding-energy (Table 2.1). The G1 oligonucleotides were used to change the $Gly_{1036\text{-}1038}$ residues to Ala and produced the mutant protein A/OpG1; the G2 oligonucleotides were used on the A/OpG1 recombinant plasmid to incorporate an Ala at the Gly_{1083} site, which resulted in the double mutant (A/OpG1G2).

Table 2.1: The oligonucleotides used for site directed mutagenesis of Gly-residues in the parasite-specific region O1

Primer	Sequence	Properties
ODC-G1 FORWARD	5'GGA TTT AAT TTT TAT ATA ATA AAT TTA **GCA GCA GCA** TAT CCA GGA GGA TTA G3'	Tm = 67 °C 52 bases
ODC-G1 REVERSE	5'CTA ATT CTT CTG GAT A**TG CTG CTG C**TA AAT TTA TTA TAT AAA AAT TAA ATC C3'	
ODC-G2 FORWARD	5'CAT TTC TCA AGA CGA AAT AT**G CA**T ACT ATA GTT TTG AAA AAA TAA CAT TGG3'	Tm = 68 °C 51 bases
ODC-G2 REVERSE	5'CCA ATG TTA TTT TTT CAA AAC TAT AGT A**TG C**AT ATT TCG TCT TGA GAA ATG3'	

The mutation sites are indicated in red.

2.3.2 Restriction digestion of plasmids with the ODC mutations

Mutated A/OpG1 and A/OpG1G2 plasmids were transformed (section 2.2.8) with subsequent screening for the correct recombinant plasmids. Screening was done by isolation of the plasmid with the STET-prep method (section 2.2.9.1) followed by restriction digestion mapping for identification of the correct size mutant plasmids. The recombinant plasmids were digested with *Hind*III, ran on a 1% agarose gel and compared to the sizes of the wild type plasmid. The *Hind*III restriction map of the pASK-IBA3 vector containing the *Pf*AdoMetDC/ODC sequence is illustrated in Figure 2.3.

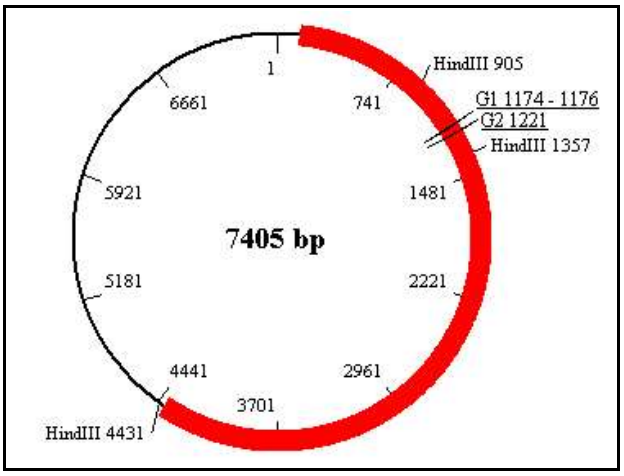

Figure 2.3: The *Hind*III restriction map of the pASK-IBA3 vector containing the *Pf*AdoMetDC/ ODC insert. The insert is illustrated as the red bar, the *Hind*III restriction positions and the G1 and G2 mutation sites are illustrated together with the respective nucleotide sequence positions.

*Hind*III is expected to digest the mutated A/OpG1 and A/OpG1G2 plasmids at 3 sites, two sites are situated in the *Pf*AdoMetDC/ODC coding region and one is situated in the pASK-IBA3 vector (three bands of approximately 3800, 3000 and 450 base pairs). Analysis of the products with electrophoresis proved that the correct plasmids were obtained (Figure 2.4).

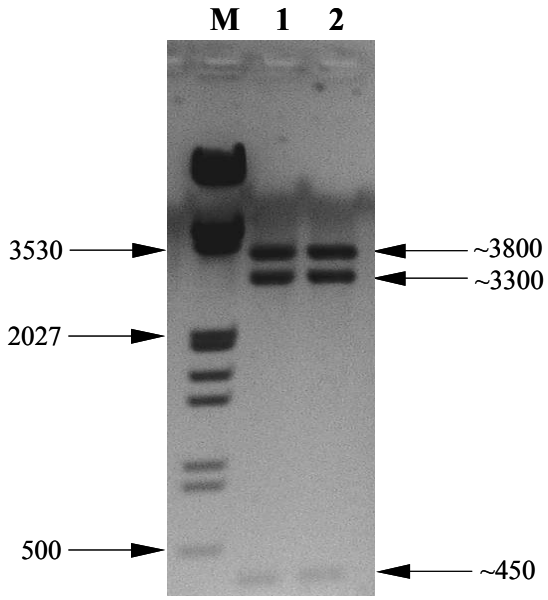

Figure 2.4: *Hind*III restriction digestion of mutant plasmids to screen for correct plasmid size. 1% Agarose electrophoresis of the A/OpG1 (1) and the A/OpG1G2 (2) recombinant plasmids. M: *EcoR*I-*Hind*III digested λ-phage DNA used as a high molecular mass marker. The sizes of the bands are given as base pairs.

The A/OpG1 mutation furthermore altered the *EcoR*V restriction site at position 3254 of the pASK-IBA3-*Pf*AdoMetDC/ODC plasmid. Figure 2.5 shows the restriction sites and sequence positions of *EcoR*V as well as the site altered with the G1 mutation.

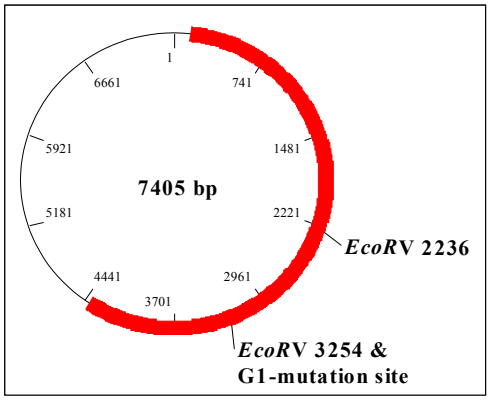

Figure 2.5: The *EcoR*V restriction map of the pASK-IBA3 vector containing the *Pf*AdoMetDC/ODC insert. The insert is illustrated as the red bar, the *EcoR*V restriction positions and the respective nucleotide sequence positions are indicated for the wild type plasmid. The G1 mutation removes the *EcoR*V 3254 restriction site as indicated.

After digestion of the various A/OpG1 mutated plasmids, the products were visualized on a 1% agarose gel and the band sizes were compared to that of a standard marker (Figure 2.6).

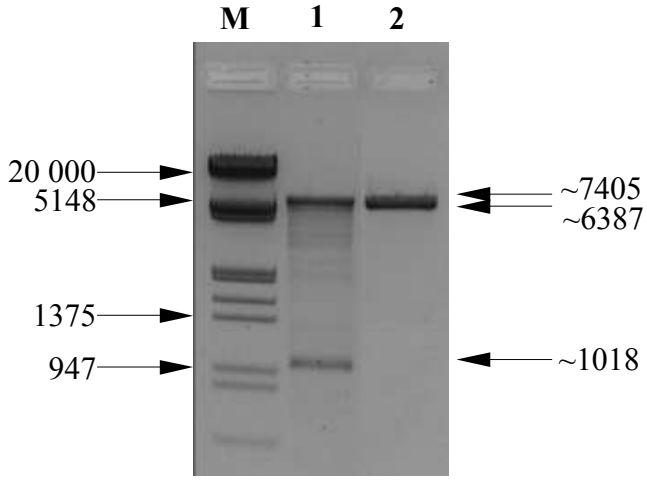

Figure 2.6: *EcoR*V restriction digestion of mutant plasmids to screen for G1 mutation. 1% agarose electrophoresis of the wild type (1) and A/OpG1 (2) recombinant plasmid. M: *EcoR*I-*Hind*III digested λ-phage DNA used as a high molecular mass marker. The sizes of the bands are given as base pairs.

Figure 2.6 shows the single linear band of A/OpG1 (lane 2) compared to that of the wild type plasmid (lane 1), which generated two bands of ~6387 and ~1018 respectively. Due to the gel resolution, a size difference between the ~7405 and ~6387 bands were not expected. A single linear band was obtained as expected. From the results obtained in Figure 2.6, it was clear that the G1 mutation was present. This was subsequently used as template for the G2 mutation. However, this mutant plasmid could not be screened for with *EcoR*V. Therefore, both the A/OpG1 and A/OpG1G2 plasmids were sequenced in order to verify the mutations.

2.3.3 SDS-PAGE

The wild type, A/OpG1 and A/OpG1G2 plasmids were transformed into electrocompetent *E. coli* EWH 331 expression cells (section 2.2.8). Protein expression was induced with AHT and the recombinant proteins were isolated by means of cell disruption, centrifugation and *Strep*-tag affinity chromatography (sections 2.2.11 and 2.2.12). Only a very small amount of protein could be expressed in *E. coli* ranging from 10 to 30 µg/ml. The total amount of protein obtained from 1L culture ranged between 50 to 150 µg. The various point mutations did not influence the expression levels of the recombinant proteins as it was comparable to the expressed concentrations of the wild type bifunctional protein (Table 2.2).

Table 2.2: Expression levels of the A/OpG1 and A/OpG1G2 recombinant proteins.

Protein	Expressed concentrations*	Standard Deviation
WT	25 µg/ml	± 10.2 µg/ml
A/OpG1	29.4 µg/ml	± 11.4 µg/ml
A/OpG1G2	20.3 µg/ml	± 1.8 µg/ml

* Values are the mean of three independant experiments.

The correct size protein bands were obtained after recombinant protein expression of the wild type *Pf*AdoMetDC/ODC as well as both the A/OpG1 and A/OpG1G2 proteins. The amount of recombinant protein loaded onto the SDS polyacrylamide gel ranged between 1.5 and 4.5 µg per lane. The recombinant proteins were visualized as ~160 kDa bands corresponding to the single bifunctional protein polypeptide (Figure 2.7).

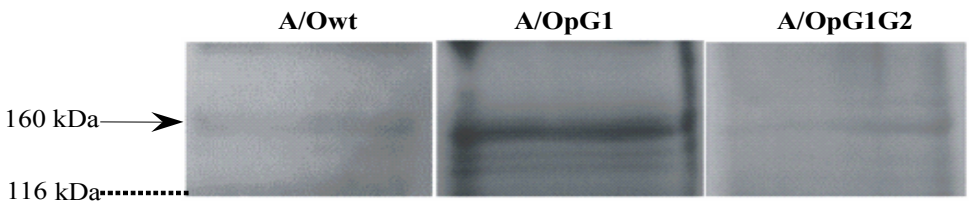

Figure 2.7: SDS-PAGE of the expressed WT and the two recombinant proteins (A/OpG1 and A/OpG1G2). The denatured protein is observed as a ~160 kDa single polypeptide. The position of the molecular weight marker is indicated with the dotted line.

2.3.4 Activity assays

The expressed and isolated recombinant proteins were subjected to activity assays where ^{14}C-labelled substrate was utilized to release $^{14}CO_2$, which was captured and counted (section 2.2.15). Three independent experiments were performed in duplicate; the results obtained were normalized against the specific activity (nmol/min/mg protein) of the wild type protein performed in parallel.

Figure 2.8 represents the normalized activities of AdoMetDC in the respective A/OpG1 and A/OpG1G2 recombinant bifunctional proteins.

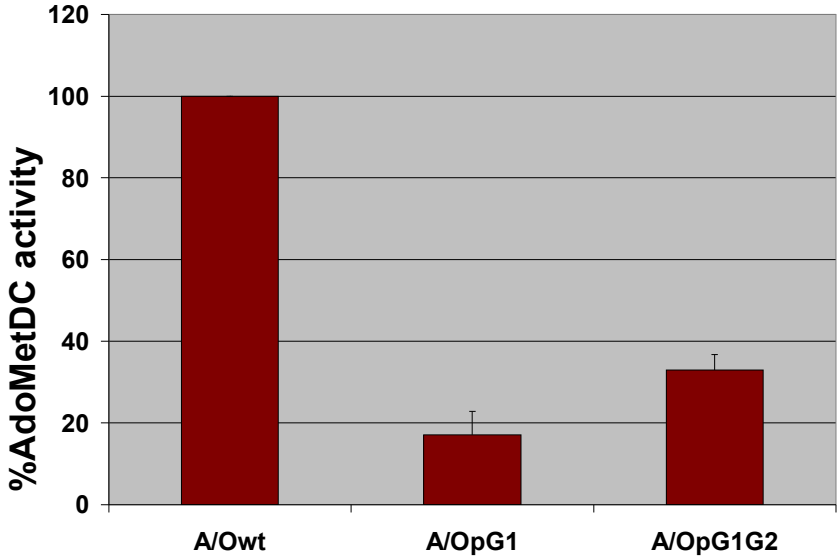

Figure 2.8: AdoMetDC activity assay. The mutant protein activities (A/OpG1 and A/OpG1G2) are normalized against the wild type activity (A/Owt) and are given as a percentage. Both results have a significance of $p < 0.001$. The error bars represent the standard deviation of the mean of 3 independent experiments performed in duplicate.

The results show a decrease of 83% in the AdoMetDC activity of the A/OpG1 recombinant protein and a loss of 67% in the A/OpG1G2 AdoMetDC activity.

Figure 2.9 represents the normalized activities of the ODC domain in the respective A/OpG1 and A/OpG1G2 recombinant bifunctional proteins.

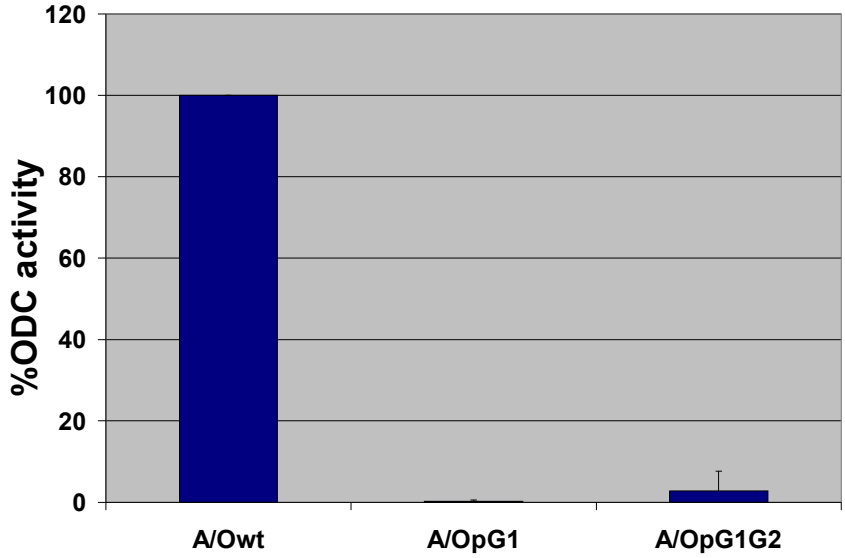

Figure 2.9: ODC activity assay. The mutant protein activities (A/OpG1 and A/OpG1G2) are normalized against the wild type activity (A/Owt) and are given as a percentage. Both results have a significance of $p < 0.001$. The error bars represent the standard deviation of the mean of 3 independent experiments performed in duplicate.

Figure 2.9 shows that the activity of the ODC domain in the A/OpG1 recombinant protein was totally depleted. The ODC activity of the A/OpG1G2 recombinant protein was decreased by 97%.

2.3.5 Molecular dynamics

From the results obtained with the activity assays, it was speculated that restriction of the O_1 loop movement altered the conformation of the ODC monomers thereby affecting dimerization of this domain or steric hindrance of this loop that interfere with protein-protein interactions in the bifunctional protein. In order to analyze the effect of movement restriction on the ODC monomer, the various recombinant proteins were subjected to molecular dynamic studies and were compared to the wild type protein.

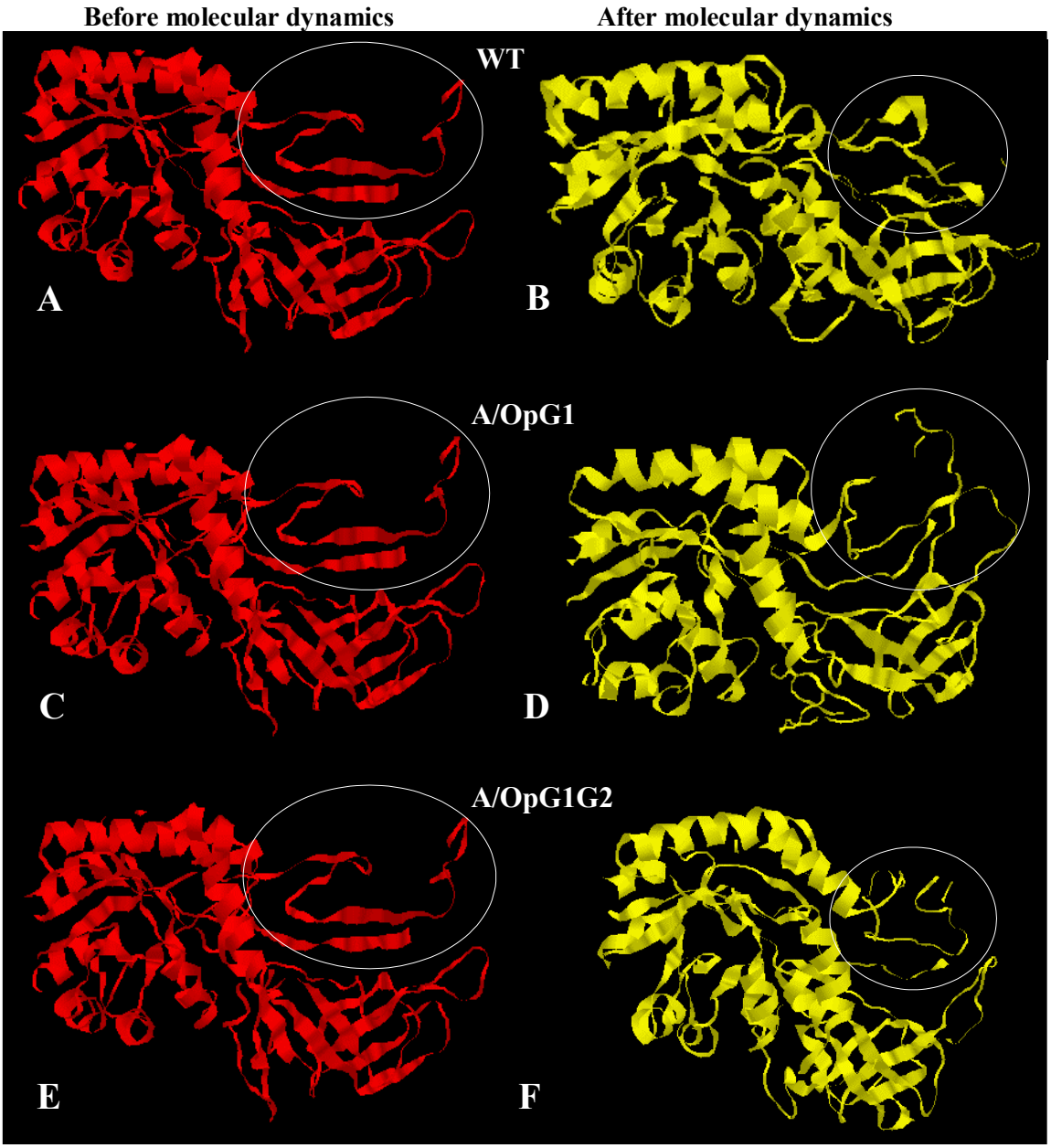

Figure 2.10: The WT, A/OpG1 and A/OpG1G2 proteins after minimization and molecular dynamics. The proteins given as red ribbons depict the different proteins after minimization. The respective proteins after 1000 000 dynamic steps are indicated with the yellow ribbons. The wild type proteins are numbered as A and B, the A/OpG1 proteins are given as C and D, and the double mutant protein (A/OpG1G2) is given as E and F. The various proteins' O_1 loops are indicated with the white circles. The respective proteins are identified.

Figure 2.10A depicts the WT monomeric ODC domain after minimization and before dynamics. Figure 2.10C represents the A/OpG1 recombinant monomeric ODC before dynamics and Figure 2.10E represents the A/OpG1G2 monomer before dynamics. No real difference could be seen between these three figures (red proteins) before dynamic studies.

However, after the 1000 000 dynamic steps a couple of interesting differences occurred. In the wild type protein (Figure 2.10A and B), the O_1 loop was totally folded onto the protein subunit to form a tightly folded monomeric ODC. The A/OpG1 protein (containing the $Gly_{1036\text{-}1038}Ala$ mutation) depicted in Figure 2.10C and D, did not resume a tightly packed conformation after dynamics and the O_1 loop protruded from the monomeric ODC. On the A/OpG1G2 recombinant monomeric protein (with both the $Gly_{1036\text{-}1038}Ala$ and $Gly_{1083}Ala$ mutations), the O_1 loop was slightly folded back onto itself after dynamics although it still protruded towards the surface in contrast to the wild type protein. The conformation of the A/OpG1G2 monomer was also altered, it formed a compactly folded monomer but the structure was twisted compared to the wild type protein.

2.4 Discussion

The recombinant plasmid containing the bifunctional *Pf*AdoMetDC/ODC coding sequence (Müller, *et al.*, 2000) was successfully isolated and mutated to result in the Gly$_{1036\text{-}1038}$Ala mutant (G1) and the Gly$_{1036\text{-}1038}$Ala - Gly$_{1083}$Ala double mutant (G1G2). The three Gly residues at positions 1036-1038 are conserved between *Plasmodia* species (Birkholtz, *et al*, 2004) and are therefore also studied separately in addition to the double mutation. The wild type and recombinant proteins were successfully expressed and isolated and adequate amounts of protein were obtained for subsequent activity assays. Given the importance of the O$_1$ insert, the current study focused on the flexibility of the insert because of the significance of protein dynamics in biological systems (Garrity, *et al.*, 2004; Ramasubbu, *et al.*, 2003; Taylor, *et al.*, 2003).

In previous experiments it was shown that the wild type *Pf*AdoMetDC and *Pf*ODC domains form a heterotetrameric complex when the monomers were independently expressed and subsequently co-incubated (Birkholtz, *et al.*, 2004). However, upon deletion of the 38 residue O$_1$ insert, the wild type *Pf*AdoMetDC and the mutant *Pf*ODC did not form a heterotetrameric protein complex. In addition, the ODC monomers failed to dimerize as a result of the O$_1$ deletion (Birkholtz, *et al.*, 2004). From these findings it was proposed that the removal of the O$_1$ insert caused a conformational change at the dimer interface, which prevented ODC dimerization, which in turn prevented complex formation between the *Pf*AdoMetDC and *Pf*ODC. Deletion of the O$_1$ insert in the bifunctional *Pf*AdoMetDC/ODC resulted in an ODC activity decrease of 94% (again due to proposed failure to dimerize) and an AdoMetDC activity decrease of 77% (due to inability to form a heterotetrameric complex) (Birkholtz, *et al.*, 2004). The two active sites of ODC are situated at the dimer interface between the two monomers, therefore, involvement of the O$_1$ loop in dimerization of ODC would directly affect formation of the active sites of ODC.

In this study, the mobility of the O$_1$ insert was studied in order to obtain a more defined idea of the function of this insert. Gly has the ability to assume multiple conformations resulting in flexibility of the O$_1$ loop. The flanking Gly residues of the O$_1$ loop was mutated to Ala in order to deprive the loop of its possible flexibility.

The resulting mutant proteins were studied in terms of activity loss or gain due to this change in flexibility of the O_1 insert. The results obtained from three independent experiments showed that the G1 mutation resulted in an activity decrease of 83% in the AdoMetDC domain and an almost complete loss of activity in the ODC domain. Figure 2.8 and 2.9 also show that the A/OpG1G2 double mutant resulted in an activity decrease of 67% in the AdoMetDC domain and an activity decrease of 97% in the ODC domain of the *Pf*AdoMetDC/ODC protein. The single G1 mutation and the double G1G2 mutation have greater influences on the ODC activity than the AdoMetDC activity as expected. Birkholtz, *et al.* (2004) showed that deletion of a parasite-specific insert has a more remarkable effect on its own domain than on the neighbouring domain. The results obtained in this study from movement restriction of the O_1 loop are comparable to those performed by Birkholtz *et al.*, where the entire O_1 insert was deleted. From this it can thus be predicted that O_1 mobility plays an important role in the activity of ODC, which may also affect the homodimerization of the ODC domain and its heterotetrameric complex formation with AdoMetDC.

Birkholtz, *et al.* (2004) proposed that deletion of the O_1 insert cause a conformational change at the dimer interface of the ODC monomers. It was questioned if mobility restriction of O_1 also results in a conformational change of the ODC monomers. To visualize the conformational changes that occur as a result of O_1 movement restriction, molecular dynamic studies were utilized. The results obtained with the molecular dynamic studies showed that the O_1 loop of the wild type monomeric ODC folds back onto itself and the protein surface (Figure 2.10A and B). Folding of the O_1 loop onto the protein subunit causes a conformational change that might be favoured in ODC dimer formation. Folding of this loop may also serve as an active site “lid” necessary for the catalytic function of the enzyme. In the double mutant protein (A/OpG1G2) depicted in Figure 2.10E and Figure 2.10F, the O_1 loop did not fold back after dynamics, which is even more pronounced in the A/OpG1 protein (Figure 2.10C and D). In both the mutant proteins the O_1 loop remained protruding from the subunit surface. Molecular dynamics studies also show that alterations of the flanking Gly residues caused a conformational change of the ODC monomers so that it differs from that of the wild type monomers. This change in conformation may negatively affect the dimer formation of the ODC protein, thereby affecting the activity of ODC as well as that of AdoMetDC. On the other hand, if the O_1 insert functions as an active site “lid”, the substrate will potentially no longer be enfolded into the active site, thereby negatively

affecting the activity. If the O_1 insert is only involved in the active site function of ODC, it is reasonable to suggest that only the ODC activity will be affected. The assumptions made based on the molecular dynamics studies of the monomeric ODC might greatly be supported with the attempted docking of the mutagenic monomers to form an ODC dimer. In the latter case, evidence for dimer interference of the O_1 loop might be obtained.

From the activity results it was clear that restriction of the O_1 loop mobility through alteration of the flanking, flexible Gly residues to Ala, resulted in activity loss of both AdoMetDC and ODC domains of the bifunctional protein. From the molecular dynamics results obtained, it is shown that hindrance of O_1 flexibility causes a conformational change in the ODC monomers. It is proposed that the conformational change occurring throughout the ODC molecule affects the dimerization interface, thereby affecting the ODC dimerization and its association with the AdoMetDC domain. This conformational change may also be communicated to the AdoMetDC domain active site, which is reflected in the activity loss of that domain. The fact that activities of both domains were altered upon movement restriction of the O_1 insert, suggests that the insert is more probably involved in protein-protein interactions that is communicated throughout the bifunctional molecule rather than functioning as an active site “lid” for ODC.

It is clear that insert O_1 mobility plays an essential role in complex formation of the bifunctional *Pf*AdoMetDC/ODC protein, which is then extrapolated to the functionality of both domains. ODC dimer formation and heterotetrameric complex formation between the domains can be studied with HPLC where the domains are independently expressed and co-incubated. Higher expression levels of *Pf*AdoMetDC/ODC will aid additional structural, interaction and mobility studies of this insert. Interference with the mobility of the O_1 loop by peptidomimetics *in vivo* will provide a novel strategy to combat malaria. This strategy involves inhibition of enzyme function by compounds targeted beyond the active site.

This chapter investigated the role of the mobility of the O_1 parasite-specific insert on the *Pf*AdoMetDC/ODC. The next chapter will focus on secondary structural elements in the hinge and ODC parasite-specific inserts in order to delineate protein-protein interacting sites.

Chapter 3
Secondary structures in the parasite-specific inserts of the *Pf*AdoMetDC/ODC protein

3.1 Introduction

Regions of low-complexity and amino acid bias are a common feature in *P. falciparum* proteins (Pizzi and Frontali, 2001; Xue and Forsdyke, 2003). It is believed that these low-complexity areas encode non-globular protein domains, the functions of which are largely still unknown. The non-globular domains extrude from the protein core and is presumed not to impair the functional fold of the protein (Pizzi and Frontali, 2001). However, it has recently been shown that some of these non-globular domains, or parasite-specific inserts, are important for protein-protein interactions and activities of the *P. falciparum* DHFR-TS (Yuvaniyama, *et al.*, 2003) and *Pf*AdoMetDC/ODC (Birkholtz, *et al.*, 2004).

Essential protein-protein interactions are evident between the domains of *P. falciparum* bifunctional proteins. In the bifunctional *P. falciparum* DHFR-TS protein, the C-terminal TS domain is inactive in the absence of the DHFR domain or both the DHFR and JR regions (Shallom, *et al.*, 1999), proving that protein interactions between DHFR and TS are important for the catalytic function of TS.

The *Plasmodial* DHFR and TS subunits are connected with an 89-residue junction region (JR). The JR contains two α-helices that are separated by a disordered, flexible loop and are involved in interdomain interactions (Yuvaniyama, *et al.*, 2003). *Pf*DHFR has two extra parasite-specific inserts: Insert 1 comprises 16 amino acid residues and the second insert consists of 35 amino acids. Insert 1 contains a short α-helix of 3 residues and protrudes from the protein surface, therefore it does not influence the protein core structure. One part of insert 1 interacts with the TS domain thereby stabilizing the domain attachment to DHFR. The flexible loop present in insert 1 is involved in substrate channeling (Yuvaniyama, *et al.*, 2003). Insert 2 contains a longer α-helix of 14 residues and a disordered region of 9 residues. In the crystal structure of the dimer, the two α-helices of insert 2 protrude from the surface and are situated close to the JR on the one side of the protein. It is believed that the α-helices of this insert may provide recognition sites for external molecules; part of insert 2 also interacts with the JR (Yuvaniyama, *et al.*, 2003).

Likewise, in the *P. falciparum* AdoMetDC/ODC protein, the hinge region is important for the catalytic activity of the ODC domain and is thought to support the correct folding of the ODC domain (Krause, *et al.*, 2000). The recombinant hinge/ODC domain is ten times less active than the ODC in the bifunctional protein where interaction with the AdoMetDC domain is involved. However, the monofunctional AdoMetDC domain is twice as active as in the bifunctional construct (Wrenger, *et al.*, 2001). It is thus apparent that the activities of the two domains are reliant on the interdomain interactions between the AdoMetDC and ODC of the bifunctional protein.

*Pf*AdoMetDC and *Pf*ODC is connected via a 260 residue hinge region of which 180 amino acids forms the core region of the hinge. The parasite-specific inserts in the *Pf*AdoMetDC/ODC protein are not solely responsible for the enlarged size of the bifunctional protein but are involved in specific intra- and interdomain protein-protein interactions in the bifunctional protein (Birkholtz, *et al.*, 2004). The hinge is involved in specific interdomain interactions between the AdoMetDC and ODC as was confirmed with deletion mutagenesis (Figure 3.1). Deletion of the hinge region in the bifunctional protein had an effect on both decarboxylase activities.

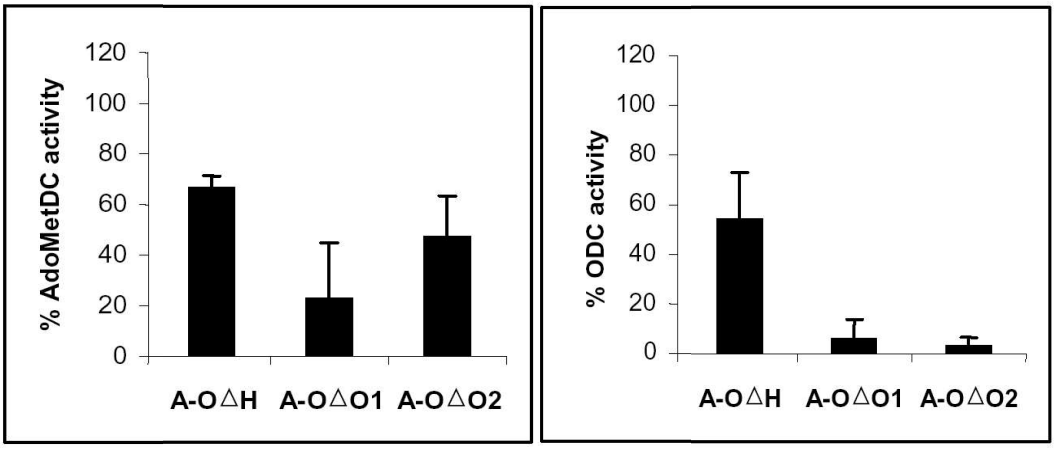

Figure 3.1: AdoMetDC and ODC activity in the *Pf*AdoMetDC/ODC after deletion mutagenesis. Activities were measured after deletion of the hinge (H), short ODC insert (O_1) and long ODC insert (O_2) and are expressed as a % of the wild type activity. Adapted from Birkholtz, *et al*., 2004.

In addition to the importance of the hinge in the catalytic activity of ODC, the hinge also plays an important role in protein-protein interactions (Birkholtz, *et al.*, 2004). Deletion of the core hinge region affected both the AdoMetDC and ODC activities and was shown to be involved in interdomain interactions between the two catalytic units (Birkholtz, *et al.*, 2004).

The O_1 insert is important for the dimerization of ODC, which also ensures ODC's association with AdoMetDC and initiates heterotetrameric complex formation (Birkholtz, *et al.*, 2004). It seems that both decarboxylases have optimum activity once a heterotetrameric complex is formed (Figure 3.1 shows the activity decrease of both domains with the O_1 deletion) (Birkholtz, *et al*., 2004)

The O_2 parasite-specific insert is essential for ODC activity of the bifunctional protein and is also relatively important for the AdoMetDC activity (Birkholtz, *et al.*, 2004). The O_2 parasite-specific insert is rich in Asn and Asp residues with a 23 amino acid stretch of (Asn-Asn-Asp)x repeats. Deletion of the O_2 parasite-specific insert almost depleted the ODC activity of the bifunctional protein and had a marked effect on the AdoMetDC activity. The polar-repeat region could act as a 'polar zipper' between protein domains because of the hydrogen bond networks present between the amino acid side chains (Birkholtz, *et al.*, 2004).

It is not yet known how the domains of *Pf*AdoMetDC/ODC interact and what specific residues are involved in these interactions. The exact protein interacting areas need to be delineated further. In order to confirm that the activity and interaction loss in the bifunctional enzyme is not as a result of the large deletions of these inserts (180 residues of hinge deleted, 145 residues deleted for O_2) (Birkholtz, *et al.*, 2004) this chapter will focus on secondary structural elements within the parasite-specific inserts that might be involved in domain interactions and activities. Secondary structures have been shown to act as nucleation sites for initiation and as guide for the folding of proteins (Richardson, 1981). α-Helices are especially essential for initiating protein folding and often teams up with β-plates, and furthermore play vital roles in the stability and organization of proteins (Richardson, 1981; Srinivasan and Rose, 1999). Certain amino acids in α-helices and β-plates are therefore important for protein folding while others are more involved in stabilization of proteins via protein-protein interactions (Kwok, *et al.*, 2002).

The parasite-specific inserts are mostly disordered but with specific localized secondary structural elements (except for the O_1 region, refer to Chapter 2). Taking the importance of secondary structures in protein-protein interactions into consideration, functional roles of selected, predicted α-helices and β-plates present in the parasite-specific inserts are investigated in this Chapter.

3.2 Methods

3.2.1 Secondary structure predictions

Secondary structure predictions were previously performed (G.A. Wells, personal communications) and are described briefly. All full-length bifunctional AdoMetDC/ODC sequences of *Plasmodia* were subjected to 23 secondary structure prediction algorithms. The GARNIER algorithm was included in the EMBOSS suite. The other algorithms were obtained from different web servers (Table 3.1). From the alignments, three overlapping segments were generated; the segments correspond to the N-terminal, middle and C-terminal regions of the proteins. Secondary structure images were generated with CLUSTALX. The same algorithms were used to predict known secondary structure regions present in the DHFR-TS crystal structure (Yuvaniyama, *et al.*, 2003) in order to establish the best performing method.

Table 3.1: Algorithms applied for secondary structure predictions in the hinge and ODC regions of *Pf*AdoMetDC/ODC.

Program	Source
GARNIER	EMBOSS
JNETPRED JNETHMM JNETALIGN JNETPSSM JNETFREQ JPRED	http://www.compbio.dundee.ac.uk
PHD DoublePrediction HNNC SOPM SIMPA96 PREDATOR DSC Sec.Cons GOR4	http://npsa-pbil.ibcp.fr
SAM-T99	http://www.cse.ucsc.edu
HMMSTER	http://www.bioinfo.rpi.edu
PROF PROFSUB PHD PHDSUB PSIPRED	http://cubic.bioc.columbia.edu

3.2.2 Primer design

Primers were designed with the same principles as described in Chapter 2, section 2.2.5. The sites for site-directed mutagenesis were incorporated in the middle of the primers, as were the sites for deletion mutagenesis. The resulting primers (Inqaba Biotechnology) are listed in Table 3.3. The positions of the various mutagenic primers (5 sets in total) are given in Figure 3.2 as reference.

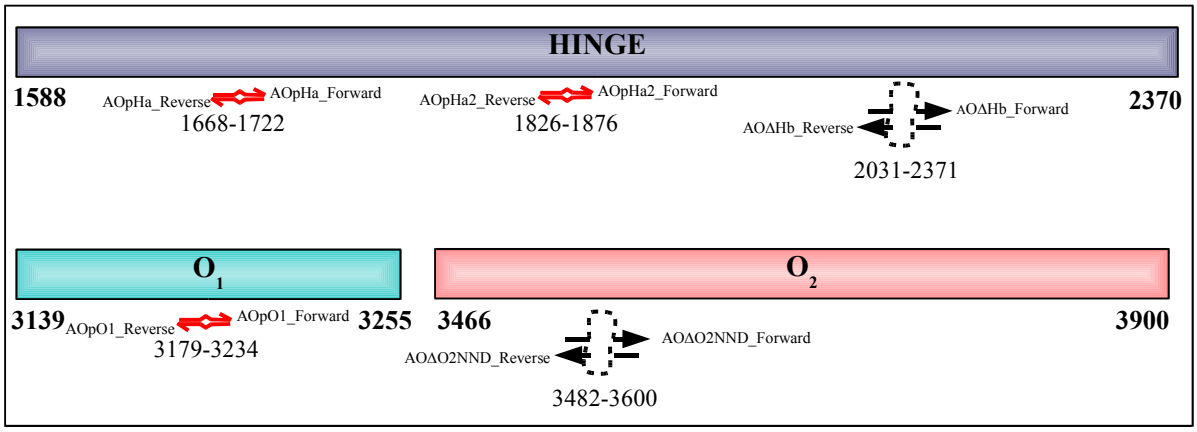

Figure 3.2: The mutagenic primer positions on the parasite-specific inserts. The start and end nucleotides of the inserts are represented. Primer positions are indicated with the exact nucleotide numbers. Site-directed mutagenesis primers are indicated with the red arrows; deletion mutagenesis primers are indicated with the black arrow containing dashed loops. The primer names are given next to the respective primers.

3.2.3 Site directed mutagenesis and nucleotide deletion

The *Pf*AdoMetDC/ODC sequence was cloned into the pASK-IBA3 vector as described (Müller, *et al*., 2000; Chapter 2, section 2.2.1). Mutations were incorporated in the *Pf*AdoMetDC/ODC sequence and nucleotides were deleted following the PCR protocol described in Chapter 2, section 2.2.6. The plasmid was isolated and purified prior to PCR (Chapter 2, section 2.2.2) as well as after site-directed mutagenesis to produce pure mutated plasmid (Chapter 2, section 2.2.7)

The correct sizes of the recombinant plasmids were screened by *Hind*III restriction digestion and were compared to the wild type sizes with electrophoretic analysis on a 1% agarose gel (Chapter 2, section 2.2.9.2). The β-plate deletion in the hinge region was pre-screened by restriction mapping with *Eco*RV, which is an indicator of the deletion (STET-prep screening is described in Chapter 2, section 2.2.9). Mutations and deletions were confirmed by nucleotide sequencing (method described in Chapter 2, section 2.2.10).

The sequencing primers used were as follows:

ODC seq1: **5' TATGGAGCTAATGAATATGAATG 3'**

ODC seq2: **5' TATGAATTACATACATTTACCG 3'**

ODC seq3: **5' GAATTAAAAGACCATTACGATCC 3'**

The positions of the sequencing primers are indicated on the *P. falciparum* hinge-ODC sequence in Figure 3.7.

3.2.4 Recombinant protein expression and activity assays

The mutation-containing expression vectors were transformed into electrocompetent EWH331 cells (described in Chapter 2 section 2.2.8). After culturing, protein expression was induced with AHT and the recombinant proteins were subsequently harvested (described in Chapter 2, section 2.2.11). The recombinant proteins were isolated by means of lysozyme and sonification to disrupt the cell walls, centrifugation and filtration to remove cell debris from the protein suspension and *Strep*-tag affinity chromatrography to isolate the recombinant proteins (methods described in Chapter 2, section 2.2.12 to 2.2.13).

The purity of the isolated proteins was analysed with SDS polyacrylamide gel electrophoresis and silver staining (described in Chapter 2, section 2.2.14).

The isolated proteins were subjected to activity assays as described in Chapter 2, section 2.2.15. The activities of the recombinant proteins were measured as the mean of 3 independent experiments performed in duplicate and were normalized to the wild type protein activity.

3.3 Results

3.3.1 Secondary structures

Structure-based alignments were used to identify the secondary structures of the parasite-specific inserts. The results of the secondary structure predictions indicated that the parasite-specific inserts do contain some α-helices and β-plates (Figures 3.3 to 3.5). Specifically, in the *Pf*AdoMetDC/ODC hinge region about 21% of the 260 residues are involved in 4 α-helices and 21% are present in 12 β-plates. In the 38-residue *Pf*AdoMetDC/ODC O_1 region, four residues form a single β-plate and approximately 51% of the residues form an α-helix. The 145-residue *Pf*AdoMetDC/ODC O_2 parasite-specific insert consists mostly of coils with approximately 24% of the residues forming 5 β-plates and a mere 4% of the residues are predicted to form a single α-helix. In all cases the α-helices and β-plates are interspersed with coils and turns.

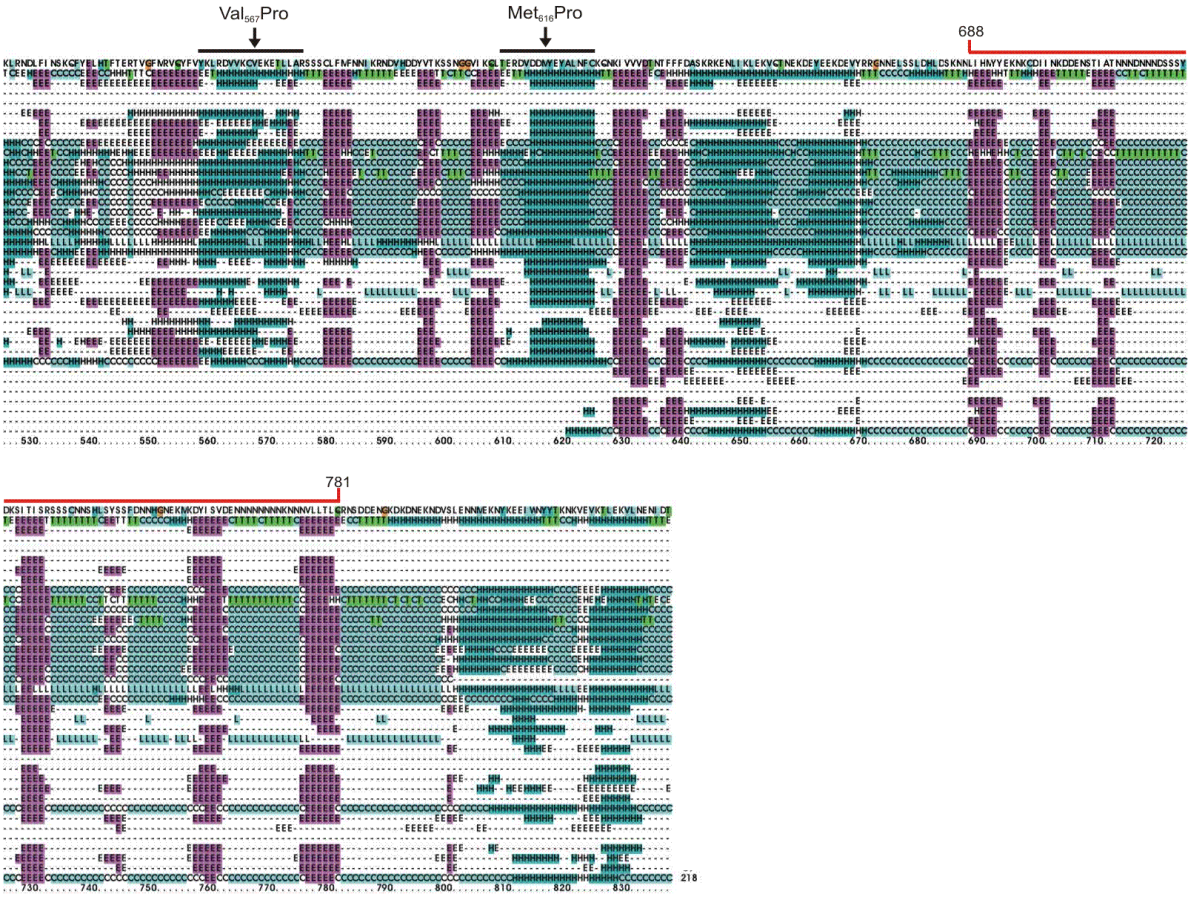

Figure 3.3: Secondary structure predictions of the Hinge region of the bifunctional AdoMetDC/ODC in *P. falciparum*. The black bars at the top of the figure illustrate the α-helices disrupted by site-directed mutagenesis and the arrows indicate the position where the helix breaker was inserted. The red bar presents the area deleted (residues 688 to 781) to disrupt the β-plate of the hinge. H: helix, C/L: coils, E: β-plates, T: turns. Amino acid residue numbers are given at the bottom of the figure. The secondary structue prediction programs used are the same than that indicated in Figure 3.4. The dashed lines represent areas with no predicted secondary structures with the specific algorithm used.

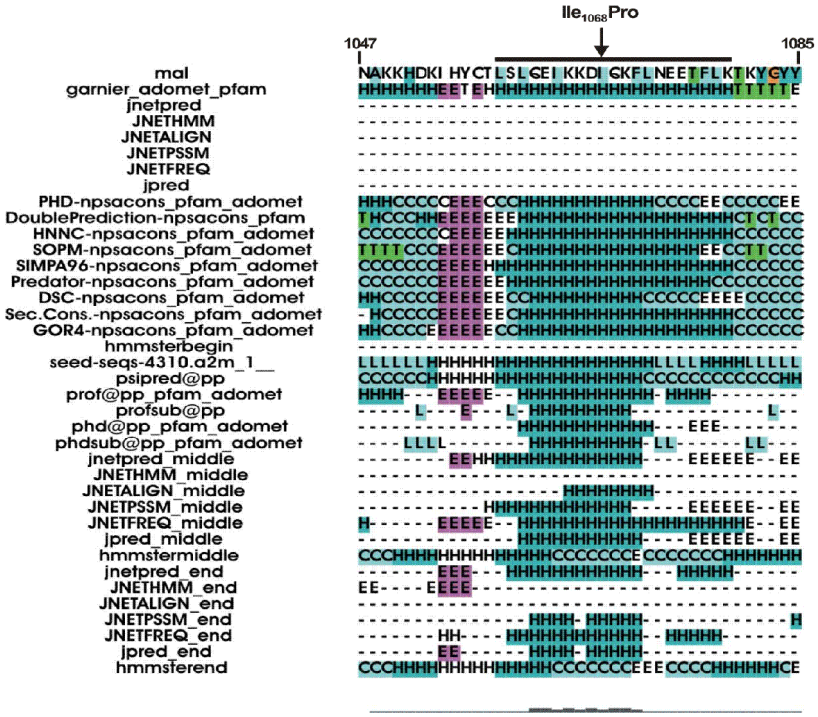

Figure 3.4: Secondary structure predictions of the O_1 region in the bifunctional AdoMetDC/ODC in *P. falciparum*. The black bar at the top of the figure illustrates the α-helix disrupted by site-directed mutagenesis and the arrow indicates the specific residue replaced with a helix breaker ($Ile_{1068}Pro$). H: helix, C/L: coils, E: β-plates, T: turns. Residue numbers are indicated at the top of the figure. Legends shown on the left of the figure indicates the secondary structure prediction programs used. The dashed lines represent areas with no predicted secondary structures with the specific algorithm used.

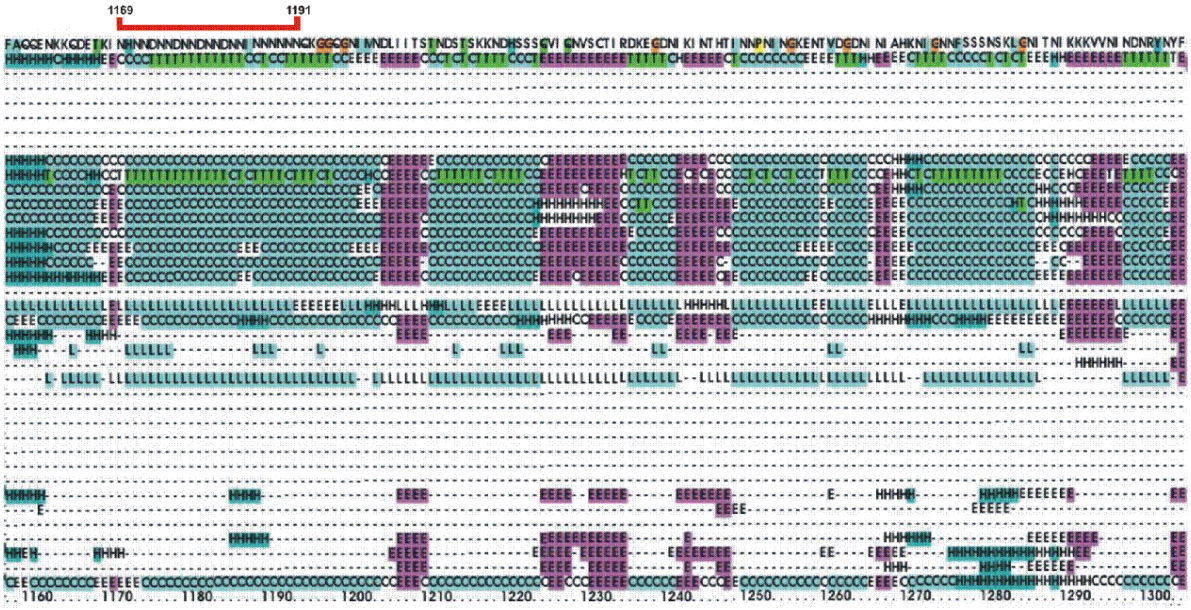

Figure 3.5: Secondary structure predictions of the O_2 region in the bifunctional AdoMetDC/ODC of *P. falciparum*. The red bar at the top of the figure illustrates the '(NND)x' repeat region that was deleted (residues 1169 to 1191). H: helix, C/L: coils, E: β-plates, T: turns. Amino acid residue numbers are indicated at the bottom of the figure. The secondary structure prediction programs used are indicated in Figure 3.4. The dashed lines represent areas with no predicted secondary structures with the specific algorithm used.

From the predictions, the secondary structures thought to be important for functionality including protein-protein interactions and activity, were selected and are represented in Figure 3.6. These secondary elements were chosen based on the fact that they are conserved between most of the prediction programs used (Figures 3.3 to 3.5).

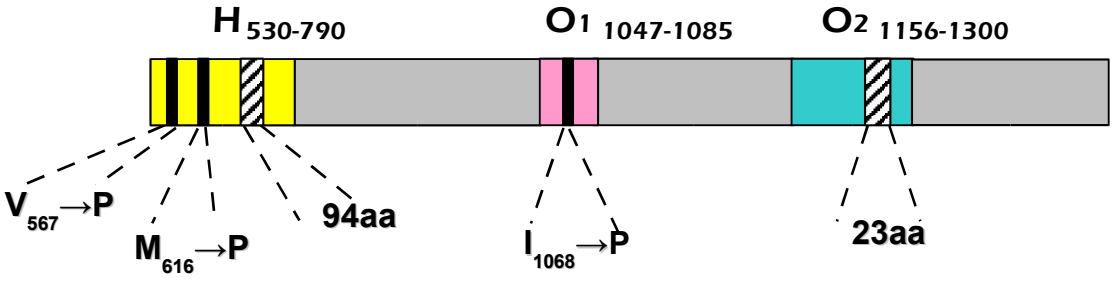

Figure 3.6: The regions in the parasite-specific inserts thought to be important for functionality. The figure depicts the three parasite-specific inserts focused on in this study; the hinge (H, yellow), the short ODC insert (O_1, pink) and the long ODC insert (O_2, blue) and their respective lengths. The black blocks represent the helices that were disrupted and the patterned blocks represents the deletions performed.

For disruption of the α-helices, a specific residue (conserved between secondary structure predictions) close to, or at the middle of the respective helices was replaced with a conformationally rigid Pro residue to act as helix breaker. The first helix in the hinge region was disrupted by transforming a Val_{567} residue to Pro (refer to Figure 3.6). The second helix in the hinge region was disrupted by changing Met_{616} to Pro (Figure 3.6). In the O_1 insert, Pro replaced Ile_{1068} as a helix breaker (Figure 3.6). In the hinge region a β-plate of 94 amino acids was removed. The '(NND)x' repeat region consisting of 23 amino acids in the O_2 parasite-specific insert was deleted. The various mutants were named as shown in Table 3.2.

Table 3.2: The designations of the various mutants.

Name	Mutant
A/OpHa1	The bifunctional *Pf*AdoMetDC/ODC sequence (A/O) with a point mutation incorporated (p) in the hinge region (H) at the first α-helix (a1).
A/OpHa2	A helix breaker was inserted in the second α-helix of the hinge region
A/OΔHb	The bifunctional *Pf*AdoMetDC/ODC sequence (A/O) with a β-plate (b) deletion (Δ) in the hinge region (H).
A/OpO1a	A site-specific helix breaker was inserted in the O_1 α-helix.
A/OΔO2NND	The bifunctional *Pf*AdoMetDC/ODC sequence (A/O) with a deletion of the '(NND)x' repeat region in the O_2 insert

3.3.2 Mutagenic and deletion primers

The Tm's of the primers range from 66˚C to 69˚C and the annealing temperature for the PCR cycles set was at 60˚C. The primers used for the disruption of the hinge α-helix 1 are AOpHa_Forward and AOpHa_Reverse. Disruption of the hinge α-helix 2 was obtained with the use of the AOpHa2_Forward and AOpHa2_Reverse primers. The AOpO1a_Forward and AOpO1a_Reverse primers were used for disruption of the O_1 helix. The 282 base pairs in the hinge region were removed with the AOdHb_Forward and AOdHb_Reverse primers. The '(NND)x' repeat region in the O_2 insert was deleted with the AOdO2NND_Forward and AOdO2NND_Reverse primers. The respective primer properties are listed below in Table 3.3 and their priming positions on the sequence are given in Figure 3.7.

Table 3.3: Mutagenic primers and their respective properties. Residues indicated in red are the mutation sites for helix disruption; the red arrows indicate the respective deletion sites.

Oligonucleotide	Sequence	Properties	Alteration
AOpHa_Forward	5' GTT TAT AAA TTA AGA GAT GTT GTT AAA TGT **CCA** GAA AAA GAA ACT TTG CTA GCT AGG A 3'	58 bases Tm = 68˚C	Val to Pro *Helix breaker*
AOpHa_Reverse	5' T CCT AGC TAG CAA AGT TTC TTT TTC **TGG** ACA TTT AAC AAC ATC TCT TAA TTT ATA AAC 3'		
AOpHa2_Forward	5' CG GAA AGA GAT GTT GAT GAT **CCA** TAT GAG TAT GCT TTA AAT TTT TGT AAA C 3'	51 bases Tm = 68˚C	Met to Pro *Helix breaker*
AOpHa2_Reverse	5' G TTT ACA AAA ATT TAA AGC ATA CTC ATA **TGG** ATC ATC AAC ATC TCT TTC CG 3'		
AOdHb_Forward	5' CG TTG GAT CAT TTA GAT AGT AAG AAT AAT▼AGG AAC AGT GAT GAT GAA AAT GGT AAA G 3'	57 bases Tm = 69˚C	282 bp *β-sheet deletion*
AOdHb_Reverse	5' C TTT ACC ATT TTC ATC ATC ACT GTT CCT▼ATT ATT CTT ACT ATC TAA ATG ATC CAA CG 3'		
AOpO1a_Forward	5' GT CTT CAA GAA ATT AAA AAA GAT **CCA** CAA AAA TTT CTT AAT GAA GAA ACA TTT CTC 3'	56 bases Tm = 66˚C	Ile to Pro *Helix breaker*
AOpO1a_Reverse	5' GAG AAA TGT TTC TTC ATT AAG AAA TTT TTG **TGG** ATC TTT TTT AAT TTC TTG AAG AC 3'		
AOdO2NND_Forward	5' G AAA CAA GAC GAA ACA AAA ATA▼CAA AAA GGG GGC CAA GGA AAT ATT ATG 3'	49 bases Tm = 69˚C	69 bp *Conserved repeat region deletion*
AOdO2NND_Reverse	5' CAT AAT ATT TCC TTG GCC CCC TTT TTG▼TAT TTT TGT TTC GTC TTG TTT C 3'		


ODC seq2
A/OpHa1
A/OpHa2
A/OΔHb
ODC seq1
A/OpO1a
ODC seq3…

Figure 3.7: The Hinge-ODC region of *Pf*AdoMetDC/ODC with the sequence positions of the mutagenic primers. The different mutants are indicated on the right side of the sequence. The respective priming sites are given as the black arrows. Specific residues that were mutated are indicated with red stars; deletions are indicated with dashed lines incorporated in the primer arrows. The three sequencing primers; ODC seq1, ODC seq2 and ODC seq3 are indicated with the red arrows.

3.3.3 Screening for mutant plasmids

Mutated plasmids obtained after *Dpn*I treatment was transformed into competent cells and subsequently screened for the correct size and mutations. Plasmid isolated from bacterial cells with the STET-prep method (section 2.2.9.1) was digested with *Hind*III to verify the presence of the pASK-IBA3 plasmid containing the *Pf*AdoMetDC/ODC mutant inserts. The *Hind*III restriction map of the pASK-IBA3 vector containing the *Pf*AdoMetDC/ODC sequence is given in Chapter 2, Figure 2.3.

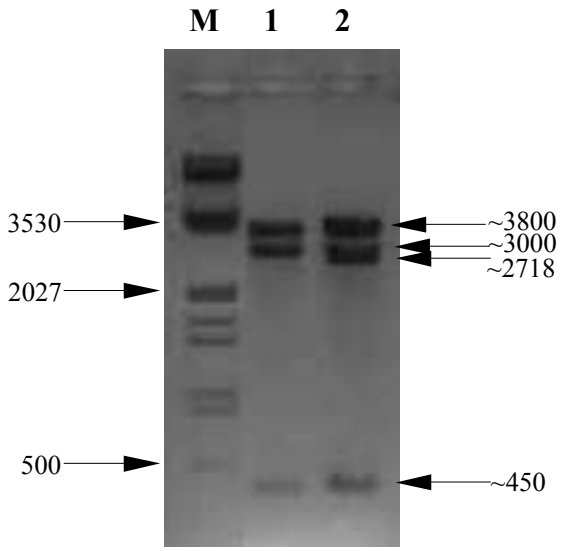

Figure 3.8: *Hind*III restriction digestion of plasmids to screen for correct plasmid size. 1% Agarose electrophoresis of WT (1) and A/OΔHb (2) recombinant plasmid. M: *Eco*RI-*Hind*III digested λ-phage DNA used as a high molecular mass marker. The sizes of the bands are given as base pairs.

Three bands were observed after digestion with *Hind*III: Approximately 3800, 3000 and 450 base pairs, respectively (Figure 3.8). Although all mutants were screened with *Hind*III mapping, only the WT and A/OΔHb plasmids are presented in Figure 3.8. The results for all the size-screens of the point-mutations look similar to that of the WT, confirming the correct plasmids. The A/OΔHb is shown to indicate the size difference in the second largest band of 2718 nucleotides. Deletion of the 94 amino acid region would result in a 282 nucleotide deletion which is visible on a 1% agarose gel if compared to the wild type sizes.

The A/OΔHb mutation was further verified with *EcoR*V restriction digestion. The deletion of the β-plate in the hinge region (A/OΔHb) removed an *EcoR*V restriction site and therefore could be screened by means of restriction mapping (Figure 3.9).

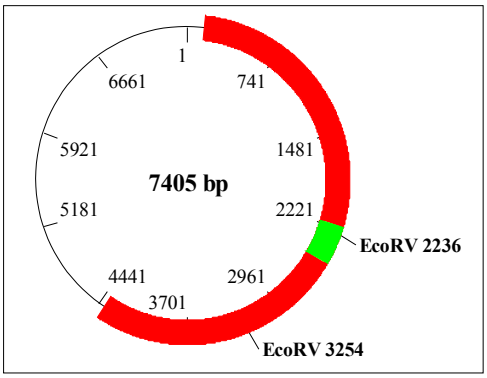

Figure 3.9: The *EcoR*V restriction map of pASK-IBA3-*Pf*AdoMetDC/ODC. The wild type plasmid has two *EcoR*V restriction sites. The *Pf*AdoMetDC/ODC insert is indicated with the red bar. The Hb deletion (shown in green) removes one of the *EcoR*V sites.

*EcoR*V digestion of the pASK-IBA3 vector containing the A/OΔHb sequence resulted in one linear band of 7123 base pairs (Figure 3.10). Restriction digestion of the WT plasmid with *Eco*RV resulted in two bands of 6387 and 1018 base pairs each.

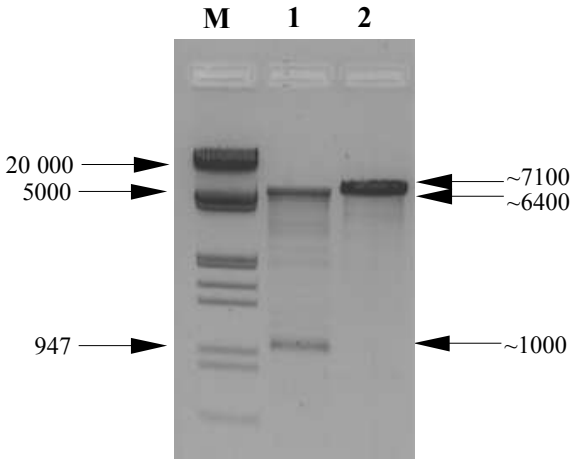

Figure 3.10: *EcoR*V restriction digestion of mutant plasmids to screen for the hinge deletion. 1% agarose electrophoresis of WT (1) and A/OΔHb (2) recombinant plasmids. M: *EcoR*I-*Hind*III digested λ-phage DNA used as a high molecular mass marker. The sizes of the bands are given as base pairs.

Figure 3.10 gives the wild type plasmid (lane 1) and the A/OΔHb (lane 2) mutant plasmid after *EcoR*V restriction digestion. Due to the gel resolution, a size difference between the 7100 and 6400 bands were not expected. A single linear band for A/OΔHb was obtained as expected. The results obtained showed a positive screen for the 282-base pair deletion. All the other mutants were identified and verified with automated nucleotide sequencing. Confirmed mutated plasmids were transformed into expression cells (EWH331) for recombinant protein expression and subsequent activity assays.

3.3.4 SDS-PAGE

The various mutations and deletions on the *Pf*AdoMetDC/ODC bifunctional protein did not influence the expression levels of most of the recombinant proteins, as the expected protein concentrations (10 µg/ml to 30 µg/ml) were obtained (Table 3.4). The A/OpO1a recombinant protein is the only protein with a reduced expression level of 15 µg/ml. The total amount of recombinant protein obtained from 1L culture ranged between 50 and 150 µg.

Table 3.4: Expression levels of the various recombinant proteins.

Protein	Expressed concentrations*	Standard Deviation
WT	25 µg/ml	± 10.2 µg/ml
A/OpHa1	31.3 µg/ml	± 8.2 µg/ml
A/OpHa2	29.6 µg/ml	± 6.3 µg/ml
A/OΔHb	30 µg/ml	± 12.4 µg/ml
A/OpO1a	15 µg/ml	± 3.3 µg/ml
A/OΔNND	29 µg/ml	± 7.3 µg/ml

*Values are the mean of three independant experiments.

The expressed, isolated and purified wild type and mutant proteins were analysed with a 12% SDS-PAGE (Figure 3.11). The amount of recombinant protein loaded per lane varied between 1.5 and 4.5 µg. All the recombinant proteins were visible on the gel.

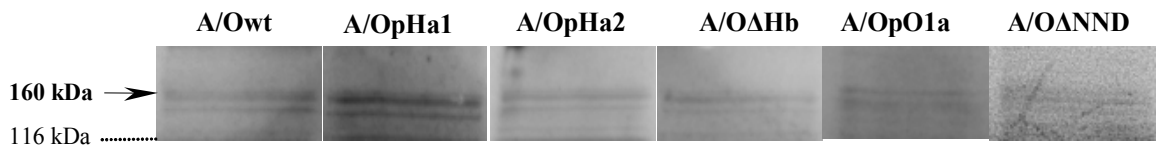

Figure 3.11: Silver stained SDS-PAGE of the wild type and various recombinant bifunctional proteins. The proteins were revealed with silver staining. The position of the molecular weight marker is indicated with the dotted line.

Two bands are observed, one being the recombinant protein and the other band possible unprocessed protein or degradation products. No size difference is observed between the A/Owt (160 kDa) and the A/OΔHb (150 kDa) and A/OΔNND (158 kDa) because of the resolution of the gel.

3.3.5 Activity assays

The isolated mutant and wild type recombinant proteins obtained with *Strep*-tag affinity chromatography were dialyzed overnight for use in activity assays. The assays entailed the addition of ^{14}C-labelled substrate to the active protein solution, resulting in the release and capture of $^{14}CO_2$ (described in Chapter 2, section 2.2.15). The amount of protein used per activity assay ranged between 1.5 µg and 4.5 µg. The results obtained were the means of three independent experiments, each performed in duplicate. The specific activities (nmol/min/mg protein) obtained for each recombinant protein were normalized to the wild type activity and is given as a percentage of the wild type activity. Figure 3.12 represents the normalized activities of AdoMetDC in the various recombinant mutant bifunctional proteins.

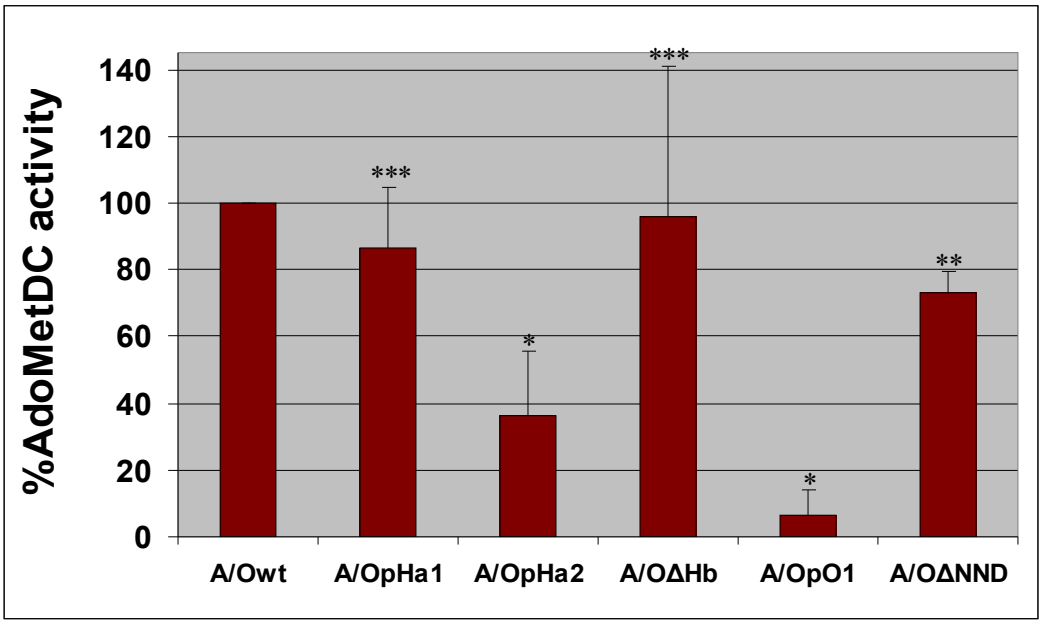

Figure 3.12: The AdoMetDC activities of the various recombinant proteins. The results are normalized and represented as % of the wild type activity. * These results have a significance of $p < 0.005$, ** a significance of $p < 0.02$. *** These results are not significant with $p > 0.1$. The error bars represent the standard deviation of the mean of 3 independent experiments performed in duplicate.

The activity results show a decrease of 13% in the AdoMetDC activity upon disruption of α-helix 1 in the hinge region (A/OpHa1) and a more dramatic decrease of 64% in the AdoMetDC activity upon disruption of α-helix 2 in the hinge region (A/OpHa2). The decrease in AdoMetDC activity of about 4% after the hinge-β-plate deletion (A/OΔHb) was not considered to be significant according to the student t-test and in view of the large standard deviation. The protein containing the helix breaker in the O_1 region (A/OpO1) shows a marked decrease in AdoMetDC activity of ~94% and the '(NND)x' repeat region deletion mutant (A/OΔNND) shows a decrease of 27%. The results for A/OpHa2 and A/OpO1 have significances of $p < 0.005$, the A/OΔNND result has a significance of $p < 0.02$. The A/OpHa1 and A/OΔHb assay results are considered not significant with student t-test values of $p > 0.1$.

Figure 3.13 represents the normalized activities of the ODC domain in the various recombinant mutant bifunctional proteins.

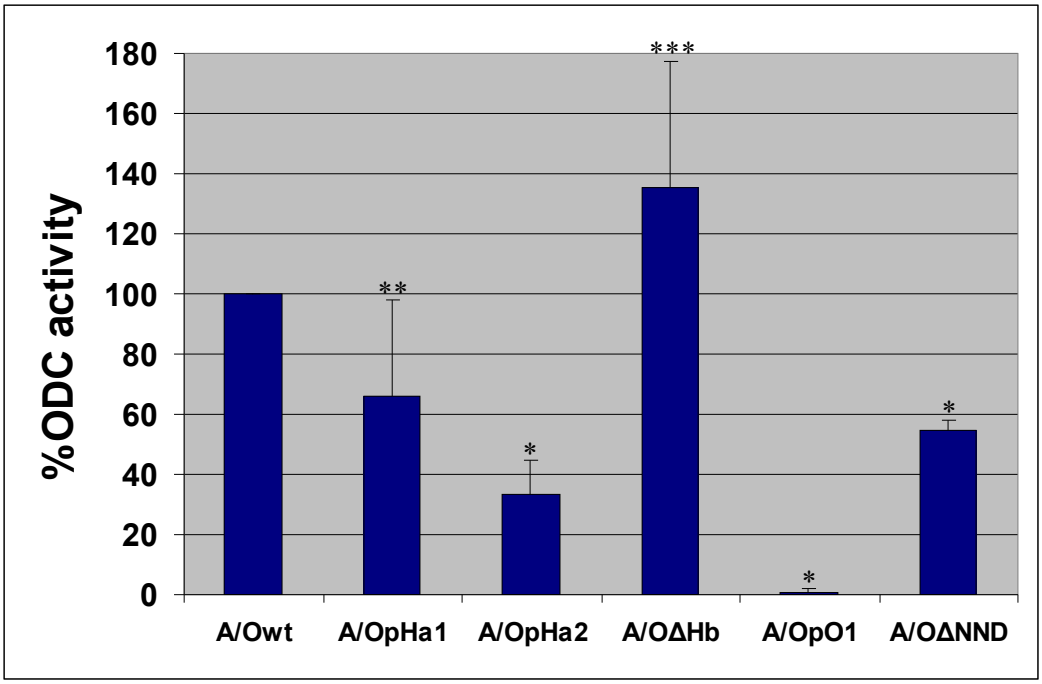

Figure 3.13: The ODC activities of the different recombinant proteins. The results are normalized and represented as % of the wild type activity. All the results are significant with * $p < 0.001$, ** $p < 0.02$ and *** $p < 0.05$. The error bars represent the standard deviation of the mean of 3 independent experiments performed in duplicate.

From the results given in Figure 3.13, the A/OpHa1 mutant (disruption of the first helix in the hinge region), it is apparent that ODC activity was reduced with 34%. The A/OpHa2 mutant (disruption of the second helix in the hinge region) reduced the ODC activity with

67%. The disruption in the O_1 helix (A/OpO1) resulted in an almost total activity depletion in the ODC domain of the bifunctional enzyme. However, the A/OΔNND mutant protein (deletion of the '(NND)x' repeat region in O_2) showed a decrease of only 46% in ODC activity. In contrast, the ODC activity was increased with 35% upon removal of the β-plate in the hinge region (A/OΔHb) with a large standard deviation.

All the above results for ODC are significant according to the student t-test analysis. The A/OpHa2, A/OpO1 and A/OΔNND have significances of $p < 0.001$. The A/OpHa1 result is significant with a p value < 0.02 and the A/OΔHb result has a significance of $p < 0.05$.

3.4 Discussion

In *T. brucei*, mutation of a dimer-interface Lys residue to an Ala had remarkable effects on the catalytic activity of ODC (Jackson, *et al.*, 2004). The Lys residue is distant from the active sites of ODC (10Å) and is part of a β-sheet domain. Mutation of this residue caused another hydrogen-bonded loop to become destabilized and disordered; the changes in stability were then propagated to the active site loop, which ultimately affected the catalytic function (Jackson, *et al.*, 2004). The Lys-Ala mutation resulted in a more accommodating active site and weakened the density of the protein, suggesting a relaxation in the protein structure that more readily adapt multiple conformations. The conformation of the protein containing the Lys-Ala mutation differs little from the wild type protein and the conformational differences are distributed throughout the protein (Jackson, *et al.*, 2004).

Long-range interactions are essentially propagated by protein-protein interactions in specific proteins. The protein-protein interactions become especially important in bifunctional proteins where intra- and interdomain protein-protein interactions play a role in enzyme function.

The secondary structure of a protein can be thought of as the local conformation of the polypeptide chain (Bourne, *et al.*, 2003). Secondary structures are important for the initiation of protein folding (Richardson, *et al.*, 1981; Srinivasan and Rose, 1999) and are the most important factors involved in conformational stabilization (Srinivasan and Rose, 1999). These secondary structures can be broken down into various important amino acids where some of these residues are more involved in protein folding while others are more involved in stabilization of proteins (Kwok, *et al.*, 2002). A number of algorithms (Table 3.1) were used to predict the secondary structures in the parasite-specific inserts of the hinge and ODC regions of the *Pf*AdoMetDC/ODC. The two most important methods in secondary structrue prediction is the Chou-Fasman method and the Garnier-Robson method. The Chou-Fasman method utilizes 3D proteins in order to assign preferences for α-helices, β-plates or turns to the respective amino acids. These assigned conformational preferences of the amino acids are used to predict secondary structures in proteins with no available structural data (Sternberg, 1996). The Garnier-Robson method is very similar to the Chou-Fasman method but it also states that the conformation of a residue is influenced by its nearest neighbouring residue (Sternberg, 1996).

Despite previous beliefs that the low-complexity containing parasite-specific inserts do not contain any significant structures, the algorithms predicted a number of α-helices and β-plates. In the DHFR-TS crystal structure it was also shown that the parasite-specific inserts do contain structures (Yuvaniyama, *et al.*, 2003). These secondary structures in the parasite-specific inserts were disrupted in order to investigate its importance in protein function and stability. The α-helices focused on in this study are conserved between *P. falciparum, P. berghei* and *P. yoelii* (results not shown). The α-helices were disrupted by the introduction of a Pro residue in each helix. Pro provides steric hindrance to the normal conformation of the α-helix and prevents stabilizing H-bonds between CO (residue n) and NH (residue n+4) (Richardson, 1981). The β-plate in the hinge region is not as conserved between *Plasmodia* species, the corresponding regions in *P. berghei* and *P. yoelii* are shorter and are predicted to be more structured. The '(NND)x' repeat region in O_2, thought to be important for protein-protein interactions by means of a polar-zipper (Birkholtz, *et al.*, 2004), was deleted to disturb the zipper effect. The repeat region is not conserved between *Plasmodia* but the possible involvement of a polar zipper motivated the deletion of this region.

Table 3.5 summarizes the previous and current results obtained with studies performed on the two domains of the *Pf*AdoMetDC/ODC. Wrenger, *et al.* (2001) and Krause, *et al.* (2000) focused on the separate domains and the effect observed when expressed on its own. Interestingly, the AdoMetDC activity increased when expressed without its partner domain, whereas the ODC domain showed a remarkable decrease in activity. The ODC however showed a slight increase in activity when expressed with 140 amino acids of the preceeding hinge region. From studying the domains on its own, it is clear that intra-domain protein-protein interactions stabilizes the heterotetrameric conformation of the bifunctional protein in order to obtain optimal activity of both catalytic domains. It is also possible that this protein-protein interactions can be utilized to regulate the activities of the individual domains by its partner domain.

Birkholtz, *et al*. (2004), focused on the deletion of the parasite-specific inserts in both domains. It is apparent that deletion of the inserts had a greater influence on the domain from which it has been removed than on the neighbouring domain. However, the fact that deletion of a parasite-specific insert influences both domain activities is an indication of interdomain protein-protein interactions that might stabilize the heterotetrameric complex. Deletion of the hinge had a more remarkable effect on the ODC domain than on the

AdoMetDC domain. This finding, together with that of Krause, *et al* (2000), proves that the ODC domain is much more dependent on association with the hinge region for activity/stability. Removal of the hinge indirectly affects both domain activities and appears to be important for interdomain interactions between the AdoMetDC and ODC domains (Birkholtz, *et al.*, 2004). The hinge region of *Pf*AdoMetDC/ODC appears to mediate the correct folding of the ODC domain and is therefore important for the stability and activity of ODC as an active homodimer (Birkholtz, *et al.*, 2004).

It was however suspected that the large deletions of entire parasite-specific inserts could be responsible for the extreme decrease of domain activities as a result of unstable proteins or multiple conformations. In the present study, predicted secondary structures were disrupted in the Hinge and ODC parasite-specific inserts. Disruption of the structures in all cases had a more remarkable effect on ODC activity. Figure 3.5 summarizes the outcomes of secondary structure disruptions in the parasite-specific inserts on the activity of the bifunctional *Pf*AdoMetDC/ODC. Disruption of α-helix 1 in the Hinge region negatively affected the bifunctional protein with an activity decrease of 13% in AdoMetDC and 34% in ODC. Similarly, disruption of the second helix in the Hinge resulted in an activity decrease of both domains with 64% in AdoMetDC and 67% in ODC. Deletion of the Hinge β-plate decreased the AdoMetDC activity with a mere 4% and caused a35% increase in the ODC activity. Disruption of the O_1 α-helix depleted the ODC activity and decreased the AdoMetDC activity with 94%. Removal of the '(NND)x' repeat region caused the AdoMetDC activity to decrease with 27% and that of ODC with 46%. It seems that ODC is more vulnerable to small changes in the bifunctional protein, it is more dependent on the Hinge and AdoMetDC domain for stabilization and activity, and it is the domain where initialization of heterotetrameric complex formation takes place.

Table 3.5: Comparative table of previous and current studies on *Pf*AdoMetDC/ODC.

Mutant name[a]	Mutation	Bifunctional Enzyme (Bif) % Specific activity of Wt		Monofunctional Enzymes % Specific activity of Wt		Reference
		AdoMetDC	ODC	AdoMetDC	ODC	
***Pf*AdoMetDC**	Monofunctional AdoMetDC domain with part of hinge	-	-	**255** (% of Bif)	-	Wrenger, *et al.*, 2001
A-OΔA3	196 amino acid deletion	**4**	**31**	**9**	-	Birkholtz, *et al.*, 2004
A-OΔH	180 amino acid deletion of the center part of the hinge region	**67**	**50**	-	**54**	Birkholtz, *et al.*, 2004
A/OpHa1	Helix breaker	**87**	**66**	-	-	S. Roux (current study)
A/OpHa2	Helix breaker	**36**	**33**	-	-	S. Roux (current study)
A/OΔHb	94 bp β-sheet deletion	**96**	**135**	-	-	S. Roux (current study)
***Pf*ODC**	Monofunctional ODC domain without hinge	-	-	-	**8** (% of Bif)	Krause, *et al.*, 2000
***Pf*hinge-ODC**	Monofunctional ODC domain with additional 144 amino acids of hinge region	-	-	-	**11** (% of Bif)	Krause, *et al.*, 2000
A-OΔO1	39 amino acid deletion	**23**	**6**	-	**9**	Birkholtz, *et al.*, 2004
A/OpO1a	Helix breaker	**6**	**0**	-	-	S. Roux (current study)
A-OΔO2	145 amino acid deletion	**48**	**3**	-	**2**	Birkholtz, *et al.*, 2004
A/OΔNND	23 bp Conserved repeat region deletion	**73**	**54**	-	-	S. Roux (current study)
A-OΔO1O2	Deletion of both O_1 and O_2 inserts	**30**	**3**	-	**2**	Birkholtz, *et al.*, 2004

[a] A1, O1 and O2 refer to the respective parasite-specific inserts in AdoMetDC (A) and ODC (O); H refers to the Hinge region; **Δ** refers to deletion of specific amino acids in inserts; **p** refers to site-specific point mutation in inserts: **Bif** refers to the Bifunctional wild type protein.

From the results obtained in this study, it can be postulated that both hinge α-helices contribute to interdomain interaction and indirectly affects the catalytic activities of both domains by propagating a local conformational change to the active sites. Deletion of the hinge β-plate caused remarkable fluctuations in both domain activities (a large standard deviation observed for both), this suggests that the β-plate is important for the stabilization of the entire bifunctional protein. The absence of the hinge β-plate might result in an unstable construct that adopts multiple conformations, some that are catalytically favorable and others that are not.

The O_1 insert is important for the dimerization of ODC monomers. Failure of the ODC to dimerize prevents heterotetrameric complex formation with the AdoMetDC domain (Birkholtz, *et al.*, 2004). It was suggested in Chapter 2 that O_1 mobility is important for dimerization of ODC. In this chapter it was furthermore shown that the α-helix in the O_1 insert was essential for both activities in the bifunctional protein. It is possible that O_1 mobility results in the availability and positioning of the α-helix for protein-protein interaction. Disruption of the helix may be communicated to the respective active sites via long-range interactions (Jackson, *et al.*, 2004; Myers, *et al.*, 2001), which cause a conformational change at the active sites resulting in activity loss. These results suggest the involvement of this helix in protein-protein interaction between the two ODC dimers.

Single amino acid repeats (homorepeats) of *P. falciparum* proteins are predominantly located in the parasite-specific inserts (Singh, *et al.*, 2004). *P. falciparum* contains 35.7% homorepeats, far exceeding the homorepeats content of *H. sapiens* (8.9%). The large amount of homorepeats present in *P. falciparum* cannot be contributed to its high A+T content or to the *Plasmodia* family (*P. yoelli* contains 13.2% repeat regions). The amino acid repeats consists mostly of Asn (60%) and Lys (23%) residues (Singh, *et al.*, 2004). Asn/Glu-rich regions (or the abundance of other polar residues) play a role in protein aggregation and might also behave as modulators of protein-protein interactions termed ‘polar zippers’ because of side-chains forming hydrogen-bonded networks (Michelitsch and Weissman, 2000; Perutz, *et al.*, 1994; Perutz, *et al.*, 2002). Perutz, *et al* (2002) showed that poly-Asn peptides ($D_2N_{15}K_2$) form β-sheets in solution and these repeats are therefore involved in polar zipper formation.

Deletion of the 145-residue O_2 insert in previous studies depleted the ODC activity and decreased the AdoMetDC activity with about 50% (Birkholtz, *et al.*, 2004). In this study the area suspected to be important for protein interaction was delineated to the '(NND)x' repeat region that is thought to play a role as a polar zipper (Birkholtz, *et al.*, 2004). It was found that deletion of the 23-residue repeat region decreased the ODC activity with 46% and the AdoMetDC activity with 27%. The deletion of the entire O_2 insert in previous studies could be responsible for the conformational collapse of the ODC domain therefore depleting the ODC activity and decreasing AdoMetDC activity. Removal of the shorter, coiled '(NND)x' repeat region proved to be important for both domain activities although the ODC activity was more dependant on the interaction with the repeat region. The activity loss of both domains could be attributed to the disruption of a ‘polar zipper’ interaction that normally contributes to the stability/activity of the bifunctional *Pf*AdoMetDC/ODC.

This chapter discussed the studies performed on the secondary structures in the hinge and ODC regions of *Pf*AdoMetDC/ODC in order to delineate the interacting areas. From the results obtained it is clear that the secondary structures present in the parasite-specific inserts are important for the activity of the *Pf*AdoMetDC/ODC protein, possibly via interdomain protein-protein interactions. The next chapter will summarize the outcomes of the experimental studies and the relevant theories thereof.

Chapter 4
Concluding Discussion

Malaria remains one of the most devastating infectious diseases affecting humans. More people die annually of malaria than 30 years ago because of resurgence of the disease. Resurgence is caused by the spread of drug resistant parasites, the evolution of insecticide resistant mosquitoes, the increase in population density, global warming and continuing poverty especially in African countries. The rapid spread of resistance against available drugs and the difficulty of developing an effective vaccine urges the development of new, mechanistically novel chemotherapeutic drugs for the treatment of malaria. The polyamine pathway in *P. falciparum* is one of the studied pathways in this regard.

Polyamines are ubiquitous in most eukaryotic cells and are involved in the differentiation and proliferation of eukaryotic cells, transcriptional regulation, protein-protein interactions, signal transduction, enzyme regulation and apoptosis (Cohen, 1998; Criss, 2003; Wallace and Fraser, 2003). The effectiveness of DFMO against *Trypanosoma brucei gambiense* reinforced the idea that inhibition of the polyamine biosynthetic pathway is a viable target for control of malaria (Müller, *et al*., 2001). The polyamine metabolism of *P. falciparum* differs considerably from that of its human host and the differences in these pathways are studied for the design of mechanistically novel drugs specific against *P. falciparum*. Differences include the unique bifunctionality of *Plasmodia* enzymes, one of which is the bifunctional *Pf*AdoMetDC/ODC protein that contains both the regulatory enzymes of the polyamine metabolic pathway. In the bifunctional protein, the active sites of the AdoMetDC and ODC domains function independently of each other (Wrenger, *et al*., 2001) although the domains interact to stabilize the heterotetrameric *Pf*AdoMetDC/ODC conformation (Birkholtz, *et al*., 2004).

Compared to other homologous monofunctional proteins, the bifunctional *Pf*AdoMetDC/ODC contains inserted regions that double the size of the protein. The parasite-specific inserts contain hydrophilic, low-complexity regions that form non-globular domains and are not involved in the core structure of the respective domains (Pizzi and Frontali, 2001; Birkholtz, *et al*., 2004).

Disordered regions in proteins are described by Garner, *et al*., (1999) as protein regions lacking fixed tertiary structure, essentially being partially or fully unfolded. These regions consist of non-folding sequences, which either contain significant net charge or lack aromatic residues, or have an excess of hydrophilic groups or exhibit a combination of these features. Dyson and Wright (2002) further expanded by stating that regions of proteins that are intrinsically unstructured under physiological conditions, differ in amino acid composition from that of globular regions and are furthermore characterized by amino acid compositional bias, low sequence complexity and high-predicted flexibility. The characteristics of disordered regions (Garner, et al., 1999; Dyson and Wright, 2002) are comparable to those of parasite-specific inserts (Pizzi and Frontali, 2001; Birkholtz, *et al*., 2004)

A survey performed in 1994 showed that half of the protein sequences in the Swiss protein Database at that time contained segments of low complexity that correspond to non-globular regions (Wootton, 1994). Non-globular regions are not necessarily disordered, because they can include repetitive structural elements like coiled coils. It has been suggested that proteins with natively unfolded regions at physiological pH are advantageous for biological systems because it allows efficient interaction with numerous targets (Uversky, 2002). Questions however still arise as to the specific roles of these inserts in biological processes.

Dunker *et al*. (2002) did literature searches of 115 predicted disordered protein regions in order to determine functions for these regions. They found 98 different functions for the disordered regions, which can be categorized in a number of classes involving molecular interactions, membrane associations, molecular recognition and chemical modifications. Molecular interactions include protein-protein binding as well as binding of proteins to nucleic acids such as DNA, rRNA mRNA and tRNA. Disordered regions can also bind multiple partners in regulatory processes (Dunker, *et al.*, 2002). The study of disordered regions and their functions are still a new field of study and mostly rely on predictive methods.

As is the case with the disordered regions, the functions of the *Pf*AdoMetDC/ODC parasite-specific, non-globular inserts are not yet clear although they appear to be involved in protein-protein interactions (Birkholtz, *et al.*, 2004). In Chapter 3, the parasite-specific inserts were analysed with secondary structural prediction algorithms in order to confirm

any structural elements. It was found that the low-complexity, parasite-specific inserts of the protein contain local secondary structures. The importance of secondary structures in protein-protein interactions motivated the delineation of the interacting areas of the parasite-specific inserts to the local structures. The α-helices and β-plates in the parasite-specific inserts that were conserved between the secondary structure prediction algorithms used were the main focus of this study.

The hinge region, connecting the AdoMetDC and ODC domains, is important for the conformational stability and correct folding of the ODC domain (Krause, *et al*., 2001). The hinge mediates interdomain interactions between the AdoMetDC and ODC, which stabilizes the heterotetrameric complex (Birkholtz, *et al*., 2004). Disruption of the two α-helices and deletion of the hinge β-plate in this study affected both domain activities. Similarly, a decrease is observed in the activities (% of wild type activity) upon deletion of the 180 amino acid core region of the hinge (summarized in Figure 4.1). It is thus proposed that the secondary structures of the hinge region are the important elements responsible for complex stabilization via protein-protein interactions. These results delineated the possible protein-protein interaction areas, which was the initial aim.

The coiled '(NND)x' repeat region present in the O_2 parasite-specific insert was thought to play a role as a polar zipper (Birkholtz, *et al*., 2004). Deletion of the 23 amino acid region caused an activity decrease of 27% in the AdoMetDC domain and 46% in the ODC domain. It was suggested that previous deletions of the entire 145 residue O_2 insert (Birkholtz, *et al.*, 2004) may have been responsible for the activity depletion of the ODC domain and the 50% decrease of the AdoMetDC activity because of conformational collapse of the protein. Deletion of the '(NND)x' repeat region (23 amino acids) was responsible for approximately half the activity loss brought about by deletion of the 145 residue insert (summarized in Figure 4.1). From these results it is clear that the repeat region plays an essential role in protein activity, possibly via indirect protein-protein interactions brought upon by a polar zipper effect.

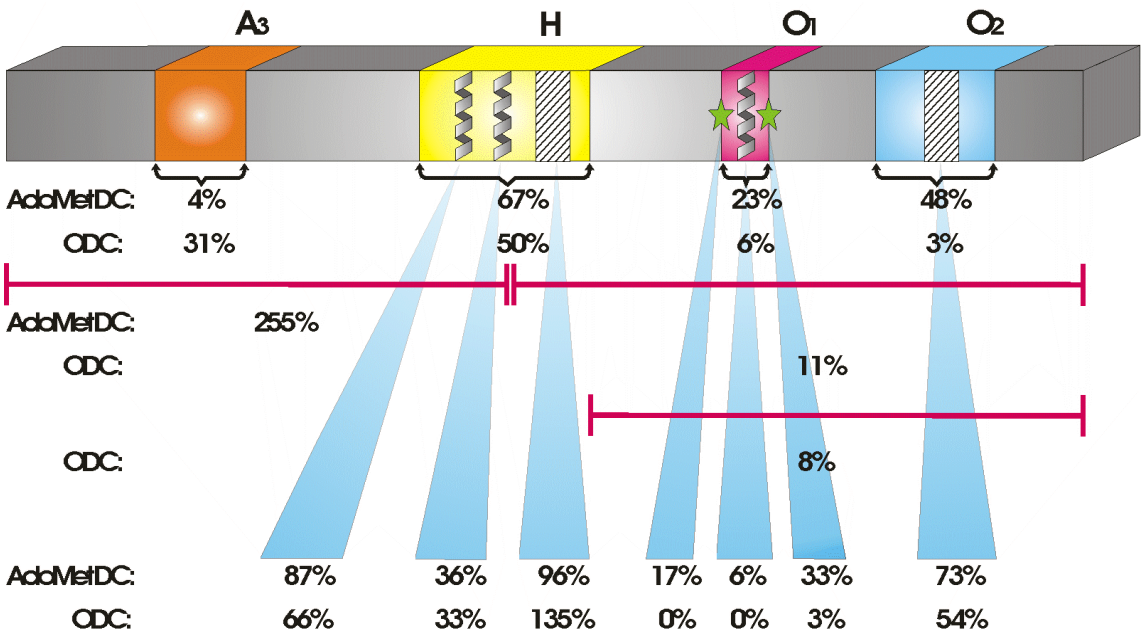

Figure 4.1: Summary of previous and current structure-function relationship studies on the bifunctional *Pf*AdoMetDC/ODC protein. The black brackets represent the deletion mutagenesis of the respective parasite-specific inserts (Birkholtz, *et al.*, 2004). The red bars depict the domains expressed as recombinant monofunctional proteins with or without part of the Hinge region (Krause, *et al*., 2000; Wrenger, *et al.*, 2001). The blue blocks represent the secondary structure disruptions (current study). The green stars indicate the G1 and G1G2 mutations respectively (current study). The values given are the percentage activity remaining after normalization against the wild type *Pf*AdoMetDC/ODC.

The 38-residue O_1 insert in the ODC domain of the *Pf*AdoMetDC/ODC differs from the other parasite-specific inserts because of its conservation between *Plasmodia* and the absence of low-complexity regions. The O_1 insert is also flanked by Gly residues, which was thought to provide mobility to the O_1 insert. Chapter 2 focused on the alteration of the flanking Gly residues to Ala to investigate its possible function in the dimerization of ODC or its involvement in the active site function. Mutation of the $Gly_{1036\text{-}1038}$ and both the $Gly_{1036\text{-}1038}$ and Gly_{1083} residues had a remarkable effect on both the AdoMetDC and ODC domain activities. Molecular dynamics (Figure 2.10) of the homology models of the wild type, single mutant and double mutant proteins confirmed that the activity loss (Figure 2.8 and Figure 2.9) was a result of possible insert immobility. Insert O_1 is essential for the dimerization of ODC thereby initiating the folding of the heterotetrameric *Pf*AdoMetDC/ODC structure (Birkholtz, *et al*, 2004). Insert O_1 might also function as an active site "lid" that potentially acts as gate-keeper for entry of substrate into the ODC active site pocket. Immobility of the insert might either prevent ODC dimerization or it may

prevent access to the active site of ODC because of the rigidity of the active site "lid". Enzyme kinetics of AdoMetDC and ODC will give a clear indication of how the active site is influenced upon O_1 immobilization. Vmax and Km are the two parameters which define the kinetic behaviour of an enzyme as a function of substrate concentration, where Vmax is defined as the maximum rate of the enzyme reaction and Km as the concentration of substrate where the enzyme reaches half of Vmax. Km is an indication of the affinity of the active site for substrate. In the situation where access to the active site might be influenced by the immobile O_1 insert, the Km will remain the same as in the wild type protein and the Vmax will be affected. In addition, when O_1 movement restriction affects the dimer interface, the active site conformations of ODC and potentially AdoMetDC will also be influenced. This will result in a increase/decrease of both the Km and Vmax values. It is thus essential to perform enzyme kinetic studies before any firm conclusions can be extrapolated from the results obtained in this study. However, from the results obtained in Chapter 2 it is suggested that O_1 is involved in ODC dimerization because of the effect of insert immobility on both domain activities of the heterotetrameric protein.

The O_1 insert also contains a single α-helix predicted by the secondary structure prediction algorithms. In Chapter 3, the α-helix was disrupted, by introduction of a Pro residue, to study its importance in the functionality of the two domains. Disruption of the α-helix depleted the ODC activity and decreased the AdoMetDC acitivity with 94%. These results confirm the importance of the O_1 insert in the activity and protein-protein interaction of the heterotetrameric complex.

The O_1 insert has been proven to be important on a number of occasions (Birkholtz, *et al.*, 2004, Chapter 2 and Chapter 3). Preventing the O_1 insert from interacting with the protein has devastating effects on both decarboxylase activities. The ideal way of inhibiting the polyamine pathway in parasitic protozoa is to inhibit the two regulatory proteins, AdoMetDC and ODC. In *Plasmodia*, these two proteins are part of a bifunctional construct and inhibiting the O_1 insert with peptidomimetics can result in the functional knockout of both these proteins at the same time. The use of small peptides as inhibitors has been explored in a number of systems up to date; these include HIV-1 protease (Schramm, *et al.*, 1996; Zutshi, *et al.*, 1998), *Lactobacillus casei* thymidylate synthase (Prasanna, *et al.*, 1998), herpes simplex virus DNA polymerase and human glutathione reductase (Zutshi, *et*

al., 1998) and *T. brucei* farnesyltransferase (Okhanda, *et al.*, 2004). Synthetic peptides were also developed to inhibit the dimerization of *P. falciparum* triosephosphate isomerase by interfering with protein-protein interaction (Singh, *et al.*, 2001). A small peptide directed against the α-helix of the O_1 loop could prove to be effective in the treatment of *P. falciparum* malaria for an extended time because resistance might not develop rapidly against a molecule targeted at a site beyond the active site. Inhibition of both regulatory enzymes with one molecule might be cytotoxic - the ideal drug in the combat against malaria.

Although certain areas of the parasite-specific inserts important for protein activity, possibly due to protein-protein interactions, have been delineated, it is still crucial to obtain visual confirmation of the predicted interactions. Disruption of the secondary structures affects the local conformation of the protein and this is then propagated to the rest of the protein via protein-protein interactions. The exact effect of these disruptions are still unclear and it would be interesting to know if the local conformational change causes order-to-disorder transition of the nearby loops, helices and plates, which might be responsible for destabilization of the protein. The specific changes occuring at both active sites of the bifunctional protein could also be studied with the availability of a structural model. An accurate protein structure is thus needed for further structural studies in this regard. Two separate homology models exist for the AdoMetDC domain (Wells, 2004) and ODC domain (Birkholtz, *et al.*, 2003), it is still troublesome to combine these two models *in silico* because of its large combined size and software limitations. In addition, the parasite-specific inserts could not be modelled (except for the O_1 insert) because of the absence of a known template, the low-complexity of the inserts and its uniqueness to *Plamodia.*

Another approach to obtain a structure for the bifunctional enzyme is to use *Toxoplasma gondii* as a model organism. The close family relationship between *T. gondii* and *P. falciparum* may aid the structural studies of the *Pf*AdoMetDC/ODC enzyme. The expression levels of *P. falciparum* proteins are problematic and the major reason for the lack of structural information for the *P. falciparum* proteins. Higher expression levels and possible stability of expressed proteins could be obtained with alteration of the *P. falciparum* codons to favour the *E. coli* codon preferences.

In the absence of definitive structural information, additional protein-protein interaction data could be obtained with the use of the yeast-2-hybrid system or the phage display system to determine specific interaction areas and residues between the AdoMetDC and ODC domains.

Although drug development against malaria is problematic, scientists are breaking down its defences one-by-one. Hopefully in the near future, malaria would be a problem of the past.

Summary

Malaria is a global health threat that causes 300 – 500 million clinical cases annually, resulting in approximately 2 million deaths. Chemotherapy and prophylaxis are becoming less effective because of increasing drug resistance by the parasite. Resurgence of malaria calls for the development of mechanistically novel drugs. The bifunctional organization of the two rate-limiting enzymes, AdoMetDC and ODC, in the *P. falciparum* polyamine pathway and the presence of six parasite-specific inserts, present potential target sites for novel *Plasmodia*-specific drugs. The inserts are species-specific, hydrophilic, low complexity segments and form non-globular domains. The inserts are involved in intra- and interdomain interactions, which are important for stability and activity of the bifunctional construct. This study investigated properties of the parasite-specific inserts, one being the mobility of the O_1 insert and the other the secondary structures present in the parasite-specific inserts.

It is postulated that the mobility of the O_1 insert plays a role in either heterotetrameric complex formation of the bifunctional construct or that the O_1 insert acts as a "lid" to the ODC active site, which is necessary for catalytic function. Successful mutagenesis of the O_1 flanking Gly residues to Ala, rendered the O_1 insert immobile. The probable immobility of the O_1 insert had a detrimental effect on the activity of both the AdoMetDC and ODC domains of the bifunctional protein. Molecular dynamics studies showed that movement restriction of the insert caused a conformational change in the ODC monomers. The decrease of both domain activities upon movement restriction of the O_1 insert suggests that the insert is involved in protein-protein interactions, which is communicated throughout the protein.

In addition, the roles of selected, predicted secondary structures in the Hinge, O_1 and O_2 parasite-specific inserts were investigated. α-Helices were disrupted by the introduction of a Pro residue, β-plates were removed with deletion mutagenesis. The effects of the secondary structure alterations on protein activity were monitored in the bifunctional *Pf*AdoMetDC/ODC protein. Both domain activities were affected by the disruptions, although the ODC domain was more sensitive to the small changes. The results obtained in this study showed that the secondary structures in the parasite-specific insert are important

for activity of both the AdoMetDC and ODC domains of the bifunctional protein, possibly via interdomain protein-protein interactions.

The delineation of essential intra- and interdomain protein-protein interactions presents possible interaction sites for disruptive molecules in the combat against malaria.

Bibliography

Alonso, P. L., Sacarlal, J., Aponte, J.J., Leach, A., Macete, E., Milman, J., Mandomando, I., Spiessens, B., Guinovart, C., Espasa, M., Bassat, Q., Aide, P., Ofori-Anyinam, O., Navia, M.M. Corachan, S., Ceuppens, M., Dubois, M.-C., Demoitié, M.-A., Dubovsky, F., Menéndez, C., Tornieporth, N., Ballou, W.R., Thompson, R. and Cohen, J. (2004). Efficacy of the RTS,S/ASO2A vaccine against *Plasmodium falciparum* infection and disease in young African children: randomised controlled trial. *Lancet,* **364,** 1411-1420.

Ballou, W. R., Arevalo-Herrera, M., Carucci, D., Richie, T.L., Corradin, G., Diggs, C., Druilhe, P., Giersing, B.K., Saul, A., Heppner, D.G., Kester, K.E., Lanar, D.E., Lyon, J., Hill, A.V.S., Pan, W. and Cohen, J.D. (2004). Update on the clinical development of candidate malaria vaccines. *Am J Trop Med Hyg,* **71,** 239-247.

Berman, P. A. and Adams, P.A. (1997). Artemisinin enhances heme-catalysed oxidation of lipid membranes. *Free Rad Biol Med,* **22,** 1283-1288.

Birkholtz, L., Joubert, F., Neitz, A.W.H. and Louw, A.I. (2003). Comparative properties of a three-dimensional model of *Plasmodium falciparum* ornithine decarboxylase. *Proteins,* **50,** 464-473.

Birkholtz, L., Wrenger, C., Joubert, F., Wells, G.A., Walter, R.D. and Louw, A.I. (2004). Parasite-specific inserts in the bifunctional S-adenosylmethionine decarboxylase/ ornithine decarboxylase of *Plasmodium falciparum* modulate catalytic activities and domain interactions. *Biochem J,* **377,** 439-448.

Bitonti, A. J., Dumont, J.A., Bush, T.L., Edwards, M.L., Stemerick, D.M., McCann, P.P. and Sjoerdsma, A. (1989). Bis(benzyl)polyamine analogs inhibit the growth of chloroquine-resistant human malaria parasites (*Plasmodium falciparum*) *in vitro* and in combination with α-difluoromethylornithine cure murine malaria. *Proc Natl Acad Sci USA,* **86,** 651-655.

Bourne, P. E. and Weissig, H.. (2003). "Structural Bioinformatics." Wiley-Liss, Inc., Hoboken, New Jersey.

Bradford, M. M. (1976). A rapid and sensitive method for the quantitation of microgram quantities of protein utilizing the principle of protein-dye binding. *Anal Biochem,* **72,** 248-254.

Brandon, C. and Tooze, J. (1999). "Introduction to protein structure." Garland Publishing, Inc., New York.

Brooks BR, Bruccoleri RE, Olafson BD, States DJ, Swaminathan S, Karplus M. (1989) CHARMM: a program for macromolecular energy, minimization and dynamics calculations. *J Comput Chem,* **4,** 187-217.

Ceriani, C., Conzález, N.S., and Algranati, I.D. (1992). Ornithine decarboxylase from *Crithidia fasciculata* is metabolically unstable and resistant to polyamine down-regulation. *FEBS,* **301,** 261-264.

Cohen, S. S. (1998). "A guide to the polyamines." Oxford University Press, Oxford.

Cooke, B. M., Wahlgren, M., and Coppel, R.L. (2000). Falciparum malaria: Sticking up, standing out and out-standing. *Parasitol Today,* **16,** 416-420.

Criss, W. E. (2003). A review of polyamines and cancer. *Turk J Med Sci,* **33,** 195-205.

Dunker, A. K., Brown, C.J., Lawson, J.D., Iakoucheva, L.M. and Obradovic, Z. (2002). Intrinsic disorder and protein function. *Biochemistry,* **41,** 6573-6582.

Dyson, H. J. and Wright, P.E. (2002). Coupling of folding and binding for unstructured proteins. *Curr Opin Struct Biol,* **12,** 54-60.

Garner, E., Romero, P., Dunker, A.K., Brown, C. and Obradovic, Z. (1999). Predicting binding regions within disordered regions. *Genome Inf,* **10,** 41-50.

Garrity, J. D., Pauff, J.M. and Crowder, M.W. (2004). Probing the dynamics of a mobile loop above the active site of L1, a Metallo-β-lactamase from *Stenotrophomonas maltophilia*, via site-directed mutagenesis and stopped-flow fluorescence spectroscopy. *J Biol Chem,* **279,** 39663-39670.

Gornicki, P. (2003). Apicoplast fatty acid biosynthesis as a target for medical intervention in apicomplexan parasites. *Int J Parasit,* **33,** 885-896.

Grishin, NV., Osterman, AL., Brooks, HB., Phillips, MA., and Goldsmith, EJ.(1999). X-ray structure of ornithine decarboxylase from *Trypanosoma brucei*: the native structure and the structure in complex with alpha-difluoromethylornithine. *Biochemisty,* **38**,15174–15184.

Hafner, E., Tabor, C. and Tabor, H. (1979) Mutants of *Escherichia coli* that do not contain 1,4-diaminobutane (putrescine) or spermidine. *J Biol Chem*, **254,** 12419-12426.

Hartl, D. L. (2004). The origin of malaria: mixed messages from genetic diversity. *Nat Rev Microbiol,* **2**(1):15-22.

Heby, O., Roberts, S.C. and Ullman, B. (2003). Polyamine biosynthetic enzymes as drug targets in parasitic protozoa. *Biochem Soc Trans,* **31,** 415-419.

Heddini, A. (2002). Malaria pathogenesis: a jigsaw with an increasing number of pieces. *Int J Parasitol,* **32,** 1587-1598.

Hillary, R. A. and Pegg, A.E. (2003). Decarboxylases involved in polyamine biosynthesis and their inactivation by nitric oxide. *Biochim Biophys Acta,* **1647,** 161–166.

Jackson, L. K., Baldwin, J., Akella, R., Goldsmith, E.J. and Phillips, M.A. (2004). Multiple active site conformations revealed by distant site mutation in Ornithine Decarboxylase. *Biochemistry,* **43,** 12990-12999.

Kilpelainen, P. T. and Hietala, O.A. (1998). Mutation of aspartate-223 to valine in mouse ornithine decarboxylase reduces enzyme activity. *Int J Biochem Cell biol,* **30,** 803-809.

Kim, K and Weiss, L.M. (2004) *Toxoplasma gondii:* the model apicomplexan. *Int J Parasitol,* **34**, 423-432.

Ko, T., Chen, Y., Robinson, H., Tsai, P., Gao, Y., Chen, A.P., Wang, A.H. and Liang, P. (2001). Mechanism of product chain length determination and the role of a flexible loop in *Escherichia coli* Undecaprenyl-pyrophosphate synthase catalysis. *J Biol Chem,* **276,** 47474-47482.

Krause, T., Lüersen, K., Wrenger, C., Gilberger, T.-W., Müller, S., and Walter, R.D. (2000). The ornithine decarboxylase domain of the bifunctional ornithine decarboxylase/S-adenosylmethionine decarboxylase of *Plasmodium falciparum*: recombinant expression and catalytic properties of two different constructs. *Biochem J,* **352,** 287-92.

Kwok, S. C., Mant, C.T. and Hodges, R.S. (2002). Importance of secondary structural specificity determinants in protein folding: Insertion of a native β-sheet sequence into an α-helical coiled-coil. *Protein Sci,* **11,** 1519-1531.

Lee, B. J., Singh, A., Chiang, P., Kemp, S.J., Goldman, E.A., Weinhouse, M.I., Vlasuk, G.P. and Rosenthal, P.J. (2003). Antimalarial activities of novel synthetic cysteine protease inhibitors. *Antimicrob Agents Chemother,* **47,** 3810-3814.

Merril, C. R., Goldman, D., Sedman, S.A. and Ebert, M.H. (1981). Ultrasensitive stain for proteins in polyacrylamide gels shows regional variation in cerebrospinal fluid proteins. *Anal Biochem,* **72,** 248-254.

Meshnick, S. R. (2002). Artemisinin: mechanisms of action, resistance and toxicity. *Int J Parasitol,* **32,** 1655-1660.

Michelitsch, M. D. and Weissman, J.S. (2000). A census of glutamine/asparagine-rich regions: Implications for their conserved function and the prediction of novel prions. *Proc Natl Acad Sci USA,* **97,** 11910-11915.

Milhous, W.K. and Kyle, D.E. (1998). Introduction to the modes of action of and mechanisms of resistance to antimalarials. *In* "Malaria: Parasite biology, pathogenesis and protection" (I. W. Sherman, Ed.). ASM Press, Washington, D.C.

Mitamura, T. and Palacpac, N.M.Q. (2003). Lipid metabolism in *Plasmodium falciparum*-infected erythrocytes: possible new targets for malaria chemotherapy. *Microb Infect,* **5,** 545-552.

Moldoveanu, T., Campbell, R.L., Cuerrier, D. and Davies, P.L. (2004). Crystal structures of Calpain-E64 and -Leupeptin Inhibitor complexes reveal mobile loops gating the active site. *J. Mol. Biol.* **343,** 1313-1326.

Müller, S., Coombs, G.H. and Walter, R.D. (2001). Targeting polyamines of parasitic protozoa in chemotherapy. *Trends Parasitol,* **17,** 242-249.

Müller, S., Da'dara, A., Lüersen, K., Wrenger, C., Das Gupta, R., Madhubala, R., and Walter, R.D. (2000). In the human malaria parasite *Plasmodium falciparum*, polyamines are synthesized by a bifunctional Ornithine Decarboxylase, *S*-Adenosylmethionine Decarboxylase. *J Biol Chem,* **275,** 8097-8102.

Myers, D. P., Jackson, L.K., Ipe, V.G., Murphy, G.E. and Phillips, M.A. (2001). Long-range interactions in the dimer interface of Ornithine Decarboxylase are important for enzyme function. *Biochemistry,* **40,** 13230-13236.

Okhanda, J., Buckner, F.S., Lockman, J.W., Yokoyama, K., Carrico, D., Eastman, R., De Luca-Fradley, K., Davies, W., Croft, S.L., Van Voorhis, W.C., Gelb, M.H., Sebti, S.M. and Hamilton, A.D. (2004) Design and synthesis of peptidomimetic protein farnesyltransferase inhibitors as anti-*Trypanosoma brucei* agents. *J Med Chem*, **47**, 432-445.

Olliaro, P. (2001). Mode of action and mechanisms of resistance for antimalarial drugs. *Pharmacol Ther,* **89,** 207-219.

Pandey, A. V., Babbarwal, V.K., Okoyeh, J.N., Joshi, R.M., Puri, S.K., Singh, R.L. and Chauhan, V.S. (2003). Hemozoin formation in malaria: a two-step process involving histidine-rich proteins and lipids. *Biochem Biophys Res Comm,* **308,** 736-743.

Persson, K., Aslund, L., Grahn, B., Hanke, J. and Heby, O. (1998). *Trypanosoma cruzi* has not lost its S-adenosylmethionine decarboxylase: characterization of the gene and the encoded enzyme.. *Biochem J,* **333,** 527-537.

Perutz, M. F., Johnson, T., Suzuki, M. and Finch, J.T. (1994). Glutamine repeats as polar zippers: their possible role in inherited neurodegenerative diseases. *Proc Natl Acad Sci USA,* **91,** 5355-5358.

Perutz, M. F., Pope, B.J., Owen, D., Wanker, E.E. and Scherzinger, E. (2002). Aggregation of proteins with expanded glutamine and alanine repeats of the glutamine-rich and asparagine-rich domains of Sup35 and of the amyloid β-peptide of amyloid plaques. *Proc Natl Acad Sci USA,* **99,** 5596-5600.

Phillips, R. S. (2001). Current status of malaria and potential for control. *Clin Microbiol Rev,* **14,** 208-226.

Pizzi, E. and Frontali, C. (2001). Low-complexity regions in *Plasmodium falciparum* proteins. *Genome Res,* **11,** 218-229.

Prasanna, V., Bhattacharjya, S. and Balaram, P. (1998) Synthetic interface peptides as inactivators of multimeric enzymes: inhibitory and conformational properties of three fragments from *Lactobacillus* casei thymidylate synthase *Biochemistry*, **37**, 6883-6893.

Ralph, S. A., D'Ombrain, M.C., McFadden, G.I. (2001). The apicoplast as an antimalarial drug target. *Drug Resist Updat,* **4,** 145-151.

Ramasubbu, N., Ragunath, C. and Mishra, P.J. (2003). Probing the role of a mobile loop in substrate binding and enzyme activity of human salivary amylase. *J Mol Biol,* **325,** 1061-1076.

Rasti, N., Wahlgren, M., and Chen, Q. (2004). Molecular aspects of malaria pathogenesis. *FEMS Immunol Med Microbiol,* **41,** 9-26.

Richardson, J. S. (1981). The anatomy and taxonomy of protein structure. *Adv Prot Chem,* **34,** 168-340.

Richie, T. L., and Saul, A. (2002). Progress and challenges for malaria vaccines. *Nature,* **415,** 694-701.

Ridley, R. G. (2002). Medical need, scientific opportunityand the drive for antimalarial drugs. *Nature,* **415,** 686-693.

Rosenthal, P. J. and Meshnick, S.R. (1998). Hemoglobin processing and the metabolism of amino acids, heme and iron. *In* "Malaria: Parasite biology, pathogenesis and protection" (I. W. Sherman, Ed.). ASM Press, Washington, D.C.

Sambrook, J., Fritsch, E.J. and Maniatis, T. (1989). Molecular cloning: A laboratory manual (2nd ed).

Schramm, H.J., Boetzel, J., Buttner, J., Fritsche, E., Gohring, W., Jaeger, E., Konig, S., Thumfart, O., Wenger, T., Nager, N.E. and Schramm, W. (1996) The inhibition of human immunodeficiency virus proteases by 'interface peptides' Antiv*iral Res*, **30**, 155-170.

Seiler, N. (2003). Thirty years of polyamine-related approaches to cancer therapy. Retrospect and prospect. Part 1. Selective enzyme inhibitors. *Curr Drug Targets,* **4,** 537-564.

Seiler, N (2005). Pharmacological aspects of cytotoxic polyamine analogs and derivatives for cancer therapy. *Pharmacol Ther,* **107**, 99-119.

Shallom, S., Zhang, K., Jiang, L., and Rathod, P.K. (1999). Essential protein-protein interactions between *Plasmodium falciparum* Thymidylate synthase and Dihydrofolate reductase domains. *J Biol Chem,* **274,** 37781-37786.

Shantz, L. M. and Pegg, A.E. (1999). Translational regulation of ornithine decarboxylase and other enzymes in the polyamine pathway. *Int J Biochem Cell Biol,* **31,** 107-122.

Sherman, I. W. (1998). A brief history of malaria and the discovery of the parasite's life cycle. *In* "Malaria: Parasite biology, pathogenesis and protection" (I. W. Sherman, Ed.). ASM Press, Washington, D.C.

Singh, P. S., Beeram, R.C., Bhattacharya, A., Akhouri, R.R., Singh, S.K. and Sharma, A. (2004). Hyper-expansion of asparagines correlates with an abundance of proteins with prion-like domains in *Plasmodium falciparum*. *Mol Biochem Parasitol,* **137,** 307-319.

Singh, S.K., Maithal, K., Balaram, H. and Balaram, P. (2001). Synthetic peptides as inactivators of multimeric enzymes: inhibition of *Plasmodium falciparum* triosephosphate isomerase by interface peptides. *FEBS letters,* **501,** 19-23.

Srinivasan, R. and Rose, G.D. (1999). A physical basis for protein secondary structure. *Proc Natl Acad Sci USA,* **96,** 14258-14263.

Sternberg, M.J.E. (1996). "Protein structure prediction." (Rickwood, D. and Hames, B.D., Ed). Oxford University Press, New York.

Suya Subbayya, I. N., Balaram, P. and Balaram, H. (1997). Metabolic enzymes as potential drug targets in *Plasmodium falciparum*. *Indian J Med Res,* **106,** 79 – 94.

Taylor, J. C. and Markham, G.D.. (2003). Conformational dynamics of the active site loop of *S*-adenosylmethionine synthetase illuminated by site-directed spin labeling. *Arch Biochem Biophys,* **415,** 164-171.

Thomas, T. and Thomas, T.J. (2003). Polyamine metabolism and cancer. *J Cell Mol Med,* **7,** 113-126.

Tompa, P. (2003). Intrinsically unstructured proteins evolve by repeat expansion. *BioEssays,* **25,** 847-855.

Trouiller, P. Olliaro, P., Torreele, E., Orbinski, J., Laing, R., and Ford, N. (2002) Drug development for neglected diseases: A deficient market and a public health policy failure. *Lancet,* **359**, no. 9324, 2188–2194.

Uversky, V. N. (2002). What does it mean to be natively unfolded? *Eur J Biochem,* **269,** 2-12.

Vaidya, A. B. (1998). Mitochondrial physiology as a target for atovaquone and other antimalarials. *In* "Malaria: Parasite biology, pathogenesis and protection" (I. W. Sherman, Ed.). ASM Press, Washington, D.C.

Wallace, H. M. and Fraser, A.V. (2004). Inhibitors of polyamine metabolism. *Amino Acids,* **26,** 353-365.

Wallace, H. M., Fraser, A.V. and Hughes, A. (2003). A perspective of polyamine metabolism. *Biochem J,* **376,** 1-14.

Webster, D., and Hill, A.V.S. (2003). Progress with malaria vaccines. *Bull World Health Org,,* **81,** 902-909.

Wells, G.A. (2004). Stuctural model and properties of the AdoMetDC domain of the bifunctional *Plasmodium falciparum* S-Adenosylmethionine/Ornithine decarboxylase. Magister Scientiae Dissertation, Department of Biochemistry, University of Pretoria.

White, N. J. (1998). Malaria pathophysiology. *In* "Malaria: parasite biology, pathogenesis and protection" (I. W. Sherman, Ed.). ASM Press, Washington, D.C.

Wootton, J. C. (1994). Non-globular domains in protein sequences: automated segmentation using complexity measures. *Comput Chem,* **18,** 269-285.

Wrenger, C., Lüersen, K., Krause, T., Müller, S. and Walter, R.D. (2001). The *Plasmodium falciparum* bifunctional ornithine decarboxylase, *S*-adenosyl-L-methionine decarboxylase, enables a well balanced polyamine synthesis without domain-domain interaction. *J Biol Chem,* **276,** 29651-29656.

Xue, H. Y. and Forsdyke, D.R. (2003). Low-complexity segments in *Plasmodium falciparum* proteins are primarily nucleic acid level adaptations. *Mol Biochem Parasitol,* **128,** 21-32.

Yerlikaya, A. (2004). Polyamines and S-Adenosylmethionine Decarboxylase. *Turk J Biochem,* **29,** 208-214.

Yuvaniyama, J., Chitnumsub, P., Kamchonwongpaisan, S., Vanichtanankul, J., Sirawaraporn, W., Taylor, P., Walkinshaw, M.D. and Yuthavong, Y. (2003). Insights into antifolate resistance from malarial DHFR-TS structures. *Nat Struct Biol,* **10,** 357-365.

Zutshi, R., Brickner, M. and Chmielewski, J. (1998) Inhibiting the assembly of protein-protein interfaces. *Curr Opin Chem Biol*, **2**, 62-66.